

Karst and cave development and groundwater resources of Dong Van Karst Plateau, Northern Vietnam

Zur Erlangung des akademischen Grades eines

DOKTORS DER NATURWISSENSCHAFTEN

(Dr. rer. nat.)

von der KIT-Fakultät für

Bauingenieur-, Geo- und Umweltwissenschaften

des Karlsruher Instituts für Technologie (KIT)

genehmigte

DISSERTATION

von

M. Sc. Diep Anh Tran

aus Hoa Binh, Viet Nam

Tag der mündlichen Prüfung: 09. December 2022

Referent: Prof. Dr. Nico Goldscheider

Korreferentin: Prof. Dr. Thomas Neumann

Karlsruhe, 2022

Karst and cave development and
groundwater resources of Dong Van Karst
Plateau, Northern Vietnam

Doctoral Thesis

by

Diep Anh Tran

Karlsruhe, 2022

Abstract

Karst regions are not only valuable in terms of landscape, tourism, and culture but also offer a variety of natural resources such as freshwater and biodiversity. In particular, groundwater from karst aquifers has proven to be the major freshwater source for drinking-water supply and agricultural irrigation in many countries and regions throughout the world. In tropical and subtropical areas, like in Southeast Asia, the special climate conditions with dry and humid-rainy seasons have created numerous typical tropical karst landforms, but also hamper a continuous freshwater supply. In highland districts of Ha Giang province which is located in the Northern part of Vietnam, although the total surface water discharge is high, the large variations in rainfall, as well as discharge between dry and wet seasons, result in seasonal water scarcity. Since 2010, when Dong Van Karst Plateau was designed as a UNESCO Global Geopark, regional economic development, the number of visitors has strongly increased which has positively contributed to changing the lives of the local people, but also enhances the pressure on the already tensed water supply situation.

In order to overcome this issue, plenty of solutions have been applied to address water scarcity in the dry season, but this is not effective or sustainable due to high costs, easy damage, and easily polluted water sources. Therefore, adapted water supply strategies such as the KaWaTech project model has developed and implemented to meet the increasing water demand. However, these areas belong to the small catchment which is located in the northeastern part of the geopark and consist of favorable geological conditions for groundwater availability. Meanwhile, the karst plateau south of Dong Van town is still facing serious water scarcity. In this context, studying and understanding the processes that take place in the Dong Van karst systems is a key basis for developing adequate solutions for the protection, management and sustainable use.

Extensive field studies combined with analysis of the huge cave survey database was carried out and resulted in a karstification model which is presented in Chapter 2 of this thesis. Accordingly, the cave classification based on the cave conduit's geometric parameters indicated that the karst evolution in Dong Van Karst Plateau is in a youthful stage, with cave systems developed mainly of the isometric

form (developed almost vertically) in the vadose zone, and not yet deepened to the local base level. The development of horizontal cave passages is related to two levels of planation surfaces at 1000-1250 and 1250-1450 masl. Meanwhile, at an altitude of 240 masl, the Na Luong cave which belongs to the Na De spring system could be the local base level for karst erosion. Additionally, cave passage orientation shows that the cave system formed and developed under the influence of tectonic activities in the Cenozoic.

The second study of this thesis (Chapter 3) focuses on the approach of using concentrations of major ions, trace and rare earth elements to clarify chemical signatures, and the ability for connections among sampling areas in the study area. To this end, a combination of different methods was applied, including mapping, hydrochemical analyses, using trace elements as the natural tracers, and multivariate statistical. It results in a basic hydrogeologic conceptual model for the Dong Van karst aquifer system. Accordingly, the Na De spring system and Na Luong cave are identified as belonging to the same discharge zone of Bac Son Carboniferous karst aquifer, while the southwestern springs and Tia Sang cave were identified as typical of shallow groundwater movement in the weathered surface zone in non-karst formations. In addition, it is possible to show a connection between the mining area and Na Luong cave by the abnormally high arsenic concentrations combined with location and geologic data. Meanwhile, Hang Rong cave has the features of a carbonate reservoir that developed in Triassic siliceous limestones of the Hong Ngai Formation, but is mainly associated with the Bac Son karst aquifer. Notwithstanding the significant differences in the water-chemistry signatures, the commonalities in REE distribution patterns between Tia Sang cave and the Na De spring system, combined with geologic data, lead to speculation that it could be one of the recharge sources of the Na De discharge zone.

The results presented in this thesis have essentially clarified the development of karst and caves, as well as the hydrogeochemical processes and connectivity ability of karst aquifers on the Dong Van Karst Plateau. Although there are still some incompletions, the results obtained are rather positive, which provides the basis for future detailed hydrogeologic studies in this area.

KURZFASSUNG

Karstgebiete werden insbesondere aufgrund ihrer landschaftlichen, touristischen und kulturellen Aspekte geschätzt und bieten zudem eine Vielzahl an natürlichen Ressourcen wie Trinkwasser und ökologischer Vielfalt. In vielen Ländern und Regionen der Welt haben Karstaquifere für die Trinkwasserversorgung und Bewässerung eine hohe Bedeutung. In tropischen und subtropischen Gebieten, wie z. B. in Südostasien, haben die besonderen klimatischen Bedingungen mit ausgeprägten Trocken- und Regenzeiten tropische Karstlandschaften geformt, die eine große Herausforderung für die Trinkwasserversorgung darstellen. Im Norden von Vietnam, auf dem Hochplateau der Provinz Ha Giang, führen hohe saisonale Schwankungen der Niederschläge trotz hohen Oberflächenabflüssen zu saisonaler Wasserknappheit. Im Jahr 2010 wurde das Dong Van Karst Plateau zum UNESCO Global Geopark ernannt. Seitdem ist die wirtschaftliche Bedeutung der Region gestiegen und die Zahl der Touristen hat stark zugenommen. Dies hat auf der einen Seite zu einer deutlichen Aufwertung der Lebensqualität der einheimischen Bevölkerung geführt, andererseits aber auch den Druck auf die bereits eh schon angespannte Wasserversorgung erhöht.

Um diesem Problem entgegenzutreten, wurden zahlreiche Idee zur Verbesserung dieser Situation umgesetzt. Aufgrund der damit verbundenen hohen Kosten, Vandalismus und den vulnerablen Wasserressourcen waren diese Ansätze alleine jedoch nicht nachhaltig. Um den immer weiter steigenden Bedarf an Trinkwasser langfristig decken zu können, wurden im Rahmen des Verbundprojektes KaWaTech mehrere Strategien für die Wasserversorgung entwickelt und implementiert. Dieses Einzugsgebiet im nordöstlichen Teil des Geoparks zeichnet sich durch eine vergleichsweise hohe Verfügbarkeit von Grundwasser und eine besondere geologische Situation aus. Auf dem Karstplateau südlich der Stadt Dong Van hingegen herrscht nach wie vor große Wasserknappheit. In diesem Zusammenhang sind die durchgeführten Untersuchungen sowie das Verständnis der Prozesse im Karstsystem von Dong Van eine wichtige Grundlage für die Entwicklung angepasster Schutzkonzepte und ermöglichen eine nachhaltigere Bewirtschaftung der Karstwasserressourcen.

Im zweiten Kapitel dieser Arbeit wird ein Karstmodell der Region vorgestellt, das auf umfangreichen Geländeuntersuchungen und Datensätzen von Höhlenvermessungen basiert. Der Vergleich der geometrischen Daten der Höhlensysteme zeigt, dass sich das Karstsystem des Dong Van Karst Plateaus noch in einem frühen Entwicklungsstadium befindet. Die Höhlen verlaufen größtenteils in

isometrischen Formen (nahezu vertikal), haben sich in vadosen Zonen entwickelt, aber sind noch nicht bis zur lokalen Basis des Karstsystems erodiert. Die Entwicklung dieser horizontalen Höhlengänge steht im direkten Zusammenhang mit zwei Niveaus von Erosionsflächen auf 1000-1250 m ü. NN und 1250-1450 m ü. NN. Die Na Luong-Höhle, welche Teil des Na De-Quellsystem ist, könnte die lokale Basis auf einer Höhe von 240 m ü. NN bilden. Die Orientierung der Höhlensysteme zeigt, dass diese unter dem Einfluss der tektonischen Aktivitäten im Känozoikum entstanden sind.

Im dritten Kapitel der Arbeit werden die Konzentrationen der Hauptionen, Spurenelemente und Seltenen Erden eingesetzt, um chemische Signaturen in Wasserproben zu bestimmen. Basierend auf diesen Daten werden hydraulische Verbindungen einzelner Teilgebiete im gesamten Untersuchungsgebiet ermittelt. Hierfür wurde das Untersuchungsgebiet kartiert, hydrochemische Analysen durchgeführt, Spurenelemente als natürliche Tracer verwendet und multivariante Statistiken mit den Analysedaten gerechnet. Das Ergebnis ist ein konzeptionelles hydrogeologisches Modell für das Dong Van Karst-System. Demnach entwässern das Na De-Quellsystem und die Na Luong-Höhle den Bac Son-Karstaquifers, während die Quellen im Südwesten des Untersuchungsgebietes sowie die Tia Sang-Höhle typische Signaturen für oberflächennahen Grundwasserabfluss in verwitterten Nicht-Karst-Formationen zeigen. Darüber hinaus belegen ungewöhnlich hohe Arsenkonzentrationen in Kombination mit geologischen Daten eine hydraulische Verbindung zwischen dem Bergbauggebiet im Untersuchungsgebiet und der Na Luong-Höhle. Die Hang Rong-Höhle hingegen weist die Charakteristik eines karbonatischen Reservoirs auf, das sich in den triassischen Kieselkalken der Hong Ngai-Formation entwickelt hat, aber hauptsächlich mit dem Karst-Aquifer der Bac Son-Formation verbunden ist. Trotz der signifikanten Unterschiede in den hydrochemischen Signaturen, lassen die Gemeinsamkeiten in den REE-Spektren zwischen der Tia Sang-Höhle und dem Na De-Quellsystem in Verbindung mit den geologischen Daten die Vermutung zu, dass die Tia Sang-Höhle im Einzugsgebiet der Na De-Abflusszone liegt.

Die in dieser Arbeit vorgestellten Ergebnisse tragen wesentlich zu einem besseren Verständnis zwischen Karststrukturen und hydrogeochemischen Prozessen bei. Hydraulische Verbindungen des Grundwassers im Dong Van Karst Plateau konnten aufgezeigt werden. Wenngleich nicht alle Prozesse im Rahmen der Arbeit vollständig aufgelöst werden konnten, bilden die Ergebnisse dieser Arbeit die Grundlage für weitere hydrogeologische Untersuchungen.

Acknowledgments

This work would not have been possible without the support of all the people who helped me in various ways, and I am grateful to everyone who has accompanied me along this journey.

First and foremost, I would like to thank my supervisors: I give my special thanks to my supervisor, Prof. Nico Goldscheider, who gave me the opportunity to work in this very exciting field of karst and karst hydrogeology. His support and confidence in me also boost my courage to take risks and try new approaches from which I have improved so much in my academic knowledge. To Prof. Thomas Neumann, I am grateful for his willingness to act as external supervisor.

I am also thankful to Prof. Franz Nestmann, Assoc. Prof. Tran Tan Van, Dr. Peter Oberle for their great support and successful coordination of the KaWaTech and KaWaTech Solutions projects.

I would also like to thank the members of my PhD Commission for their support: Prof. Nico Goldscheider, Prof. Thomas Neumann, Prof. Franz Nestmann, Prof. Philipp Blum and PD Dr. Ulf Mohrlök.

Furthermore, I would like to express my sincere gratitude to the Catholic Academic Exchange Service (KAAD) and the Graduate School of the Centre for Climate and Environment (GRACE) for the financial support. Special thanks go to the Heads of the Asian Department Dr. Heinrich Geiger and Dr. Esther-Maria Guggenmos and the Asian Department assistant Ms. Karin Bialas for their support in many ways. The German Federal Ministry of Education and Research (BMBF) is acknowledged for funding the KaWaTech Project [grant number [02WCL1291A](#)] and the KaWaTech Solutions Project [grant number [02WCL1415](#)].

I want to thank Dr. Nadine Goeppert for her scientific support and her help during the past years. Her suggestions are very helpful and important for me to complete my studies.

Thank you, Prof. Dr. Arthur N. Palmer for his valuable comments on karst and cave knowledge, fruitful discussions and language editing support.

I gratefully acknowledge the colleagues at the VIGMR, as well as the member of SPEKUL for their support during the field trips, discussions, and provision of cave databases. Special thanks are given to David Lagrou, Ho Tien Chung, Doan The Anh, Nguyen Van Dong, Nguyen Cao Cuong, Nguyen Manh Tuan, and Trinh Thi Thuy.

Sincere thank goes to Dominik Richter, a colleague as well as a great friend. Step by step I was going through the very difficult beginning phase thanks to his big support. I really enjoyed conversations, hiking, and cycling with him.

In addition, I want to thank the laboratory team Daniela Blank, Chris Buschhaus, and Christine Roske-Stegemann for their support and the enjoyable collaboration.

I would also like to thank Simon Frank, Nikolai Fahrmeier, Adreas Wunsch, Yanina Müller, Tanja Liesch, Marc Ohmer, Fan Xinyang, Alexander Kaltenbrunn, and all other colleagues in the Hydrogeology and Engineering Geology Departments for the good working atmosphere and support in the last years.

Thank you my Vietnamese friends Vu Huu Long, Trinh Cong Dan, Tran Viet Hoan, Pham Cam Van, Vu Hoang Thai Duong, Tran Anh Duc and Vu Tuan Dung for sharing and helping me have a memorable time in Germany. I hope we would have successful cooperation in the near future.

Finally, I thank my whole family for supporting me all time. Special thanks to my dear wife Tran Khanh Tho, who always supported, encouraged and motivated me to carry out my research. Thanks to my children Anh Vu and Khanh Linh for being my great motivation.

Table of contents

Abstract.....	III
Acknowledgments	VII
List of figures	XII
List of tables and appendixes.....	XVII
List of abbreviations	XVIII
1 Introduction	1
1.1 Karst worldwide in tropical-subtropical regions and in Vietnam	1
1.1.1 Karst distribution over the world and in Southeast Asia	1
1.1.2 Karst in Vietnam	2
1.2 Introduction to the Dong Van Karst Plateau Geopark.....	5
1.2.1 Geography.....	5
1.2.1.1 <i>Location and topography</i>	5
1.2.1.2 <i>Weather and climate</i>	7
1.2.1.3 <i>Social and economic conditions</i>	7
1.2.2 Karst research.....	8
1.2.3 Water resources management.....	10
1.2.4 The KaWaTech project	13
1.3 Objectives and approaches of the thesis.....	15
1.3.1 Objectives.....	15
1.3.2 Approaches.....	15
1.4 Structure of the thesis.....	18
2 Karst and cave development	19
2.1 Introduction.....	20
2.2 Overview of the study area.....	22
2.2.1 Geological setting.....	23
2.2.2 Planation surfaces.....	25

2.2.3	Cave systems.....	27
2.3	Data and Methodology.....	28
2.3.1	Cave database.....	28
2.3.2	Methodology.....	29
2.4	Results and Discussion.....	32
2.4.1	Results.....	32
2.4.1.1	<i>Cave classification based on speleomorphologic features of cave conduits.....</i>	<i>32</i>
2.4.1.2	<i>Cave levels, speleomorphologic features and cave passage in different cave groups.....</i>	<i>33</i>
2.4.2	Discussion.....	40
2.4.2.1	<i>Cave passage orientation in relationship to the geological structure and tectonic periods.....</i>	<i>40</i>
2.4.2.2	<i>Relationship between cave levels and planation surfaces on Dong Van Karst Plateau.....</i>	<i>41</i>
2.5	Conclusions.....	43
3	Hydrogeology and Hydrogeochemical processes.....	49
3.1	Introduction.....	50
3.2	Study site.....	52
3.2.1	Geological and hydrogeological settings.....	52
3.2.2	Climatic features.....	53
3.3	Materials and Methods.....	54
3.3.1	Sampling campaigns and sampling sites.....	54
3.3.2	Measurements and analysis.....	55
3.3.3	Methods.....	56
3.3.3.1	<i>Presentation of hydrochemical data.....</i>	<i>56</i>
3.3.3.2	<i>Multivariate statistical analysis.....</i>	<i>57</i>
3.3.3.3	<i>Normalization and calculation of REE patterns.....</i>	<i>57</i>
3.4	Results.....	59
3.4.1	Physicochemical characteristics.....	59
3.4.2	Water-rock interaction.....	61
3.4.3	Hierarchical Cluster Analysis.....	62
3.4.4	Presentation and interpretation of REE data.....	65

3.5	Discussions	67
3.5.1	Evaluation of clustering results	67
3.5.2	Using the concentration of trace elements as a natural tracer	68
3.5.3	Estimated water balance.....	71
3.6	Conclusions	72
4	Recommendations for sustainable water resources management and future research	75
4.1	Appropriate strategies for sustainable water resources management.....	75
4.2	Outlook for future research	77
5	Conclusions	83
	Declaration of authorship	86
	References	87

List of figures

Fig. 1-1	Map of the global distribution of karstifiable carbonate and evaporite rocks based on the World Karst Aquifer Map (WOKAM, Chen et al. 2017, Goldscheider et al. 2020).	2
Fig. 1-2	Map of the investigation area; a) Map of distribution of limestone in Viet Nam (modified after Van et al. 2004) and location of Ha Giang province; b) Location of Dong Van Karst Plateau UNESCO Global Geopark in the province Ha Giang; c) Map of the study site in the DVKG on top of a DEM.....	3
Fig. 1-3	Sub-tropical karst landscapes in Vietnam: a) Son Doong Cave-the largest natural cave in the world (Photo: Quang Binh Department of Tourism); b) Mature karst topography and old karst in the Non Nuoc Cao Bang UNESCO Global Geopark (Photo: Hachi8Media); c) Karst landscape in Tam Coc, Ninh Binh (Photo: www.vnexpress.net); d) Inundated karst landscape in Ha Long Bay.	5
Fig. 1-4	Karst landscape at area of Sa Phin commune - A part of DVKG.....	6
Fig. 1-5	Average precipitation and air temperature at the climate station Dong Van District in the period 2015–2020 (Operated by NCHMF).....	7
Fig. 1-6	a) Sa Phin A “hanging pool” cannot store rainwater for the dry season due to cracks in the bottom; b) Anthropogenic inputs affects the water quality of Seo Lung A hanging pool, Sang Tung commune (Photo: HGDONRE).....	12
Fig. 1-7	a) Schematic illustration of the main components of the Seo Ho High-Pressure Plant that was planned and built within the KaWaTech project. (Modified after Oberle et al. 2017); b) The new water pumping system (PAT) installed in Seo Ho hydro-power plant.....	14
Fig. 1-8	Idealized cross-section of a karst system with a vertical spatial zonation of karst, and plan views of associated cave patterns. (Modified after Palmer 1991; Audra and Palmer 2013; and Jouves et al. 2017).....	16
Fig. 1-9	Block diagram illustrating the conceptual model of a karst aquifer (Goldscheider & Drew 2007).....	17

Fig. 2- 1	Map of the investigation area. a) Location map of Northern Vietnam illustrating the physiographic impact of the collision between the Indian and Eurasian plates; b) Location of Dong Van Karst Plateau in the Northern Vietnam and South China karst belt (based on the World Karst Aquifer Map, Goldscheider et al. 2020); c) Location map of the main study area shows the distribution of cave entrances, planation/pediment surfaces, and river terraces remnants at different altitudes on top of a DEM (After Tuy in Van et al. 2010). 21	21
Fig. 2-2	Geological setting of the study area. a) Study area position in the main structural zone in NE Vietnam (After Tri et al. 2009) (Legend: 1-Viet Bac fold system; 2-Dong Bac fold system; 3-Mesozoic riftogenous superimposed depression; 4-Neogene-Quaternary basin; 5-Accurate fault zone; 6-Supposed fault zone; 7-Capital position; 8-DVKP UGG boundary); b) Geological map (After Tinh et al. 1976; Updated by KaWaTech project); c) Lithostratigraphic profile. 24	24
Fig. 2-3	Photos showing the karst landscape and important geological structures in the study area; a) Ma Le stream fault zone; b) Overthrust fault zone North Dong Van; c) Nho Que River fault zone, d) Na De - Meo Vac fault zone; e) Lung Tao - Tu San fault zone; f) Pho Bang - Khau Vai fault zone..... 25	25
Fig. 2-4	Distribution of low gradient surfaces related to planation surfaces as revealed from topographic cross-sections in Dong Van Karst Plateau..... 27	27
Fig. 2-5	Geometric parameters computation. (a) The vertical index V on a 3D cave sample. Different color lines represent the different cave branch curvilinear length (L_i); (b) Sketch of a karst sample divided into three branches. The curvilinear length L_j and the Euclidian length D_j can be computed along each branch j . Then, the tortuosity of each branch is calculated; (c) Processing of width-height ratio for a cave survey station i : ① In-situ measurement of width ($W_i = W_l + W_r$) and height ($H_i = H_u + H_d$) at survey station i ; ② WH-ratio WH_i calculated from the in-situ measurement for an idealized shape of karst	

conduit; **(d)** Curvature parameter computation: ① Possibilities of curvature values computed at an intersection node P_i ; ② The curvature at a point P of a curve C , where the point O is the origin of the curvilinear abscissa s . The parameter k is the curvature vector and t designates the tangent vector at P . The value r is the radius of the osculating circle at P . (Modified from Jouves et al. 2017). 30

Fig. 2-6 An example to illustrate the cave passages orientation analysis. **(a)** The grid displaying general cave passage azimuths is constructed based on Hang Ong cave map on the geological background; **(b)** Rose diagram of cave passage orientations (number %, 10° classes)..... 32

Fig. 2-7 Graph showing the distribution of geometric parameters (WH, T, K, V) and classification for the 49 cave conduit systems in Dong Van Karst Plateau..... 33

Fig. 2-8 Elevation distribution of horizontal cave passages and cave class division. 35

Fig. 2-9 Graph showing the distribution of geometric parameters (WH, T, K, V) in different cave levels and local structural blocks. 37

Fig. 2-10 Rose diagrams display (a) the cave passage orientation in different cave groups and (b) the overall cave passages orientation in the study area..... 39

Fig. 2-11 Cross-sections (in Fig. 2-1) showing the development and structure of cave systems and the karstification features on Dong Van Karst Plateau..... 43

Fig. 3-1 Map of the investigation area; **a)** Location of Dong Van karst plateau in Vietnam and South China karst belt (based on the World Karst Aquifer Map, Goldscheider et al. 2020); **b)** Map of sampling sites on top of geological map of the study area (After Tinh et al. 1976; Updated by KaWaTech project); **c)** Map of distribution of individual springs belonging to the Na De spring system superposed on a satellite image (Source: Google Earth). 51

Fig. 3-2 Photos showing different sampling areas in the study area; **a)** Na De valley is located on the boundary between the Bac Son Fm. (C-Pbs) and Song Hien Fm. (T₁sh) (Photo: David

	Lagrou); b) Discharge area of the underground stream at the entrance of Na Luong cave (NLC) during the rainy season; c) BM1 spring is the main spring of Na De spring system during the dry season; d) Sampling point in the Hang Rong cave (HRC); e) A part of the mining area is located northwest of the Na De spring system; f) The hanging pool stores wastewater that is reused for the ore extraction process in the mining area.....	55
Fig. 3-3	Gibbs diagrams are used to explain the predominant processes of water hydrochemistry in the study area: (a) for cations; (b) for anions.	60
Fig. 3-4	Plots showing the ratios between the major ions of water samples in study area: (a) SO_4^{2-} vs. Ca^{2+} ; (b) $(\text{Ca}^{2+} + \text{Mg}^{2+})$ vs. HCO_3^- ; (c) Mg^{2+} vs. Ca^{2+} ; (d) $(\text{Ca}^{2+}/\text{Mg}^{2+})$ vs. Ca^{2+}	62
Fig. 3-5	Dendrograms classifying the groundwater samples according to physical-chemical composition. (a) dry season (upper display); (b) rainy season (lower display).....	63
Fig. 3-6	REE abundances in waters normalized to the PAAS standard (Post Archean Australian Shales; Taylor and McLennan 1985) and divided into the samples collected during the dry season in March 2020 (a, c) and wet season in June 2020 (b, d) . Panels (a) and (b) show all measured water data without adjustment, while panels (c) and (d) show the mean concentration of each group as well as each cave to emphasize the features in terms of their pattern slope, concentrations, and variations in primary water anomalies (Ce, Eu). Water samples were collected from the Na De spring system (NDSS; orange filled squares); from caves (Caves; blue-filled circles); in the southwest of DVKP (SW springs; green-filled triangles); and at the mining area (red-filled inverted triangles).....	65
Fig. 3-7	Conceptual model of the Dong Van karst aquifer system: a) Cross-section displays the distribution and ability of association between sampling areas based on physicochemical parameters and trace elements in water; b) Profile showing the structure of Hang Rong Cave; c) Simple conceptual model of Na De karst spring system.	70
Fig. 4- 1	ALLOWS input data (© van Afferden et al. 2015).....	77
Fig. 4- 2	Model structures applied for modeling karst spring discharge based on gridded meteorological input data. (Modified from Wunsch et al. 2022)	79

Fig. 4- 3 Map of expected ground-based rain gauge network and potential trace inject points. ... 80

Fig. 4- 4 a) Plan of the expected installation location for hydrological monitoring stations of Na De discharge zone; b) View of mainstream and NLC discharge flow from HMS1 expected site; c) An example of a hydrological monitoring station model. (Source: World Bank 2018)..... 81

List of tables and appendixes

Tables

Table 1-1 Major parameters of the main river basins in the part of Viet Nam flowing through the DVKG (Ha Giang Department of Natural Resources and Environment – HGDONRE, 2021).....	10
Table 1-2 Statistics on population, number of tourists, water use demand and capacity to produce and supply clean water on DVKG for the period 2015-2020 (Source: Ha Giang Statistical Office 2021; DVKG annual report 2020; HGDONRE 2021)	11
Table 2-1 Cave passage morphometry	30
Table 3-1 Descriptive statistics of the major physicochemical parameters of water samples in the study area.....	59
Table 3-2 Mean chemical values for seasonal groups distinguished by hierarchical cluster analysis.	64
Table 3-3 Elements for calculating the water balance on the Dong Van karst plateau.	71

Appendixes

Appendix 2-1 Summary of cave survey data and cave conduits geometric parameters in Dong Van Karst Plateau.....	46
Appendix 2-2 Summary of the statistics of horizontal cave-passage length in the Dong Van Karst Plateau	48
Appendix 3-1 REE concentration (ng/L) and REE distribution pattern parameters of water samples in the DVKP	74

List of abbreviations

DVKG	Dong Van Karst Plateau UNESCO Global Geopark (takes up most of the area of four districts namely Dong Van, Meo Vac, Quan Ba, and Yen Minh)
DVKP	Dong Van Karst Plateau: The karst plateau located at southern of Dong Van town (composing most of the area of Dong Van and Meo Vac districts)
KaWaTech project	The Vietnamese-German Cooperation Project for the Development of sustainable Technologies for Karst Water Management
KaWaTech Solutions project	The Vietnamese-German Cooperation Project for the Development of Karst Water Technologies and Sustainable Groundwater Protection (Joint project)
SPEKUL	Speleoclub of the Catholic University of Leuven
VIGMR	Vietnam Institute of Geosciences and Mineral Resources
HGDONRE	Ha Giang Department of Natural Resources and Environment
NCHMF	Vietnam National Centre for Hydro-Meteorological Forecasting
PAT	Pump as turbine
BMBF	Federal Ministry of Education and Research (<i>Bundesministerium für Bildung und Forschung</i>)
VB	Vadose branchwork cave
WTC	Water-table cave
LC	Looping cave
AM	Angular mazes cave
MC	Mixed cave
DEM	Digital elevation models
SB	Structural Block
CL	Cave class
masl	Meters Above Sea Level
HCA	Hierarchical Cluster Analysis
REE	Rare-Earth Elements
NDSS	Na De spring system
SW springs	Springs appear in the southwestern part of Dong Van Karst Plateau
NLC	Na Luong cave
HRC	Hang Rong cave
TSC	Tia Sang cave

AGW	Institute of Applied Geosciences
PAAS	Post Archean Australian Shales
TDS	Total Dissolved Solids
EC	Electric Conductivity
WHO	World Health Organization
IWRM project	Integrated Water Resource Management project
HMS	Hydrological monitoring station
SMART-IWRM project	Sustainable Management of Available Water Resources with Innovative Technologies - Integrated Water Resources Management in the Lower Jordan Rift Valley project
ALLOWS	Assessment of Local Lowest-Cost Wastewater Solutions
GIS	Geographic information system
NGOs	Non-governmental organizations

Chapter 1

1 Introduction

1.1 Karst worldwide in tropical-subtropical regions and in Vietnam

1.1.1 Karst distribution over the world and in Southeast Asia

Karst is a special type of landscape formed by the dissolution of soluble rocks (e.g., limestone, dolomite, and gypsum) combined with processes of corrosion, subsidence, and/or collapse, that is characterized by the presence of distinctive hydrological and morphological features (Ford & Williams 2007). Karst regions are not only valuable in terms of landscape, tourism, and culture but also offer a variety of natural resources such as freshwater and biodiversity. A study by Goldscheider et al. 2020 highlighted that 15.2% of the global ice-free continental surface is characterized by the presence of karstifiable carbonate rock (Fig. 1-1), while the population living on karst areas is estimated at 1.3 billion people. Groundwater from karst aquifers is the major freshwater source for drinking-water supply and agricultural irrigation in many countries and regions throughout the world. As mentioned by Ford & Williams 2007, about 25% of the global population is partly or entirely supplied by freshwater from karst aquifers, while an updated result by Stevanovic 2020 shows that the number of karst water consumers is estimated at 678 million, or 9.2% of the world's population. Not only that, most large springs on earth are karst springs, which are the water supply of many big cities, such as Vienna, Rome, and San Antonio (Kresic & Stevanović 2010). These results show the global importance of karst areas, karst aquifers as well as further research on issues related to this topic for orientation of residential planning and sustainable groundwater resources management.

Karst is widely distributed in Asia with an absolute area is 8.35 million km², which is corresponding to 18.6% of land surface (Chen et al. 2017; Goldscheider et al. 2020). Whereas in Southeast Asia, about 10% of the total land surface is characterized by karst, which occurs mainly in Lao PDR, Thailand, Vietnam, Indonesia, Philippines, Myanmar, and Malaysia. Karst in Southeast Asia belongs to the humid tropical karst type, which is mainly developed on Permian and Carboniferous carbonate rocks. In addition, in this area, karst can be also found in carbonate of the Ordovician, Silurian, Devonian, and Triassic ages (Tuyet 1998, Day 2011, Jiang et al. 2021). Due to the strong development, the karstlands of Southeast Asia are diverse, reflecting the influence of geology, uplift history, geomorphological processes, and climates (Gillieson 2005).

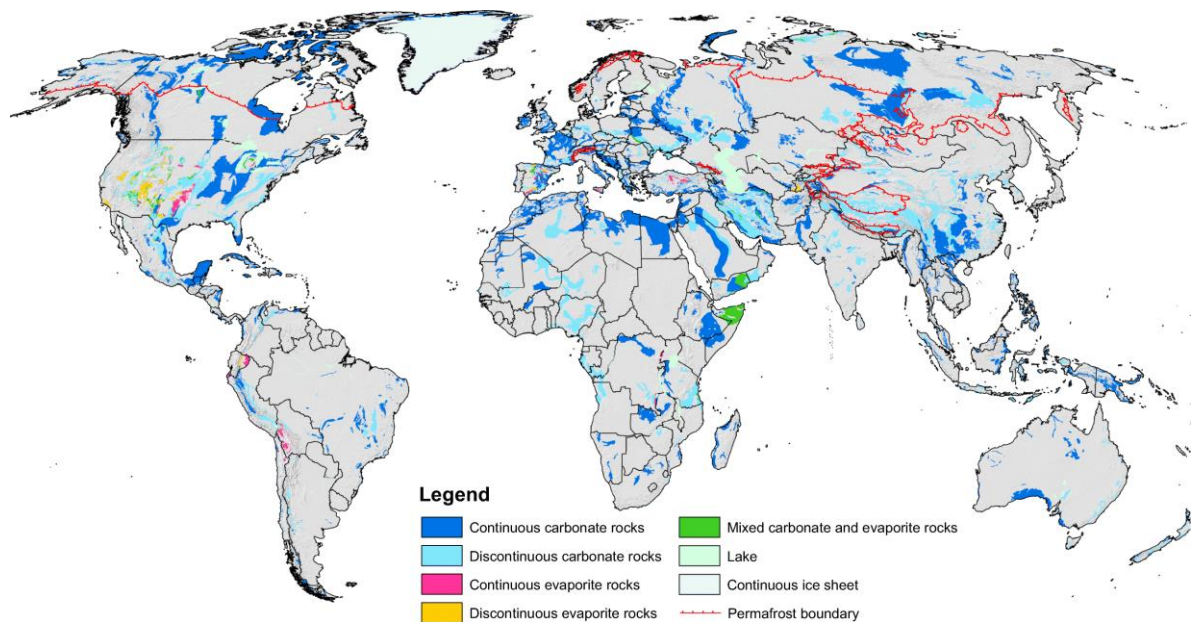


Fig. 1-1 Map of the global distribution of karstifiable carbonate and evaporite rocks based on the World Karst Aquifer Map (WOKAM, Chen et al. 2017, Goldscheider et al. 2020).

1.1.2 Karst in Vietnam

In Vietnam, as pointed out by Tuyet 2001, Van et al. 2004, limestone account for nearly 18% (about 60,000 km²) of the total area, mostly in the northern provinces (Fig. 1-2a), while an updated result by Goldscheider et al. 2020 shows that carbonate rocks cover an area of 90,000 km² (occupying 27.2% of the total area) (Fig. 1-1). Geologically, widespread carbonate rocks have been deposited from the Pre-

Cambrian up to the Middle-Triassic, of which, the dominant karst-forming rock are the Carboniferous-Permian and the Middle Triassic formations (Fig. 1-2a).

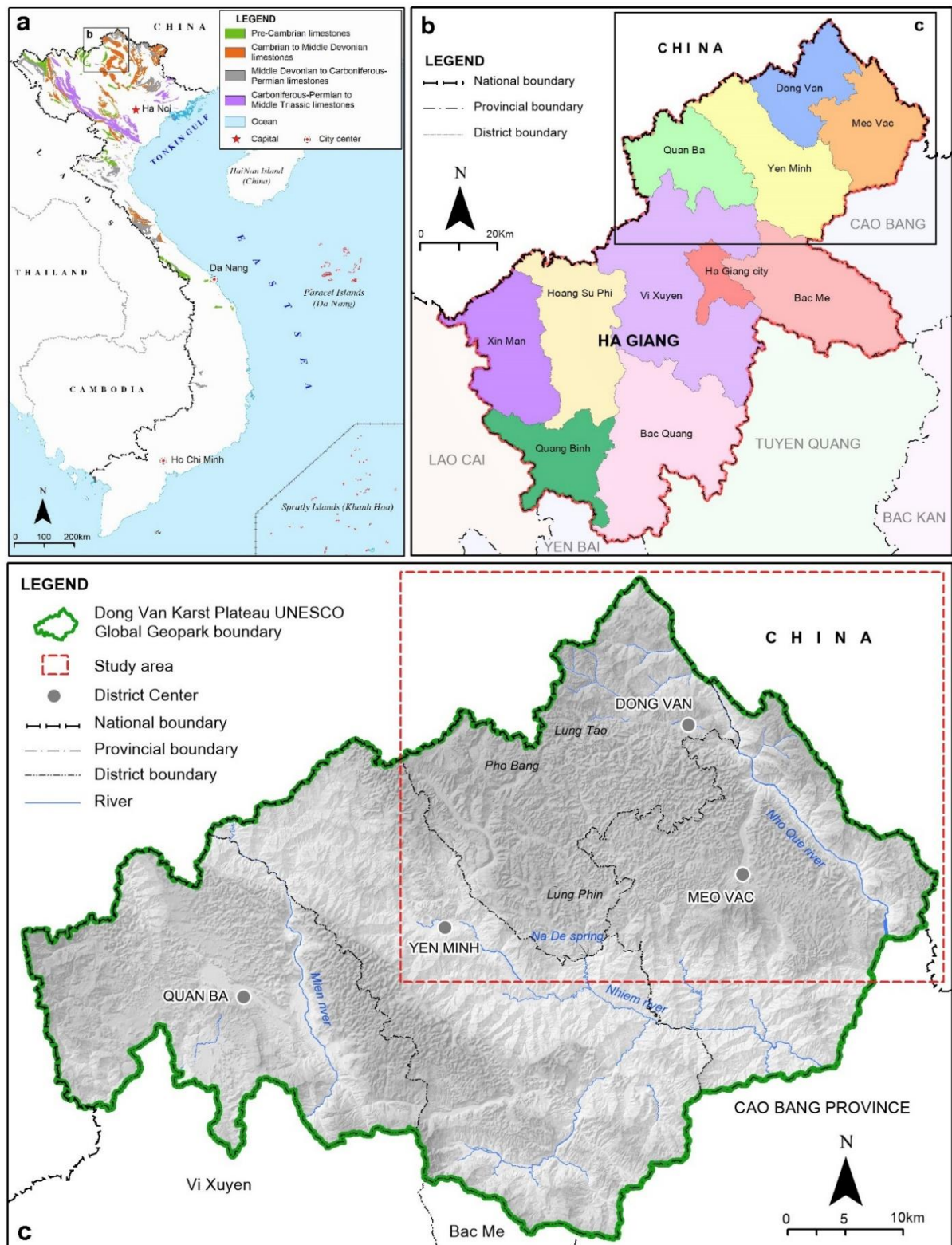


Fig. 1-2 Map of the investigation area; **a)** Map of distribution of limestone in Viet Nam (modified after Van et al. 2004) and location of Ha Giang province; **b)** Location of Dong Van Karst Plateau UNESCO Global Geopark in the province Ha Giang; **c)** Map of the study site in the DVKG on top of a DEM.

Carbonate rocks are present in all climatic zones, and the type and degree of karst development are the results of a long and complex geologic, geomorphologic and climatic history (Ford & Williams 2007). The karst regions of Vietnam are part of the tropical global karst belt, which is closely related to the South China tropical-subtropical karst and humid tropical karst of Southeast Asia (Tuyet et al. 2004). Several previous studies (Khang 1985, Van et al. 2010, Hai et al. 2013) have shown that karst in Vietnam formed and developed depending mainly on the structure and lithological properties of carbonate rocks, folding, tectonic movements combined with geomorphologic processes, and the position of ground-water levels. These factors combined with geographic location and climate features have created numerous typical tropical karst landforms such as karren, dolines, tower karst, cone karst, interior-draining valleys (poljes), pocket valleys, karst canyon, peak cluster-depression landscapes with deep dolines and closed valleys, cave systems are large in dimension and complex in structure, etc.

The Neotectonic movement created a rather diverse topographic structure in Vietnam, where the terrain surface descends from the northwest (mountainous area) to the southeast (coastal area), resulting in many special karst regions such as Ha Long Bay (Fig. 1-3c), Trang An Landscape Complex (typical examples of inundated karst landscape), the Cuc Phuong - Pu Luong Nature Park, the Phong Nha - Ke Bang National Park (with the largest natural cave in the world - the Son Doong Cave) (Fig. 1-3a) and the Dong Van Karst Plateau, Non Nuoc Cao Bang UNESCO Global Geoparks (Fig. 1-3b).

One of the outstanding features of Vietnam's humid tropical karst is its high biodiversity, which is rich in genera and species with many endemic species. Besides, karst aquifers are widely distributed in these areas, which provide domestic and irrigation water sources for most residential communities in the Northern and Central mountainous regions of Vietnam. However, these are the areas with the highest poverty rate in the country (13.4%) (published data from the General Statistics Office of Vietnam 2021), and residents are mainly ethnic minorities who have been living in remote areas under substandard conditions. The main reason for the low living standards of these people, besides living in rugged, remote terrain, is the shortage of fresh water for household use and production, as the topsoil layer is rarely conserved in karst areas and surface streams are usually short and dry up soon after the rainy season, most of them sink underground at the sinkholes.



Fig. 1-3 Sub-tropical karst landscapes in Vietnam: **a)** Son Doong Cave-the largest natural cave in the world (Photo: Quang Binh Department of Tourism); **b)** Mature karst topography and old karst in the Non Nuoc Cao Bang UNESCO Global Geopark (Photo: Hachi8Media); **c)** Karst landscape in Tam Coc, Ninh Binh (Photo: www.vnexpress.net); **d)** Inundated karst landscape in Ha Long Bay.

Recently, the rapid population growth and increasingly heated economy in Vietnam have been conducting more and more severe damage to the karst environment due to the consequence of deforestation and industrial pollution. Therefore, it is necessary to have a plan for conservation and sustainable development in the karst regions based on close collaboration between government, organizations, and local communities, on the basis of an integrated, multi-sectoral approach as well as comprehensive and detailed knowledge of the karst systems.

1.2 Introduction to the Dong Van Karst Plateau Geopark

1.2.1 Geography

1.2.1.1 Location and topography

Ha Giang is a mountainous province in the far north of Vietnam, covering an area of 7,929.48 km², which is 320 km away from Hanoi by Highway 2. Ha Giang shares a 270 km long border with Yunnan province (China) in the north, Cao Bang in the east, Lao Cai in the west, Yen Bai in the south, and

Tuyen Quang in the southeast. The administrative units include Ha Giang city and 10 rural districts of Bac Me, Bac Quang, Dong Van, Hoang Xu Phi, Meo Vac, Quan Ba, Quang Binh, Vi Xuyen, Xin Man, and Yen Minh (Fig. 1-2b).

Dong Van Karst Plateau Geopark (DVKG) is located in the northeastern province of Ha Giang (Localisation N23°11'32" and E105°11'49"), which covers a total area of 2356 km². It takes up most of the area of four districts namely Dong Van, Meo Vac, Quan Ba, and Yen Minh. In 2010, DVKG was recognized as a member of the Global Geopark Network and subsequently became a UNESCO Global Geopark in 2015 (UNESCO, 2021).



Fig. 1-4 Karst landscape at area of Sa Phin commune - A part of DVKG.

The DVKG topography is strongly dissected, mainly covered by high mountain landforms in the NW-SE direction with steep slopes and most of its surface is carbonate rocks (about 60%) (Fig. 1-4). The average elevation within the geopark is 1400 to 1600 meters above sea level (masl) with the highest peak is Mount Mieu Vac (1971m) while the deepest point is about 200m in the southeast area. The DVKG in the SW-NE direction can be divided into three main parts: 1) The southwest karst plateau covering most of Quan Ba district; 2) The terrigenous rock band occupying most of the area of Yen Minh district; and 3) The northeast karst plateau composing most of the area of Dong Van and Meo Vac districts, which is the study area of this thesis (Fig. 1-2c).

1.2.1.2 Weather and climate

Northern Vietnam's climate is generally of the subtropical monsoon type (Khang 1985). However, the DVKG belongs to the high-altitude region with strongly dissected terrain, and thus the climate is characterized as a temperate zone (Van et al. 2010), and is divided into two seasons:

- A rainy season from May to October, when winter winds blowing from the East Sea bring more moisture and. The weather is hot and wet in Yen Minh valley, but still quite cool on the plateaus of Quan Ba and Dong Van - Meo Vac.
- A dry season from November to April, when the dry monsoon winds blow from the China mainland. The weather is temperate, but there are several cold days with the appearance of frost, hoarfrost or even snow in higher areas.

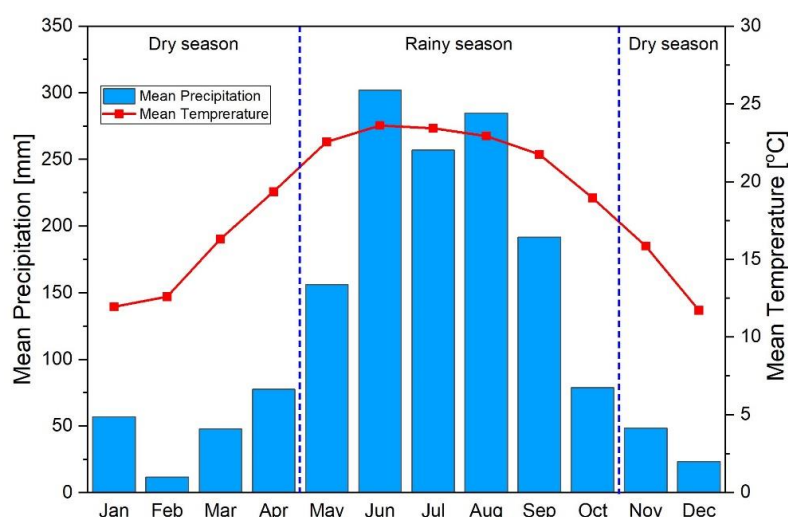


Fig. 1-5 Average precipitation and air temperature at the climate station Dong Van District in the period 2015–2020 (Operated by NCHMF).

According to the data in the period 2015–2020 at the climate station Dong Van District, operated by NCHMF, the annual average precipitation is 1537.25 mm, with the highest rainfall in June (302.2 mm average) and lowest in February (11.8 mm average). The annual average temperature is 18.4°C, with the highest reaching 23.6 °C in June and the lowest 11.7°C in December (Fig. 1-5).

1.2.1.3 Social and economic conditions

Ha Giang is among the few northern provinces with a high proportion of ethnic minorities who have low levels of education, and the economy is generally underdeveloped and mostly dependent on

government support. According to published data from the Ha Giang Statistical Office [2021](#), the total population of this province is 871,401 people, of which 87.7% belong to 22 ethnic minority groups: H'Mong 34.5%, Tay 22.4%, Dao 14.8%, Nung 9.5%, Giay 2.0%, La Chi 1.6%, etc. Covering about 30% of the total area of Ha Giang province, the DVKG is home to 326,446 people (as of 2020) belonging to 17 ethnic minority groups, about 71% of whom are H'Mong, besides ethnic groups of Dao, La Chi, Pu Peo, Lo Lo, Tay, Nung, etc. Together, they have created the unique, rich, and valuable cultural in this area.

In the period before 2010, the socio-economic life in geopark was quite poor and backward. Besides a small group who work on handicrafts and small-size businesses in the center of districts and/or communes, the local resident mainly produced subsistence agriculture on the steep slopes of limestone mountains or along the narrow river and stream valleys. Since 2010, when DVKG was established, regional economic development is gradually oriented to the tourism economy and highly supported by the local people. The effective promotional activities along with the landscape and culture values of this place have attracted many visitors. Accordingly, the number of visitors has steadily increased along with accompanying tourist services and products which have positively contributed to changing the lives of the local people and opened up favorable conditions to fight poverty in this area.

1.2.2 Karst research

The Dong Van Karst Plateau Geopark has been long time attractive to numerous geoscientists because it is probably the best place in Vietnam that can fullest represent the Earth's crust evolution history from the Paleozoic until the present (Van et al. [2010](#)). Previously, there were plenty of studies published in different geological fields in this area, including geological mapping at different scales (Dovjikov AE et al. [1965](#), Tinh et al. [1976](#)), paleontology - stratigraphy (Janvier & Phuong [1999](#); Phuong [2000](#), Truong et al. [2004](#), Huyen [2007](#)) and tectonics (Tri et al. [1977](#), Tri & Khuc [2009](#), Hai et al. [2013](#)). In addition, there were including studies on karst geomorphology by An and Bao ([2008](#)), Tuy in Van et al. ([2010](#)) that describe in detail the unique karst landscapes on DVKG compared to the South China karst features.

In addition, the DVKG is known as a notable karst region of Vietnam with strong development of cave systems, therefore this area is also a speleologists attraction. The first speleological expedition was organized in 2003 with the cooperation of Belgian (SPEKUL) and Vietnamese (VIGMR) experts. Up to date, many other expeditions have been performed with the purpose to improve the understanding of karstification and karst groundwater on the DVKG. According to the survey data, more than 135 caves were explored with a total of up to 39 km of cave passage mapped so far on this area (Masschelein et al. 2007, Bontridder et al. 2010, 2019).

Due to situated in a remote location, difficult access, lack of required equipment, limited financial resources, and complicated geological settings, thus in the previous periods, there are only a few studies have been carried out on karst water resources in the DVKG (Van et al. 2004, Tam & Batelaan 2011, Lam et al. 2013, Nhan et al. 2013, Thach et al. 2013) under the support by several projects funded by Vietnamese Government. In recent years, there have been some more detailed studies on karst water quality, artificial tracer tests, and hydrochemical and microbiological analyses (Ender et al. 2017, 2018a, 2018b, Richter et al. 2021, 2022) as the basis for groundwater protection, and establishing a hydrogeological, conceptual model for the Dong Van town and surrounding area within the framework of the Vietnamese-German Cooperation Project for the Development of sustainable Technologies for Karst Water Management (KaWaTech project). However, these updated studies mainly focus on a small karst catchment of DVKG in order to deliver a base to develop adapted and sustainable water management strategies.

It can be seen that the above studies have basically clarified the stratigraphic features and the tectonic and geomorphologic development processes on the DVKG, besides several results on hydrogeologic and caves. However, these studies are mostly on a small-scale or small catchment and are unlinked, therefore a systematic study based on updated results on stratigraphy, tectonics, geomorphologic, hydrogeologic, and speleologic is required for a better understanding of karst development and groundwater resources in the DVKG.

1.2.3 Water resources management

As a result of the strongly dissected terrain on the carbonate rocks with high porosity and infiltration rate, there are almost no or only short surface flows, which dry up soon after the rainy season (most sink underground). Therefore, on the DVKG, there are only three main rivers, namely Nho Que, Mien and Nhiem (a tributary of Nho Que river) rivers and other small streams such as Ma Le, Lung Man, Ban Thang (Fig. 1-2c).

Table 1-1 presents the annual discharge and total annual flow of some main rivers traversing DVKG. Although the total surface water discharge is high, the large variations in rainfall, as well as discharge between dry and wet seasons, result in seasonal water scarcity. In addition, due to culture and farming practices, local people are mostly living in high mountainous areas or in the district centers, however, these rivers are usually located at low altitudes and far from residential areas, making them difficult to use for domestic purposes.

Table 1-1 Major parameters of the main river basins in the part of Viet Nam flowing through the DVKG (Ha Giang Department of Natural Resources and Environment – HGDONRE, 2021)

River name	Total length (km)	Catchment area (km ²)	Annual discharge (m ³ /s)	Annual specific discharge (l/s/km ²)	Total annual flow (10 ⁶ m ³)
Nho Que	46	2010	85	15.8	233.5
Mien	60	792	23.1	23.2	727

On the other faces, as shown in Table 1-2, the total population of the DVKG in 2020 is 326,446 people, of which 89.9% of local people are living in rural areas which are sustaining themselves on agriculture, while 10.1% are living in urban places and profiting from commerce and tourism activities. At the current population level, the demand for water for domestic use is calculated at 20,247.5 m³/day (Applied water consumption of 60 litre per capita and day (lpcd) for rural areas, and 80 lpcd for urban areas, HGDONRE 2021) while the capacity to produce and supply clean water from the centers for rural water supply is only 504,400 m³/year (1382 m³/day) (Tab. 2). This is much less than the actual demand and can only be supplied to the urban population, and most rural residents cannot access clean water. In addition, the production value of agriculture and forestry in the total Ha Giang province in

2020 increased by 3.52% and 2.12% respectively compared to 2019 (Ha Giang Statistical Office 2021), while the number of tourists also increased steadily every year and boom in 2019 and 2020 with more than 1.4 and 1.5 million visitors respectively (GGN 2019, 2020). It can be seen that economic development leads to population growth in the region and, in combination with the high tourist numbers the pressure on domestic water has increased. The forecast of demand for domestic water in the DVKG by 2025 and 2030 as calculated will increase sharply, reaching 30,060 and 45,121 m³ per day, respectively (Prime Minister of Vietnam 2017, Ha Giang People's Council 2020, HGDONRE 2021; Ha Giang Department of Planning and Investment, 2021).

Table 1-2 Statistics on population, number of tourists, water use demand and capacity to produce and supply clean water on DVKG for the period 2015-2020 (Source: Ha Giang Statistical Office 2021; DVKG annual report 2020; HGDONRE 2021)

	Unit	2015	2017	2018	2019	2020
Population	people	291,033	303,070	308,911	320,450	326,446
Urban place population	people	27,066	28,098	28,774	32,704	33,035
Rural area population	people	263,967	274,972	280,137	287,746	293,411
Tourists	people	580,000	800,000	800,000	1,400,000	1,500,000
Domestic use water demand	m ³ /day	18,003.3	18,746.2	19,110.1	19,881.1	20,247.5
Annual capacity to produce and supply clean water	10 ³ .m ³	317.3	386.6	420.0	528.3	504.4

In order to overcome the shortage of domestic water in the dry season on the karst plateau, many solutions have been proposed by the local government such as providing water tanks to harvest rainwater for local people, building gravity water-supply systems on the village-scale, drilling wells to exploit groundwater and especially the project to build reservoirs funded by the Vietnamese Government budget, the World Bank, and the Asian Development Bank. Since 2007, a total of 121 reservoirs called “Hanging Pools” have been built and put in operation in the four districts of DVKG to store the water from the rainy season for use in the dry season (HGDONRE 2021). However, these constructions are not sustainable for several reasons. First, the flat areas where reservoirs can be built are mostly located on top of sinkholes with unstable foundations, which leads to a relatively short lifetime of the concrete basins due to cracks when storing water (Fig. 1-6a). Furthermore, the basins

consist of a large open water surface, resulting in high evaporation and an increasing deterioration of water quality due to natural contamination from microbial and algae growth and/or pollution from anthropogenic inputs (Fig. 1-6b). Recently, the KaWaTech project was implemented and completed in 2019, which has built a pumping (pump as turbine - PAT) plant to guarantee sustainable water supply even in the dry season with a capacity of 1,500 m³ per day for approx. 10,000 people who are living in the Dong Van town and surrounding villages. This is considered as one of the sustainable solutions for the management and exploitation of karst water and can also be applied to other regions in DVKG in the future. In terms of water for agriculture, most areas in DVKG use rainwater so farmers often arrange sowing times parallel with the rainy season which often occurs from February to May.

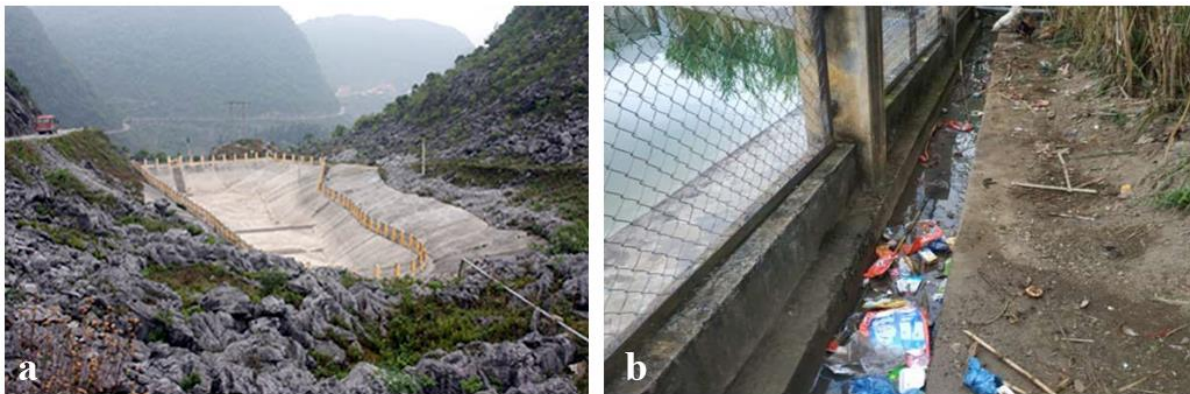


Fig. 1-6 a) Sa Phin A “hanging pool” cannot store rainwater for the dry season due to cracks in the bottom; b) Anthropogenic inputs affects the water quality of Seo Lung A hanging pool, Sang Tung commune (Photo: HGDONRE)

In summary, the highly dissected terrain combined with extreme weather conditions has led to water scarcity in the DVKG. In addition, due to population growth and rapidly increasing numbers of tourists, pressure on domestic water supplies has increased, which is why the local government has invested in numerous domestic water supply construction in this area. However, apart from the positive effects of water supply for the local people, there are still many limitations and inadequacies in these facilities, such as the main water source is rainwater and therefore cannot be actively used in the dry season; the awareness of the local people on the use and protection of the facilities is low, and there is no specialized unit for management and repair, so these water supply installations are quickly deteriorated and damaged; water pollution from anthropogenic inputs. On the other hand, to meet the further increasing water demand, private wells have been drilled to extract water from the karst aquifer below

the city centers of Quan Ba, Yen Minh, and Dong Van, except for Meo Vac due to the deep groundwater level. However, there is no study on the extent of the aquifer, the recharge rates, and the residence times of groundwater. In the worst case, uncontrolled groundwater extraction could lead to severe groundwater depletion causing potential risks of land subsidence, collapse and deterioration of the groundwater quality. Therefore, it is necessary to develop a management strategy in parallel with scientific research and solutions for the sustainable protection and use of valuable groundwater resources in DVKG.

1.2.4 The KaWaTech project

The Vietnamese-German Cooperation Project for the Development of sustainable Technologies for Karst Water Management (KaWaTech project) was implemented from 2013 to 2020 in two phases based on the cooperation between German and Vietnamese partners from universities, research institutes, industries, and authorities. The first phase of the project (BMBF, grant number 02WCL1291A, 2013-2016) is subdivided into four work packages, including 1) investigations, exploration, and monitoring; 2) hydropower and water production; 3) water distribution and supply, and 4) resource protection and socio-cultural aspects. By closely integrating these topics, an adapted hydropower-driven water supply system was built that is able to pump water from the Seo Ho River to a distribution tank in Ma U (Fig. 1-7a). By using a mechanically coupled unit of a “pump as turbine” (PAT) and a feed pump (Fig. 1-7b), even small discharge rates during dry season (20l/s) can be efficiently used to supply the water to the distribution tanks with a vertical interval of up to 500m (Fritz et al. 2012; Oberle et al. 2017). Within the project, several field studies were carried out to determine the water availability and the current and expected future water demand to design the dimensioning of the water supply system.

The second phase named KaWaTech Solutions (BMBF, grant number 02WCL1415) is scheduled to run from 2016 until 2020 with the main goal of completing the water supply and distribution system for Dong Van town and surrounding villages. In addition, water purification and pilot implementation of water pumping based on renewable energy are also important parts of this phase. Based on the information obtained in the first phase, a small pilot treatment plant will be designed for permanent

operation at the point of use in Dong Van city to provide high-quality water for public buildings, such as the hospital. After an analysis of potential locations, the Lung Lu village in Dong Van was selected as the site for a pilot implementation of decentralized photovoltaic-based pump systems (PVPS) that use solar-operated to pump water from the central storage tank to Lung Lu village (about 200 m higher). Due to the impact of the Covid-19 pandemic, implementation has been significantly delayed and is expected to be completed in the last months of 2022.

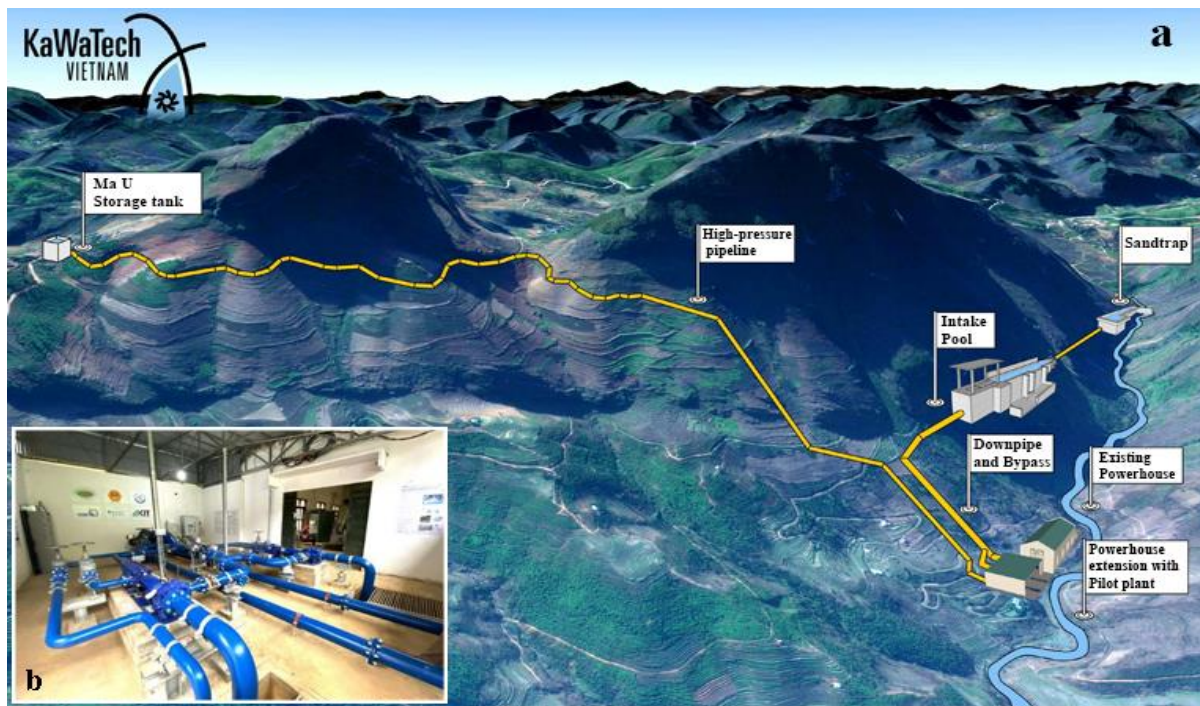


Fig. 1-7 a) Schematic illustration of the main components of the Seo Ho High-Pressure Plant that was planned and built within the KaWaTech project. (Modified after Oberle et al. 2017); b) The new water pumping system (PAT) installed in Seo Ho hydro-power plant.

To sum up, the results of the KawaTech projects have given positive signals for the development and implementation of adapted technologies for the sustainable use of water in poor and remote karst areas. Therefore, detailed geological, speleological, and hydrogeological field investigations are needed as a basis for the future application of these technologies and concepts not only in North Vietnam but also in other karst water regions in the world.

1.3 Objectives and approaches of the thesis

1.3.1 Objectives

The main aim of this work is to contribute to a better understanding of subtropical karst systems in northern Vietnam and their development based on the database of the geological, cave survey, and physicochemical parameters of groundwater. The objectives of this study are:

- To determine the development and structure of karstification in subtropical karst areas based on cave survey data along with topographic and geologic data.
- Use major ion chemistry to characterize mixing processes and water-rock interactions in the subtropical karst system.
- Verify the use of trace- and rare-earth elements as potential natural tracers when some processes are not revealed by conventional hydrochemical methods.
- To establish a conceptual model that displays the ability of association of underground water flow paths and characterize the properties of underground water transport.
- Provide scientific information on groundwater quality and identify contaminant transport processes in karst systems.

By addressing these specific topics, a profound understanding of the studied karst region could be developed. Furthermore, the results presented in this thesis are also useful for the development of strategies for the sustainable management, protection, and exploitation of groundwater resources in karst areas.

1.3.2 Approaches

The spatial organization of cave systems has been the focus of numerous karst studies (Ford and Williams 1989, Palmer 1991, Klimchouk 2009, Filipponi 2009, Piccini 2011, Audra and Palmer 2013, Jouves 2017) that describe the karst evolution and the position and shape of cave networks according to flow conditions, climatic settings and geologic discontinuities such as fractures, faults, injection horizons, etc. (Fig. 1-8). This is one of the most effective approaches to identify the relationship

between the cave system and the tectonic and geomorphologic development processes. In this study, the above approach was used to clarify the development and structure of karstification of a subtropical karst area. Accordingly, morphometric characteristics of cave conduits were computed following the approach of Jouves et al. 2017, while the "Cave passages statistics" method (mentioned by Palmer 1987, Filipponi et al. 2009, Piccini 2011) was implemented through statistical analysis of the altimetric distribution of the horizontal parts of cave passages to identify the cave levels. In addition, the cave passage orientation analysis approach (Littva et al. 2015) was also performed to compare with the geological development periods, as well as to achieve a better understanding of the speleogenetic processes that have locally dominated.

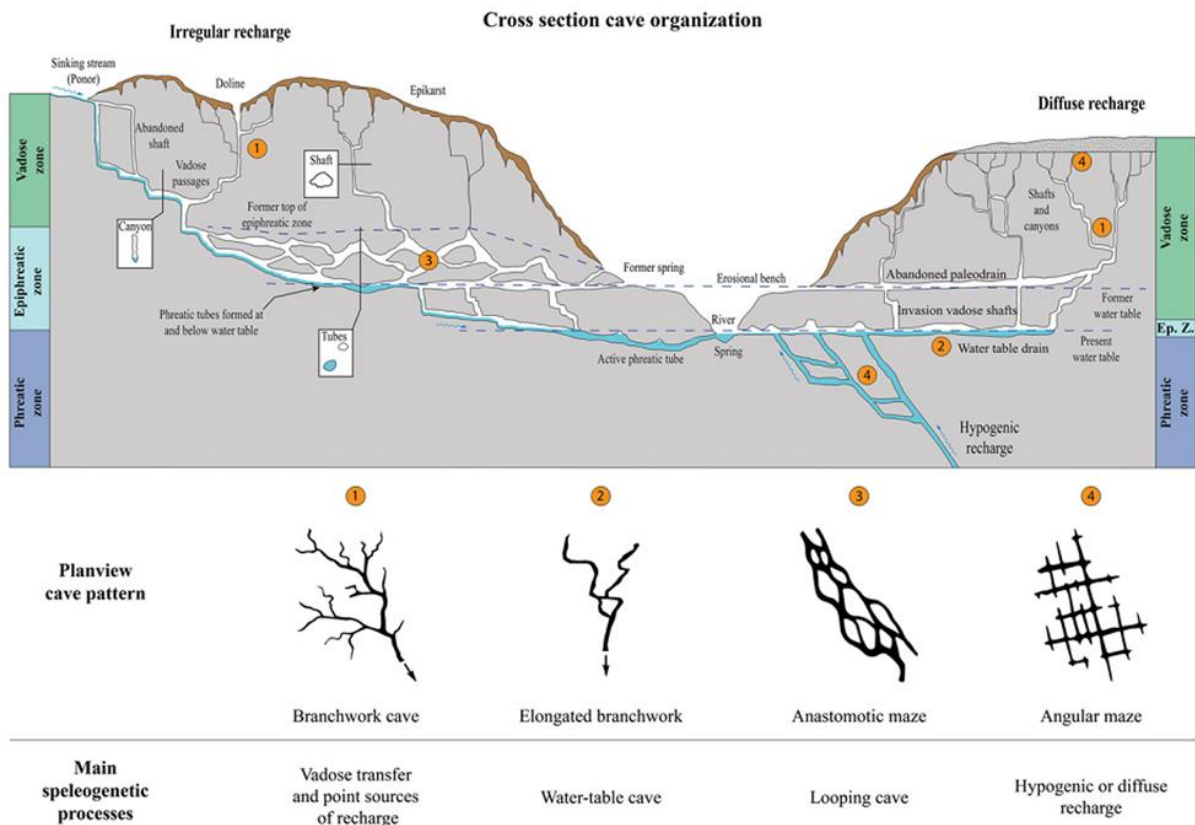


Fig. 1-8 Idealized cross-section of a karst system with a vertical spatial zonation of karst, and plan views of associated cave patterns. (Modified after Palmer 1991; Audra and Palmer 2013; and Jouves et al. 2017)

Karst aquifer forms when the water infiltration on the surface interacts and enters the underground through shallow soils and a network of interconnected fissures, fractures, and conduits emplaced in a relatively low-permeability rock matrix. Most of the groundwater flow and transport occurs through the network of openings, while most of the groundwater storage occurs in the matrix (Kovacs et al.

2005). After traveling underground, this water is then discharged from springs, many of which are cave entrances (Fig 1-9). As a result, most karst aquifers are highly heterogeneous and anisotropic, and therefore require specific investigation methods such as geological, geophysical, and speleological methods, hydrologic and hydraulic techniques, the use of natural tracers, such as isotopes and hydrochemical parameters, as well as the application of artificial tracer tests, long-term monitoring of water levels, spring discharge, and water quality (Goldscheider and Drew 2007). The selection of appropriate methods and the sequence of methods applied depend on the practical conditions or scientific research questions, but also on the level of previous knowledge and on the available time, funding, personnel, and instrumentation.

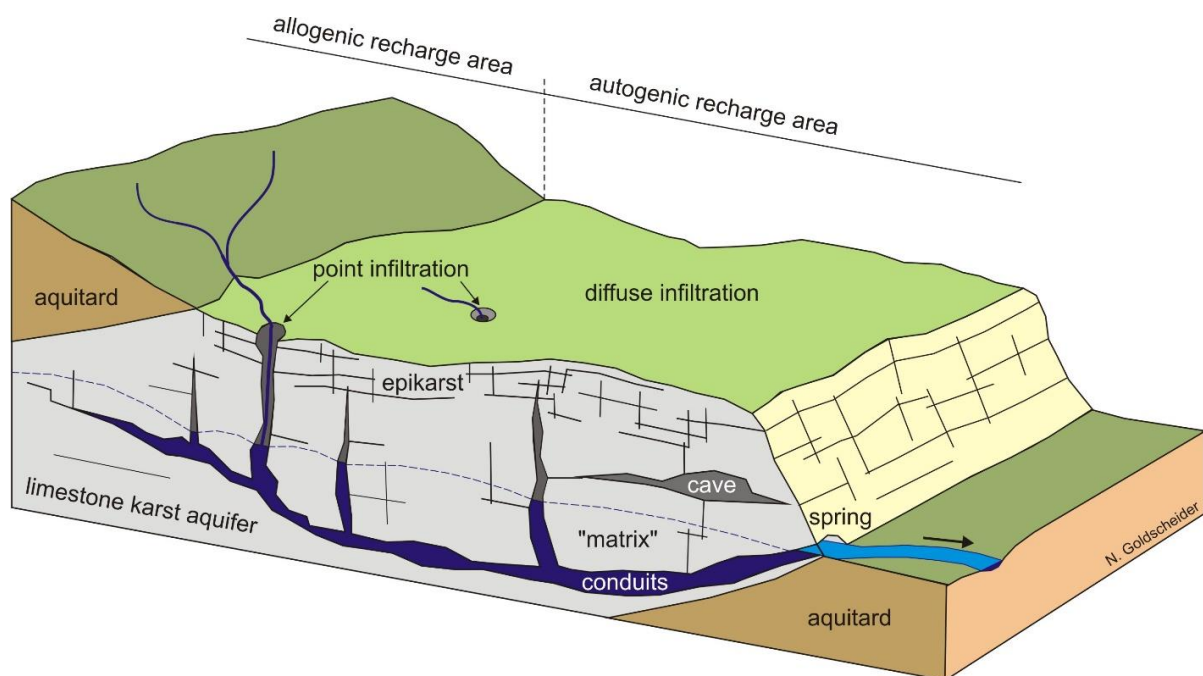


Fig. 1-9 Block diagram illustrating the conceptual model of a karst aquifer (Goldscheider & Drew 2007)

Recently, groundwater geochemistry has emerged as an operative tool that can be used to elucidate water sources, hydrochemical processes, and dynamics in karst aquifers, as well as contamination input sources. And the use of major ions to identify hydrochemical facies and the major processes controlling groundwater chemistry has become a common hydrochemical method. In addition, several studies have shown that trace elements can be used as potential natural tracers of groundwater origin when some processes are not revealed through conventional hydrochemical methods. Thus, analysis and statistics of the physicochemical parameters and the behavior of trace elements of groundwater are among the

effective approaches used in this thesis to identify the physical-chemical processes controlling groundwater chemistry, as well as for grouping and linking the underground karst flow in the subtropical karst aquifer.

1.4 Structure of the thesis

This thesis is structured cumulatively and consists of two studies (Chapters 2 and 3) that address different aspects of karst research on the Dong Van karst plateau, including karst evolution and karst hydrogeology.

Chapter 2 presents a quantitative study of the relationship between the cave system and the tectonic and karst evolution of the Dong Van Karst Plateau based on analysis and statistics of geometric parameters and orientation of cave passages.

Chapter 3 addresses the approach of using concentrations of major ions, trace- and rare-earth elements to clarify chemical signatures and the ability for connections among sampling areas in the study area. It results in a basic hydrogeologic conceptual model for the Dong Van karst aquifer system. Based on this model, strategies for the protection and management of karst water resources can be developed.

In **chapter 4**, discussions are presented based on the obtained results for the purpose of proposing practical solutions for sustainable management, protection and exploitation of karst water resources in Dong Van karst plateau as well as giving recommendations for future research and observation.

Chapter 5 gives a summary of the major results obtained from the study.

Chapter 2 has been published in peer-reviewed journals, whereas Chapter 3 is currently under review.

Chapter 2

2 Karst and cave development

Reproduced from: Diep Anh Tran, Nadine Goepfert, Arthur N. Palmer, Nico Goldscheider (2022) Development and structure of karstification of the Dong Van Karst Plateau UNESCO Global Geopark, North Vietnam based on cave survey data. International Journal of Earth Sciences 111: 1573-1592, <https://doi.org/10.1007/s00531-022-02190-5>

Abstract

This paper presents a quantitative study of the relationship between the cave system and the tectonic and karst evolution of the Dong Van Karst Plateau based on analysis and statistics of geometric parameters and orientation of cave passages. The region is located in northern Vietnam and belongs to the extended part of the South China karst belt (Yunnan karst plateau), which is composed mainly of carbonate rocks. Cave classification based on cave conduits geometric parameters shows that caves developed mainly in the vadose zone (27 vadose branchwork caves, 10 mixed caves developed under the control of fault systems, and 12 water-table caves). The degree of correlation between cave levels and planation surfaces suggests that the development of horizontal cave passages is related to two levels of planation surfaces, including one at 1250–1450 masl (equivalent to cave level at 1350–1450 masl), and at 1000–1250 masl (corresponding to cave level at 1200–1250 masl). Additionally, cave passage orientation shows that the cave system formed and developed under the influence of tectonic activities in the Cenozoic. The dominant orientation trend is roughly in the East–West direction and occurred in the early phase (Eocene–Miocene). Next is a trend roughly North–South that occurred in the late phase (Pliocene–Quaternary). The last orientation trend follows the NW–SE direction due to the reactivation of paleo-fault systems in the same direction. Although there are limitations due to

accessibility and the level of cave exploration, this research suggests that analysis and statistics of the geometric parameters and orientation of cave passages based on cave survey data can be one of the effective approaches used to identify the development and structure of karstification in the karst region.

2.1 Introduction

Dong Van Karst Plateau is located in northern Vietnam and belongs to the extended part of the South China karst belt (Yunnan karst plateau) (Fig. 2-1b). Besides its geological, geomorphologic, stratigraphic and paleontological features and values, this area is also characterized by extensive and varied karst and cave development. Karst and cave systems are not only valuable in terms of landscape, tourism and subsurface biodiversity, but caves are also places where information about paleoclimatic conditions and tectonic evolution can be recorded (Goldscheider 2019).

In this area, the average altitude is about 1500 m, up to 1800 m at some places, whereas the local erosional base is rather low, only about 200–300 m at the Nhiem River in the south or 400–500 m along the Nho Que River in the north and east (Fig. 2-1c). The topsoil layer is rarely conserved and surface streams are mostly short, becoming dry soon after the rainy season, most of them sink underground at cave entrances or sinkholes (Van et al. 2004). Several studies (Van et al. 2010, Hai et al. 2013) have shown that the distribution of cave systems, planation surfaces, and stream terraces/valleys at different elevations in this area depend on tectonic movements combined with geomorphologic development processes that occurred in cycles during the Cenozoic period. However, two major research questions that need to be clarified are: (1) When and how did the main phases of karst evolution occur? (2) How are these phases related to the tectonic and geomorphologic development of the wider region? We used cave survey data, along with topographic and geologic data, to answer these questions.

Studying caves is a challenge because, except for entrance areas, caves are largely hidden from view, so using systematic documentation of cave survey data is the main key to provide a basis for this kind of research (Kambesis 2007). In recent years, many studies have shown that the formation of karst and cave systems is chiefly controlled by a complex combination of tectonic activities, geomorphic evolution,

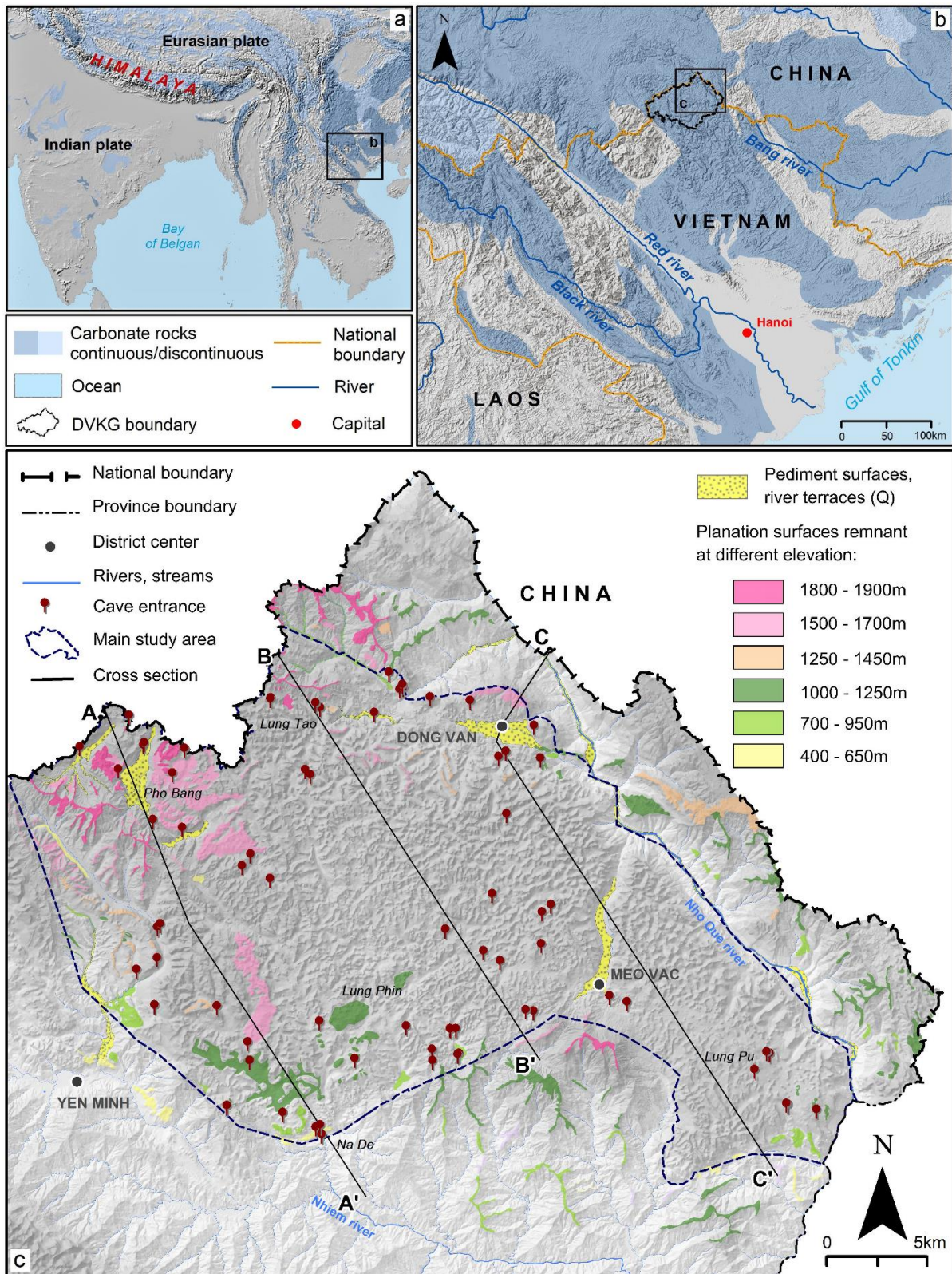


Fig. 2- 1 Map of the investigation area. **a)** Location map of Northern Vietnam illustrating the physiographic impact of the collision between the Indian and Eurasian plates; **b)** Location of Dong Van Karst Plateau in the Northern Vietnam and South China karst belt (based on the World Karst Aquifer Map, Goldscheider et al. 2020); **c)** Location map of the main study area shows the distribution of cave entrances, planation/pediment surfaces, and river terraces remnants at different altitudes on top of a DEM (After Tuy in Van et al. 2010).

climatic and hydrologic processes. From the tectonic point of view, Palmer (1991) showed that 42% cave passage of his data set was controlled by faults/fractures, while Littva et al. (2015), Shanov et al. (2015) mention the relationship between cave passage orientation and the neo-tectonics stress field. Several previous studies (Ford 1971, Palmer 1991, 2007, Klimchouk 2009, 2016, Wagner et al. 2011, Audra and Palmer 2013) indicate that the conduit network has close relations with landscape evolution and local geology, which are controlled by several factors, such as lithology, tectonics and stratigraphic boundaries. Palmer (1991) classified geomorphologic cave patterns based on speleogenetic context, while Jouves (2017) and Collon (2017) determine these cave patterns through quantitative statistics of morphometric parameters of cave conduits. In addition, the studies of Palmer (1987), Filipponi (2009), Piccini (2011) and Labib (2019) indicate that the occurrence of horizontal levels of cave passages is caused by hydrological factors when the cave passage acted as an underground water conduit in a relatively stable tectonic period. Analysis of the horizontal cave passages can be used to identify the cave levels as a consistent indicator of tectonic periods and karst evolution phases. Thus, analysis and statistics of the geometric parameters and orientation of cave passages are one of the effective approaches used to identify the relationship between the cave system and the tectonic and geomorphologic development processes based on cave survey data.

In this study, by applying the above approach, through analysis and statistics of geometric parameters and orientation of cave passages, cave survey data were used to clarify the development and structure of karstification of the Dong Van Karst Plateau.

2.2 Overview of the study area

The study area is located in Dong Van, Meo Vac district, covering an area of about 620 km², which is composed mainly (more than 60%) of carbonate rocks. The boundary of this area is delineated by Ma Le Stream and North Dong Van fault zone in the north, Nho Que River fault zone in the northeast, Na De - Meo Vac fault zone in the south, and Nhiem River fault zone in the southwest (Fig.2-2b, 2-3).

In order to provide a more general view of the main study area, basic information on geological setting, planation surfaces, and cave systems will be presented and analyzed based on published research,

digital elevation models (DEM), unpublished cave data (provided by SPEKUL, Belgium), and personal fieldwork.

2.2.1 Geological setting

According to previous and recently updated geological maps, the study area is composed of sedimentary formations from Paleozoic to Mesozoic, and local outcrops of Triassic gabbro and diabase along deep faults (Fig.2-2). Carbonate rock formations, including Bac Son (C-P *bs*), Dong Dang (P₂ *đđ*) and Hong Ngai (T₁ *hn*), are widely distributed in the central part of karst plateau, and caves are mainly developed in these formations. The Devonian formations including Mia Le (D₁ *ml*), Si Phai (D₁₋₂ *sp*) and Toc Tat (D₃ *tt*) occur in narrow bands, located along the north and northeast. In addition, Triassic formations, including Song Hien (T₁ *sh*) and Yen Binh (T_{2a} *yb*), are distributed in the South and SW of this area.

Dong Van Karst Plateau belongs to three tectonic structural zones, including from SW to NE Lo Gam Zone, Song Hien Zone and Lung Cu Zone (Tri et al. 2009) (Fig.2-2a). Together they form a large structure shaped like a synclinorium extending in the NW-SE direction. The main study area is entirely located in Song Hien zone, mainly composed of Carboniferous-Permian-Triassic carbonate rock and Early Triassic terrigenous acid eruption deposits.

Northeast Vietnam has a long history of tectonic development from Mid-Paleozoic to Cenozoic, however, only two tectonic phases occurring in Mesozoic and Cenozoic have been recorded in the study area. In the Mesozoic, the late Triassic Indosinian orogeny phase occurred consisting in large scale folding and faulting in an overthrust (Hai et al. 2013) (Fig. 2-3b). In the Neotectonic period two types of tectonics developed according to the two-phase deformation model due to the collision between the Indian and Eurasian plates occurring in Paleogene (Molnar et al. 1993, Tri et al. 2009, Hai et al. 2013). In the first phase (Eocene-Miocene), the geodynamic regime was characterized by a tectonic stress field with sub-latitude compression and sub-meridian extension (Tapponnier et al. 1990). In the later phase (Pliocene-Quaternary), the tectonic stress field changed into sub-meridian compression and sub-latitude extension (Wang et al. 1998). In summary, if the Indosinian tectonic process plays an important role in shaping

geologic structure, the strong activities of fault systems in Neotectonic is considered a factor controlling the formation and development of the topographic landscape, especially karst and cave systems in the Dong Van Karst Plateau.

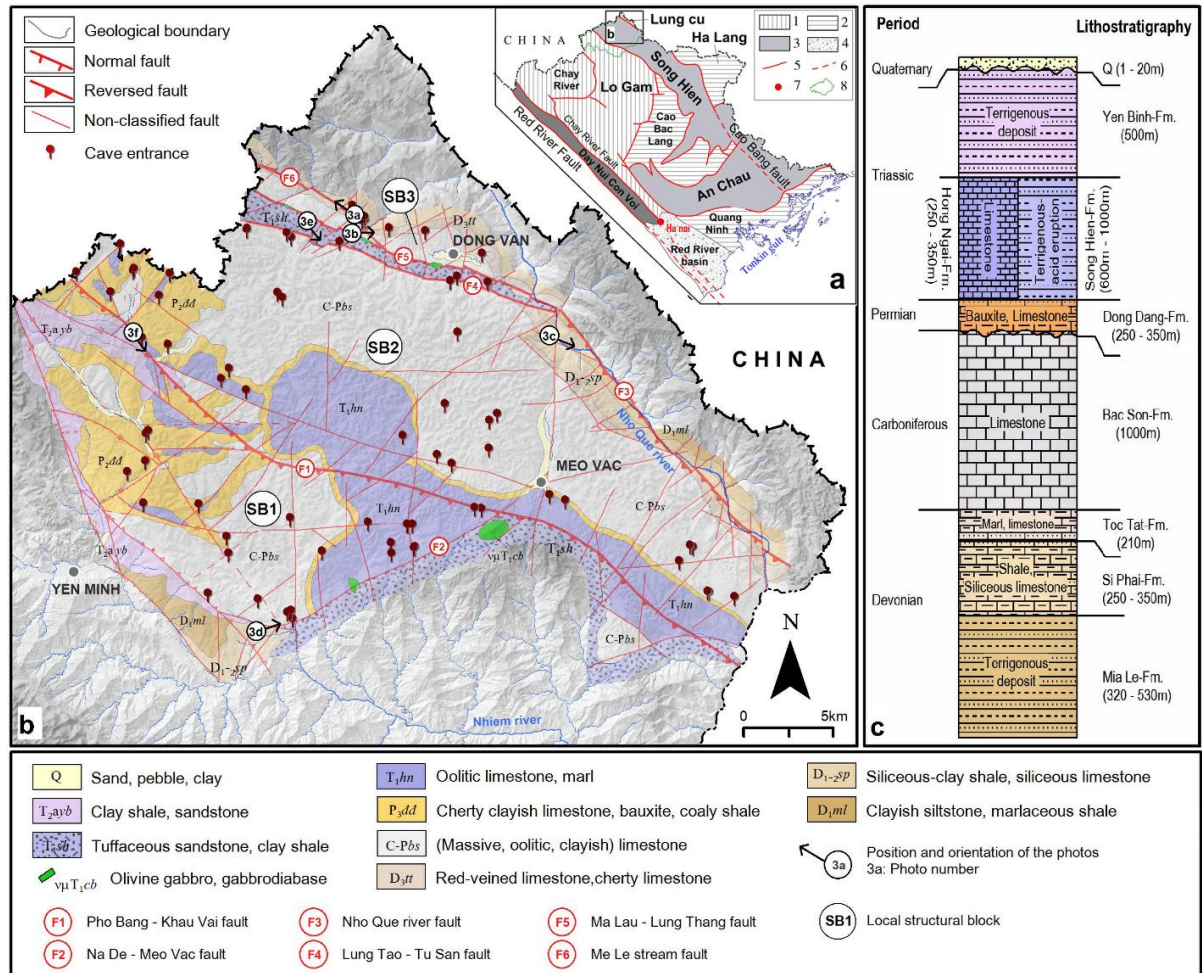


Fig. 2-2 Geological setting of the study area. **a)** Study area position in the main structural zone in NE Vietnam (After Tri et al. 2009) (Legend: 1-Viet Bac fold system; 2-Dong Bac fold system; 3-Mesozoic riftogenous superimposed depression; 4-Neogene-Quaternary basin; 5-Accurate fault zone; 6-Supposed fault zone; 7-Capital position; 8-DVKP UGG boundary); **b)** Geological map (After Tinh et al. 1976; Updated by KaWaTech project); **c)** Lithostratigraphic profile.

The study area is dissected by many fault systems (Fig. 2-2b), but the main one is the NW-SE fault system, include Pho Bang - Khau Vai fault (F1), Nho Que river fault (F3), Lung Tao - Tu San fault (F4), Ma Lau - Dong Van - Lung Thang fault (F5) và Ma Le stream fault (F6) and some of them are in a structural fault zone (F1, F4). In addition, there is the appearance of fault system with NE-SW direction such as Na De - Meo Vac fault (F2), especially sub-latitude and sub-meridian fault systems formed in the Neotectonic period such as Meo Vac fault with sub-meridian direction.

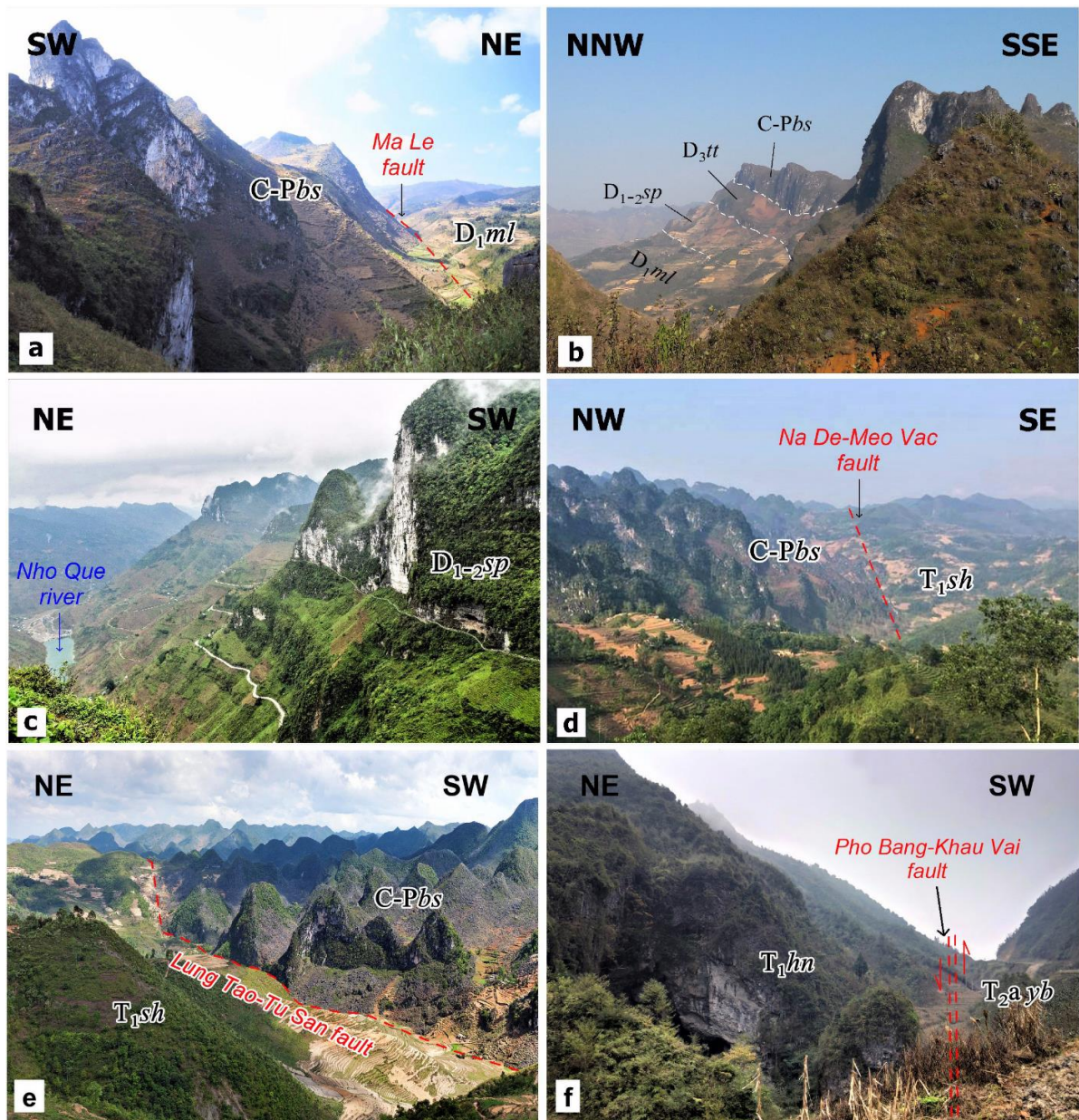


Fig. 2-3 Photos showing the karst landscape and important geological structures in the study area; a) Ma Le stream fault zone; b) Overthrust fault zone North Dong Van; c) Nho Que River fault zone, d) Na De - Meo Vac fault zone; e) Lung Tao - Tu San fault zone; f) Pho Bang - Khau Vai fault zone.

2.2.2 Planation surfaces

There are a number of studies on karst geomorphology-related denudation planation surfaces in Dong Van Karst Plateau and surrounding areas. A study by Chen (1993) determined that the 1600-2000 masl planation surface in Guizhou and the >2000 masl surface in East Yunnan (belonging to the Guizhou-Yunnan karst region, South China) are of Paleogene age, while the 1700-1900 masl karst forest in East

Yunnan is Pliocene in age. After that, An et al. (2008) when studying the Dong Van Karst Plateau, identified five levels of planation surface that can be compared with planation surfaces in South China-North Indochina blocks. The planation surface at an altitude of 1800-1900 masl corresponds to Middle Paleogene; the 1500-1600 masl planation surface corresponds to Early-Middle Miocene; the 1200-1300 masl surface corresponds to Late Miocene; the 800-1000 masl surface corresponds to Pliocene; and the 400-600 masl surface corresponds to Quaternary. Tuy in Van et al. (2010) has established the geomorphological map of the DVKP area showing six planation surfaces distinguished on the basis of previous studies. Accordingly, the planation surfaces in DVKP are the result of the cyclical activity of Neotectonic movements. At the beginning of each cycle, the terrain was uplifted and dissected. The end of each cycle corresponded to a tectonically stable period, which favored the processes of erosion, transportation, and accumulation, leading to the formation of a fairly flat surface at the local erosion level. Specifically, six planation surfaces include: 1) Paleogene (E_2-E_3) at 1700-1900 masl; 2) Early-Middle Miocene (N_1^{1-2}) at 1500-1700 masl; 3) Late Miocene (N_1^3) at 1300-1500 masl; 4) Late Miocene (N_1^3) at 1000-1300 masl; 5) Early-Middle Pliocene (N_2^{1-2}) at 750-950 masl; and 6) Late Pliocene (N_2^3) at 400-650 masl. The relative age of the planation surfaces is determined by the presence of Neogene deposits (N_1^3) in the southern Dong Van valley at 1000-1300 masl.

In this study, to accurately identify the elevation of the planation surfaces, a morphological analysis was performed by means of a series of topographic cross-sections, based on earlier studies concerning the evolution and classification of planation surfaces (An et al. 2008, Tuy in Van et al. 2010). As a result, six planation surfaces are identified (Fig. 2-1c, 2-4):

- The Paleogene planation at 1800-1900 masl (E_2) approximates the original surface atop the massif, which remains only at the top of the mountains on the west of the study area;
- The Early-Middle Miocene planation at 1500-1700 masl (N_1^{1-2}) is present as incomplete planation surface divided by valleys in the southwestern part of the study area and north Dong Van;
- The Late Miocene planation at 1250-1450 masl (N_1^3) remains as flat areas on the drainage divide zone of the limestone area east of the study area, south of Dong Van, and the flat areas along the Pho Bang, Pho Cao valleys in the western part of the region;

- The Late Miocene planation at 1000-1250 masl (N_1^3) consists of flat areas on the drainage divide zone in the karst and non-karst area, or areas with karst towers of similar altitudes;
- The Early-Middle Pliocene planation at 700-950 masl (N_2^{1-2}) is distributed in narrow areas, mainly in form of incomplete planation surfaces on mountain shoulders in limestone areas and along drainage divides in terrigenous rocky areas south of study area;
- The Late Pliocene planation at 400-650 masl (N_2^3) is distributed in narrow flat areas with shallow slopes along the river valleys in the south area (Na De, Mau Due). In addition, high river terraces (river erosion) at different altitudes with Early Pleistocene age (Q_1^1) also appear on the pediment surfaces (Nhiem, Nho Que river valley).

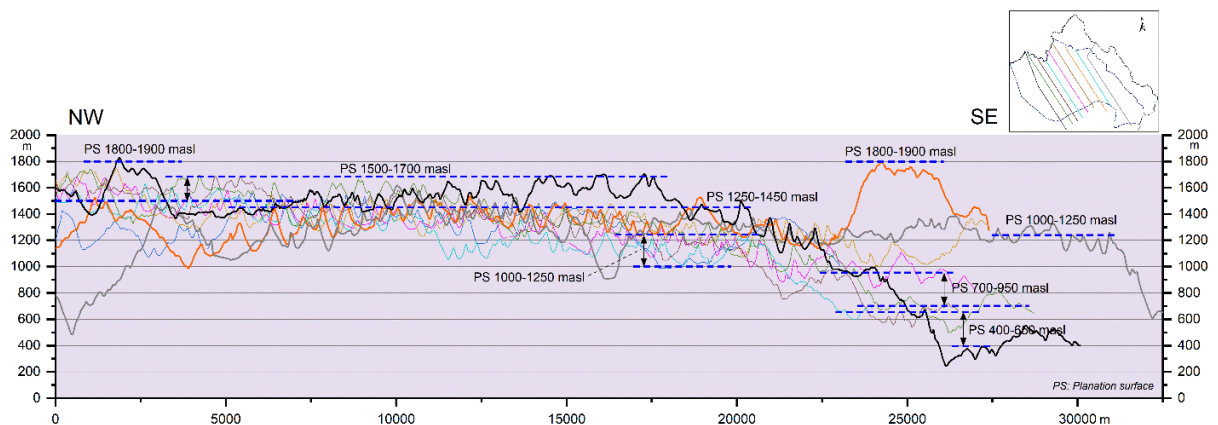


Fig. 2-4 Distribution of low gradient surfaces related to planation surfaces as revealed from topographic cross-sections in Dong Van Karst Plateau.

2.2.3 Cave systems

According to the survey data, more than 135 caves were explored with a total of up to 39 km of cave passage mapped so far on Dong Van Karst Plateau (Masschelein et al. 2007, Bontridder et al. 2010). In which, 73 caves were discovered in the main study area, and most of them are developed in three carbonate rock formations including Bac Son ($C-P_{bs}$), Dong Dang (P_2_{dd}) and Hong Ngai (T_1_{hn}).

Due to different petrographic properties, caves developed in each formation have different characteristics. Bac Son formation is composed of homogeneous, massive, partly dolomitized limestone, totaling in thickness 700-1000m, so the mapped caves in this unit are usually deep and long. Dong Dang formation consists of layers of limestone, clay-rich limestone, siliceous limestone, medium to thin-

bedded in the upper part which is a favorable environment for the formation of caves. However, the bottom part comprising siltstone, claystone, bauxite, shale, is insoluble, so most of the caves are stopped or develop horizontally here. Therefore, in Dong Dang formation, caves are short, horizontal, or in the form of sinkholes with the bottom filled by rockfall blocks and sediment. Hong Ngai formation is composed of layers of argillaceous limestone, siliceous limestone, and medium-to-thick-bedded limestone. Hence, in the Hong Ngai formation, caves developed not only along the faults/cracks but also followed the bedding planes.

2.3 Data and Methodology

2.3.1 Cave database

In order to perform this study, the digital database of 49 caves from 73 caves in the main study area was used for analysis and interpretation. These are caves with length and depth measurements large enough to meet the requirements of analyses. Unused caves are usually in the form of shallow sinkholes, or simply developed, short caves that are not valuable for analysis.

In general, the original cave survey data consisted in survey stations connected to each other by a baseline (Jeannin et al. 2007, Pardo-Iguzquiza et al. 2011). Between two survey stations, the recorded data are length, azimuth, the inclination from horizontal of the line joining these two stations, as well as the local width and height that is provided through left, right, up, and down measurements from each station.

Recently, the development of measuring devices has made the precision and validity of field measurements greatly improved. However, there are some survey errors that can still appear in the surveying process such as back-sight measurements; cycle closure errors; missing connections; fictive data that connect several entrances, survey stations; artificial cycles that correspond to loops acquired in a huge conduit or a room; etc (more details in Collonet et al. 2017, Jouves et al. 2017). For this reason, the data set needs to be cleaned before computation. In this study, based on existing cave survey data, the preprocessing step was performed manually following the knowledge of cave surveying techniques (Jeannin et al. 2007).

The data set was carefully evaluated and cleaned and then imported into the speleological software On Station 3.2 (Taco van Ieperen 1990) which enables common survey formats to be read, as well as displaying cave profiles and cave maps. Then the cave entrance (as a survey station) is precisely positioned (location, altitude) in the field by using GPS to calculate the coordinates (x_i , y_i , z_i) of each station (S_i). These are the basic databases used to carry out the calculations in this study.

2.3.2 Methodology

According to the approach mentioned in the Introduction, the analysis process includes the following steps:

- Perform geometric parameters analysis to identify and classify cave patterns;
- Apply the "Cave passages statistics" method to identify the altimetric distribution of horizontal cave passages as well as cave levels, and divide cave classes according to the elevation of planation surfaces;
- Divide cave groups by local structural blocks (horizontally) and cave classes (vertically);
- Perform geometric parameters analysis and cave passage orientation analysis for each cave group.

The obtained results can be used to interpret and identify the relationship between the cave system and tectonic and geomorphologic development periods in the study area.

The morphometric analysis of cave conduits was used to describe the condition that existed within the cave. It provides valuable information on geometries of karst conduits which are wide enough to be accessible by humans. In this study, geometric characteristics were computed following the approach by Jouvès et al. (2017): 1) the conduit cross-section shape (the width-height ratio), 2) the sinuosity (the curvature and the tortuosity), and 3) the vertical index. The parameters computed locally (per node or per branch) were averaged over the cave network in order to obtain one value per cave sample. The definition of these parameters is presented in Table 2-1 and Fig. 2-5 (more detail in Collonet et al. 2017; Jouvès et al. 2017). The results obtained from this analysis are one of the bases for cave classification, and explain the relationship of influencing factors in the development of cave passages such as lithology,

Table 2-1 Cave passage morphometry

Geometric parameter	Method	Symbol	Calculation formula locally (per node i or per branch j)	Averaged value over the cave network
Curvilinear length	Taken from the data by using OnStation 3.2 software	L_j	L_j is all segments between two branch extremities	
Euclidean length	Taken from the data by using OnStation 3.2 software	D_j	D_j is the straight distance between two branch extremities	
Width length	Taken from the data by using OnStation 3.2 software	W	$W_i = W_l + W_r$	
Height length	Taken from the data by using OnStation 3.2 software	H	$H_i = H_u + H_d$	
Total depth	Taken from the data by using OnStation 3.2 software	T_d	T_d is the straight distance between highest and deepest survey station	
Average elevation	Taken from the data by using OnStation 3.2 software	E_a	E_a is the average elevation between highest and deepest survey station	
Modal elevation	Taken from the data by using OnStation 3.2 software	E_m	E_m is the elevation of highest survey station	
Real length	Taken from the data by using OnStation 3.2 software	L_r	L_j is all segments between two branch extremities	$L_r = \sum_{j=1}^{n_b} L_j$
Width-Height ratio	Calculated from W and H data	WH	$WH_i = \frac{W_i}{H_i}$	$WH = \frac{1}{n} \sum_{i=1}^n WH_i$
Tortuosity	Calculated from L_j and D_j data	T	$T_j = \frac{L_j}{D_j}$	$T = \frac{1}{n_b} \sum_{j=1}^{n_b} T_j$
Curvature	Calculated by from coordinates (x_i, y_i, z_i) of each survey station	K	$K(P) = \frac{1}{r} = \left\ \frac{dt}{ds} \right\ = \left\ \frac{d^2(OP)}{ds^2} \right\ $	$K = \frac{1}{n'} \sum_{i=1}^{n'} K_i $
Vertical index	Calculated from total deep (T_d) and real length (L_r) data	V		$V = \frac{T_d}{L_r}$

n the number of cave passage nodes, n_b the number of branches of the cave passage, n' the number of 3-point combinations along the passage

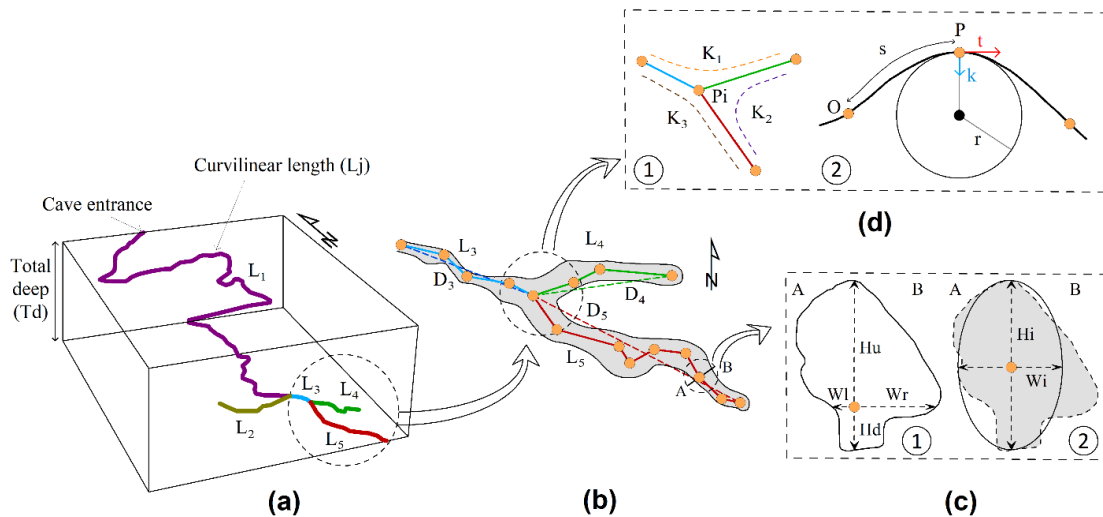


Fig. 2-5 Geometric parameters computation. **(a)** The vertical index V on a 3D cave sample. Different color lines represent the different cave branch curvilinear length (L_i); **(b)** Sketch of a karst sample divided into three branches. The curvilinear length L_j and the Euclidean length D_j can be computed along each branch j . Then, the tortuosity of each branch is calculated; **(c)** Processing of width-height ratio for a cave survey station i : ① In-situ measurement of width ($W_i = W_l + W_r$) and height ($H_i = H_u + H_d$) at survey station i ; ② WH-ratio WH_i calculated from the in-situ measurement for an idealized shape of karst conduit; **(d)** Curvature parameter computation: ① Possibilities of curvature values computed at an intersection node P_i ; ② The curvature at a point P of a curve C , where the point O is the origin of the curvilinear abscissa s . The parameter k is the curvature vector and t designates the tangent vector at P . The value r is the radius of the osculating circle at P . (Modified from Jouves et al. 2017).

fault tectonics and geological structures. Following this classification, the vadose branchwork cave (VB) type is mainly delimited by $WH < 1.5$ with high variability for K and V ; The water-table cave (WTC) and looping cave (LC) type is roughly located where $WH > 1.5$, $K < 0.2$, and $V < 0.2$; The angular mazes (AM) type is mostly confined to where $WH > 1$ and $K > 0.2$.

As mentioned by Palmer 1987, Filipponi et al. 2009, Piccini 2011, the "Cave passages statistics" method is implemented through statistical analysis of the altimetric distribution of the horizontal parts of cave passages to identify the cave levels in the study area. In this study, cave survey data and the longitudinal cave profiles are used to identify horizontal and/or low-gradient cave passages (i.e., conduits with Vertical Index $V < 0.2$ or angle of inclination between two survey stations $\alpha < 120$; for details see Jouvès et al. 2017), so that these cave passages are statistically at different elevation classes. The obtained frequency graph reflects the vertical distribution of horizontal cave passages and furnishes a database to distinguish cave levels.

Fractures/faults are considered as one of the main geologic features that have a strong influence on the development of karstic conduits (Palmer 1991). Therefore, the frequency distribution of cave passage directions is an interesting parameter that can be used to compare with the geological development periods, as well as to achieve a better understanding of the speleogenetic processes that have locally dominated (Collonet et al. 2017, Piccini 2011). As mentioned by Littva et al. 2015, to perform the cave passage orientation analysis, the plan cave map was used to construct a grid displaying the general cave passage azimuths. Cave passages were excluded which had no clear general orientation (e.g. cave chambers and/or halls), and cave passage length was not considered in this analysis. In the next step, rose diagrams were made displaying the overall orientation of cave passages of each cave by using Tectonics FP software written by Franz Reiter and Peter Acs in 1996, updated in 2020 (Reiter and Acs 1996) (Fig. 2-6). The individual results obtained are merged into different combinations for interpretation, including the overall cave passage orientation rose diagram which shows the major development direction of cave conduits in the study area; the rose diagram of cave passage orientation of cave groups that divided by local structure blocks and the cave levels show the main development direction of the cave passages of each group.

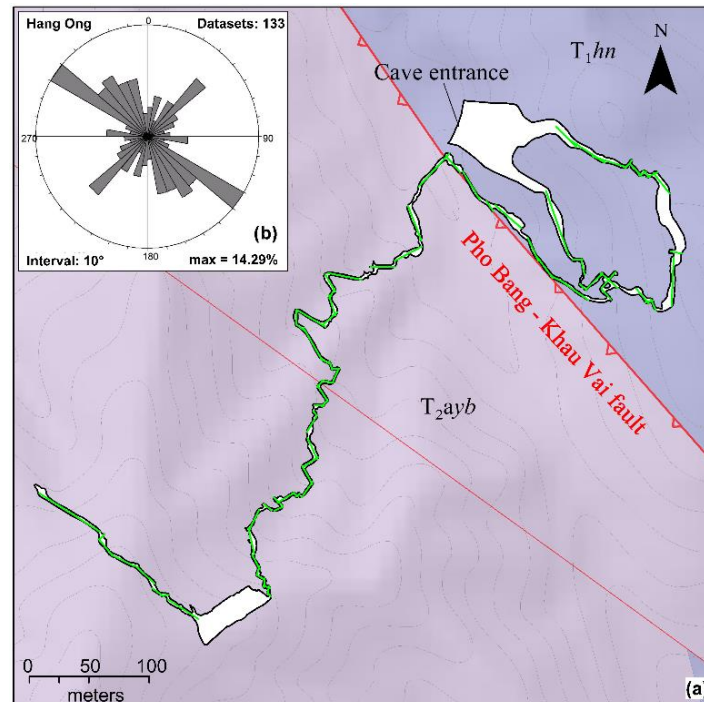


Fig. 2-6 An example to illustrate the cave passages orientation analysis. (a) The grid displaying general cave passage azimuths is constructed based on Hang Ong cave map on the geological background; (b) Rose diagram of cave passage orientations (number %, 10° classes).

2.4 Results and Discussion

2.4.1 Results

2.4.1.1 Cave classification based on speleomorphologic features of cave conduits

The complete results of the computation of geometric parameters for 49 caves which developed on different carbonate formations in the study area are shown in Appendix 2-1. The plots nicely show the relations between these parameters (WH, T, K, V) (Fig.2-7). Then, the classification of cave types based on geometric parameters features was performed (As mentioned by Jouves et al. 2017 in Sec. 2.3.2).

The results of cave classification show that there are 27 vadose branchwork caves (VB), 12 water-table caves (WTC), without the presence of angular mazes. The results also show that there is a cave type that has a low Vertical index ($V < 0.2$) with conduit sections ranging in shape from circular to vertical ($WH < 1.5$) including 10 caves. These caves are not only by definition developed horizontally but also have steeply sloping passages. However, the passages that develop laterally are dominant throughout the entire cave. Field observations show that the horizontal passages of these caves can be formed by

flow beneath the water table or developed under the control of a bedding plane or stratigraphic contact but still can be influenced by tectonically induced discontinuities. This result is supported by several studies (Jaskolla and Volk 1986, Osborne 2001, Littva 2015) which discovered that many caves formed along the intersection of a fault system with discontinuity surface, and these cave passages are usable for tectonic analysis. In this study, we propose to call this type of cave "Mixed cave" (MC).

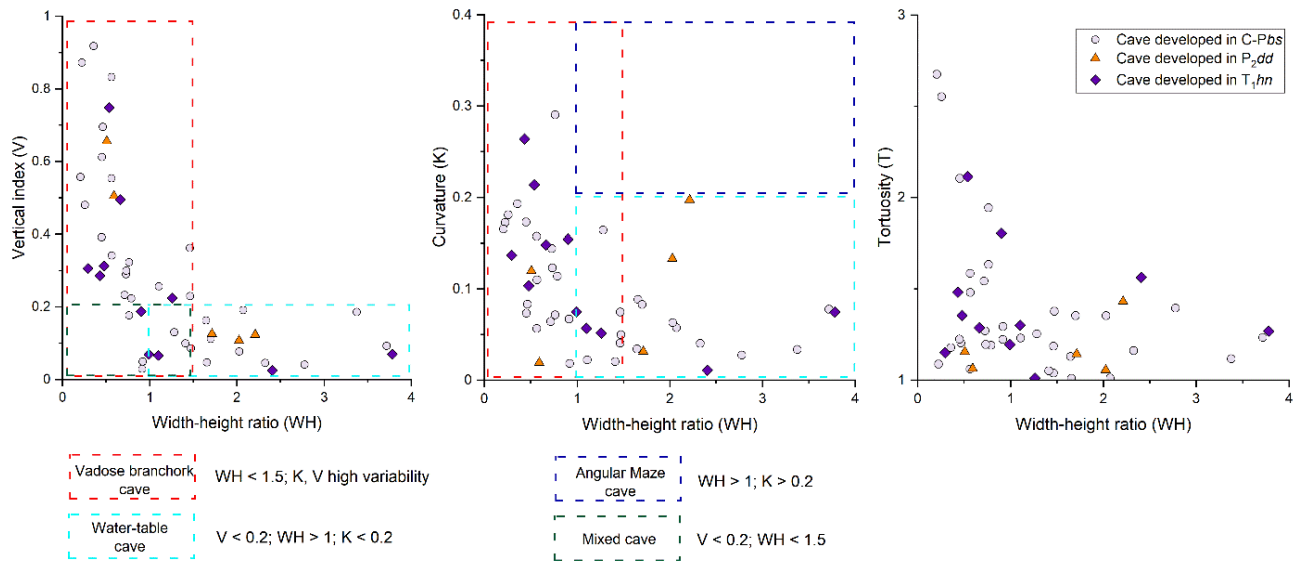


Fig. 2-7 Graph showing the distribution of geometric parameters (WH, T, K, V) and classification for the 49 cave conduit systems in Dong Van Karst Plateau.

Figure 2-7 also shows that the VB caves have vertically elongated conduit sections ($WH < 1$). The range of the vertical index is highly variable with caves developing almost vertically ($V > 0.8$) to caves developing less steeply ($0.13 < V < 0.8$). Actual observations show that the Vertical index decreased when the horizontal cave passages appeared in VB cave systems. These cave passages developed in Carboniferous carbonate unit (C-Pbs) during stable tectonic periods, while forming under the control of bedding planes in Dong Dang (P_2dd) and Hong Ngai (T_1hn) formations.

2.4.1.2 Cave levels, speleomorphologic features and cave passage orientation in different cave groups

Based on the geological data, the study area can be divided into three different “local structural blocks” (Fig. 2-2b) with the boundary delimited by major fault zones including: Structural Block 1 (SB1) which is located SW of the F1 fault, limited by the F7 fault (NE-SW direction) and Nhim River fault zone

(NW-SE direction); Structural Block 2 (SB2) which is limited by F1 fault and F4 fault, the Western boundary is F3 fault zone; Structural Block 3 (SB3) which is located NE of the F4 fault, which is limited by F6 fault and overthrust fault North Dong Van.

A statistical analyses of the elevation of horizontal cave passages was performed to identify the cave levels in the various local structural blocks and in the entire study area. Within each structural block, the cave group was divided by cave classes to conduct an analysis of the geometric parameters and cave passage orientation. Details of the cave groups are shown in Appendix 2-1.

Statistical analysis of horizontal cave passage and division cave classes

The frequency graph (Fig. 2-8) obtained from the 50 m elevation group of caves shows the vertical distribution of cave passages in the entire study area and in each structural block. Throughout the study area, horizontal cave passages were formed and distributed at different elevations from 200 to 1700 masl. Specifically, Fig. 2-8 shows five peaks of cave passage lengths ranging in the following groups: 200-250 masl, 850-900 masl, 1050-1150 masl, 1200-1250 masl, and 1350-1450 masl. In passage length, these peaks range from 890m to 2130m. (Details of the statistics of horizontal cave-passage length are shown in Appendix 2-2a).

Considering the different structural blocks, the results also show that there is a variation in the distribution of cave levels. In SB1, the horizontal cave passage has rather limited development. They are distributed at scattered elevations from 200 to 1400 masl, with a peak at 200-250 masl reaching 894 m of passage length. The SB2 has strong cave development with a total of 9184 m equivalent to 59.9% of horizontal cave passage length in the entire study area. They are distributed nearly continuously at altitudes from 850 to 1700 masl, with three peaks at 850-900 masl (950m of passage length), 1200-1250 masl (809m of passage length), and 1350-1450 masl (ranging from 1096m to 1487m of passage length). Horizontal cave passages in SB3 develop quite concentratedly at elevations from 1000 to 1250 masl with two peaks. The first peak at 1000-1050 masl reaches 1802m of passage length and another peak at 1200-1250 masl reaches 842m of passage length.

On the basis of the obtained results on the degree of development of horizontal cave passage and the elevation of planation surfaces on the DVKP identified in Sec. 2.2.2, we propose dividing the cave classes according to the elevation of their corresponding planation surfaces as a basis for calculations in the next following sections. In particular, due to rather limited development, we also propose combining the cave passages that have developed at altitudes lower than 650 masl into a single class. As a result, there are five cave classes in the study area (Fig. 2-8) divided as follows:

- Cave class 1 (CL1) at 1500-1700 masl;
- Cave class 2 (CL2) at 1250-1450 masl;
- Cave class 3 (CL3) at 1000-1250 masl;
- Cave class 4 (CL4) at 700-950 masl;
- Cave class 5 (CL5) at < 650 masl.

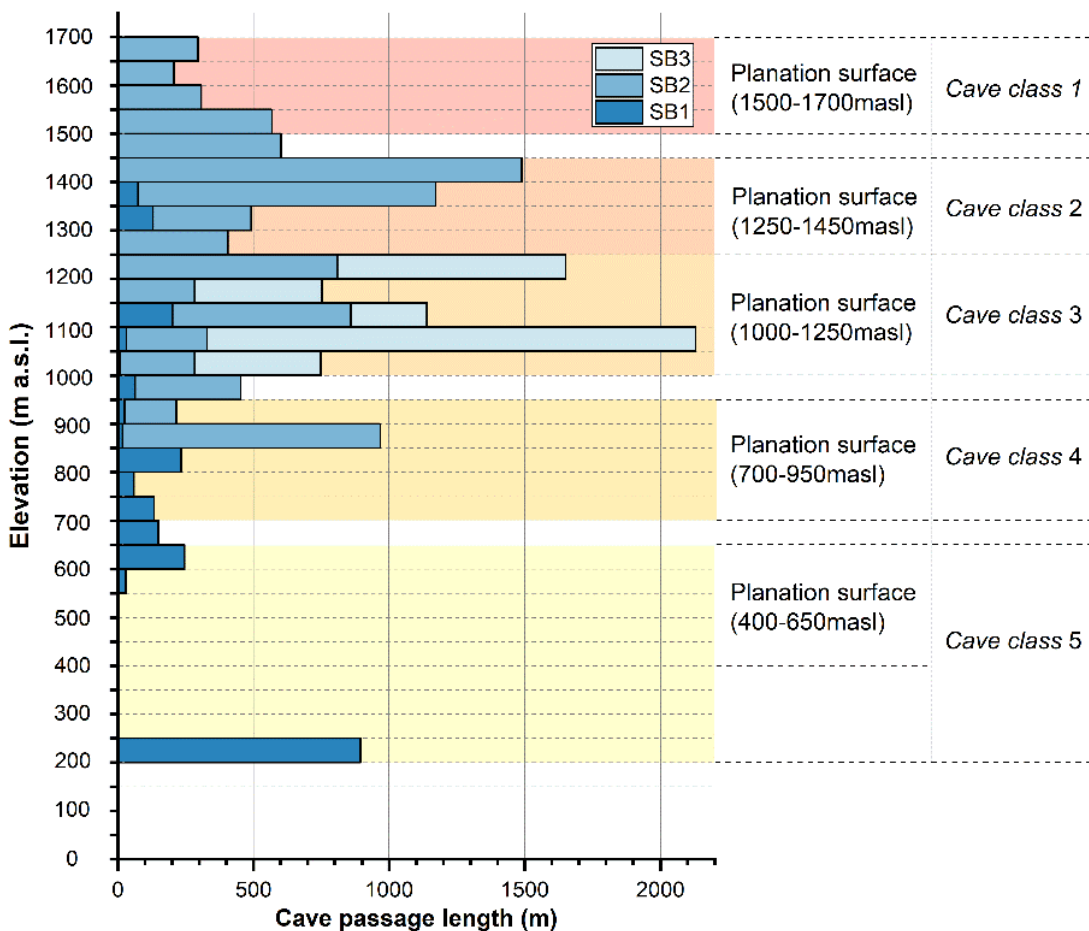


Fig. 2-8 Elevation distribution of horizontal cave passages and cave class division.

Geometric parameters of cave conduits in different cave groups

Cave entrances cannot always be used to identify cave levels because they commonly are more abundant in the upper part of a karst system and their distribution depends on many surficial geomorphic factors not linked to groundwater hydrology; this is especially the case for caves that have a large vertical range (VB cave). However, a cave with different horizontal levels linked with distinct evolution stages will have an average elevation that does not represent its real pattern. Therefore, in this study, we propose to use the average elevation (E_a) to represent the level where VB caves develop ($V > 0.2$), and the modal elevation (E_m) to represent the altitude of MC and WTC caves ($V < 0.2$).

Figure 2-9 shows the correlation of geometric parameters (WH, T, K, V) with different cave classes and local structural blocks. Based on the cave classification, the speleomorphological characteristics of the cave systems in each group are described as follows.

At class 5 (<650m), there is only Na Luong cave developed in SB1. Geometric parameters of Na Luong cave conduit show characteristics of mixed cave type which is developed horizontally at the lowest altitude (238 masl) in the limestone of Bac Son formation (C-Pbs).

At class 4, caves are developed in SB1 and SB2. Caves in SB1 are in the type of VB cave that develop in both Carboniferous - Permian (C-Pbs) and Triassic carbonate rocks (T₁hn). In this group, cave passages are not very steep (V ranges from 0.29 to 0.362), with conduit sections varying from circular to longitudinally elongated (WH ranges from 0.294 to 0.665). Only Lung Chinh Cave formed with steeply sloping passages (V = 0.75), with a sinuous pattern (T = 2.114, K = 0.21), and circular conduit sections (WH = 0.54). These parameters show the features of a cave developed in the Vadose zone that was controlled by fracture system. In the SB2, there is Tia Sang cave, developed in Carboniferous - Permian carbonate rock (C-Pbs), with a total length of 1154m. This cave developed almost in the horizontal plane (V=0.093) with horizontally elongated conduit sections (WH = 3.719). These indicators of a WTC cave, combined with geologic information show that the horizontal development of this cave was formed along the contact of lithologically contrasting rocks.

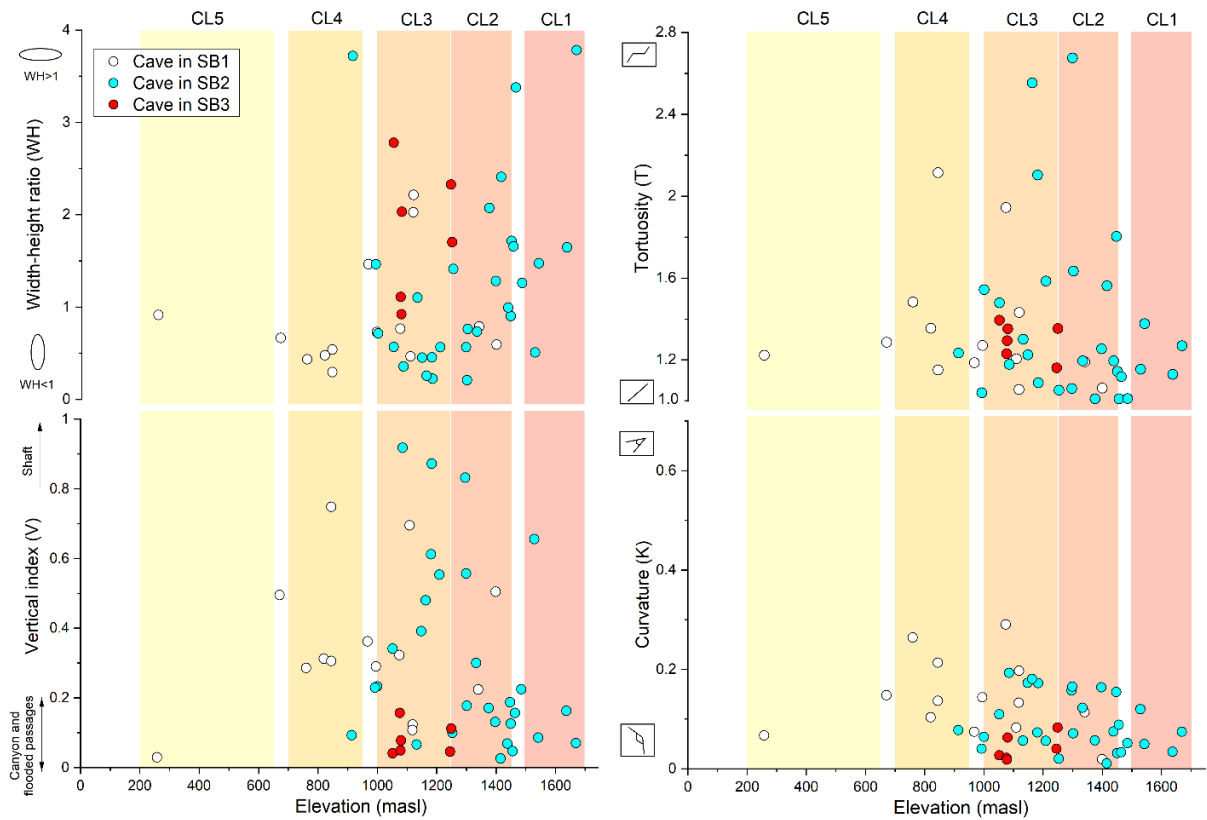


Fig. 2-9 Graph showing the distribution of geometric parameters (WH, T, K, V) in different cave levels and local structural blocks.

At class 3, caves develop in three local structural blocks, in which caves in SB3 differ from the other groups. In this group, cave passages are mostly horizontal (V ranges from 0.041 to 0.256), with conduit sections varying from circular to horizontal elongate (WH ranged from 0.921 to 2.778). These geometric values indicate that there are 3 cave types in this group, including 4 WTC caves, one MC cave (Ma Le 2), and one VB cave (Ma Le 1).

Also in class 3, caves appear scattered on SB1 (4 caves), mainly on SB2 (9 caves), and developed in different Carboniferous - Permian - Triassic carbonate rocks. It can be seen in these groups there are caves that have a low Vertical index (V from 0.07 to 0.12), including 2 WTC caves (Pho Cao 1, Pho Cao 2019) with horizontally elongated conduit sections (WH from 2.03 to 2.21) and one MC cave (Meo Vac 1) with circular conduit sections (WH=1.1). In addition, there are also caves that develop slightly inclined ($0.23 \leq V \leq 0.34$), with vertically elongated conduit sections (WH ranged from 0.57 to 0.76) in the type of VB cave (Kho Thong 1, Pai Lung, Sung Ta). In SB2, caves mainly develop vertically, starting with a sinkhole entrance, followed by passages with variable verticality, interspersed

with horizontal passages (V ranged from 0.391 to 0.917) and often ending at siphons (lake) or small cracks which are difficult to enter by a human or a horizontal section filled by rockfall blocks and sediment. These caves developed a winding (meandering) pattern ($0.06 \leq K \leq 0.19$; $1.59 \leq T \leq 2.68$) with vertically elongated conduit sections (WH ranged from 0.21 to 0.56) (this was seen in Xa Lung 1, Xa Lung 2, Pa Ca 1, Quan Si 1, Lung Pu 1, in which, Xa Lung 2 and Pa Ca 1 are the deepest caves in the study area). These features indicate tectonic and structural factors that contributed to the development of cave systems in the vadose zone.

At class 2, caves appeared mainly on SB2 (11 caves), scattered on SB1 (2 caves), and developed on the carbonate rock of three formations including T_1hn , P_2dd , and $C-Pbs$. In the SB1 cave group, slightly inclined caves developed (V ranged from 0.22 to 0.50), with vertically elongated conduit sections (WH ranged from 0.59 to 0.79) in the type of VB cave. Meanwhile, most of the caves develop in the SB2 have a low Vertical index ($0.03 \leq V \leq 0.22$), a high variation in Curvature index ($0.01 \leq K \leq 0.16$) while the Tortuosity index changes slightly ($1.01 \leq T \leq 1.80$), including five MC caves (Dong Nguyet, Rong TL, Hang Ong, Hang May, Lung Pu 3) and three WTC caves (Xa Phin B, Rong ST, Sang Tung 2). Especially, Hang Ong is evaluated as one of the deepest caves in the study area (341m depth), but the Vertical index is very low ($V=0.19$). The survey data shows that this is a long and multilevel cave (1679m length), developed over a long time under variable hydrodynamic conditions due to climate and/or tectonic evolutions ($WH=0.90$).

Sparse cave development at class 1, mostly fossil caves, developed horizontally (V ranges from 0.07 to 0.16), with horizontally elongated conduit sections (WH from 1.47 to 3.78). Only Sung La Tren 3 cave has the form of a sinkhole ($V = 0.66$, $WH = 0.51$).

In summary, these results show the diversity of speleomorphologic characteristics of cave systems in each cave group. There are significant similarities between group SB2-CL2 and SB3-CL3 where these cave groups have a low Vertical index, most of the caves are in the type of WTC and MC. Meanwhile, the geometric parameters of cave conduits in groups SB1-CL4, SB2-CL3 show the features of caves developed in the Vadose zone. The cave system has developed strongly in structure block 2 (29 caves in total) and contains the deepest and longest caves in the study area.

Orientation of cave passages at different cave classes and structural zones

Before performing the cave passage orientation analysis, water-table caves were removed from the dataset due to unclear conduit orientations. The results of the cave passage orientation analysis of overall caves and each cave group at different cave classes and local structural blocks are shown in Figure 2-10. Accordingly, the rose diagram displaying the overall orientation of all measured cave passages (Fig. 2-10b) shows two main passage orientations develop in approximately NW-SE and sub-latitude direction and there are two subsidiary orientations developed in the sub-meridian and NE-SW direction.

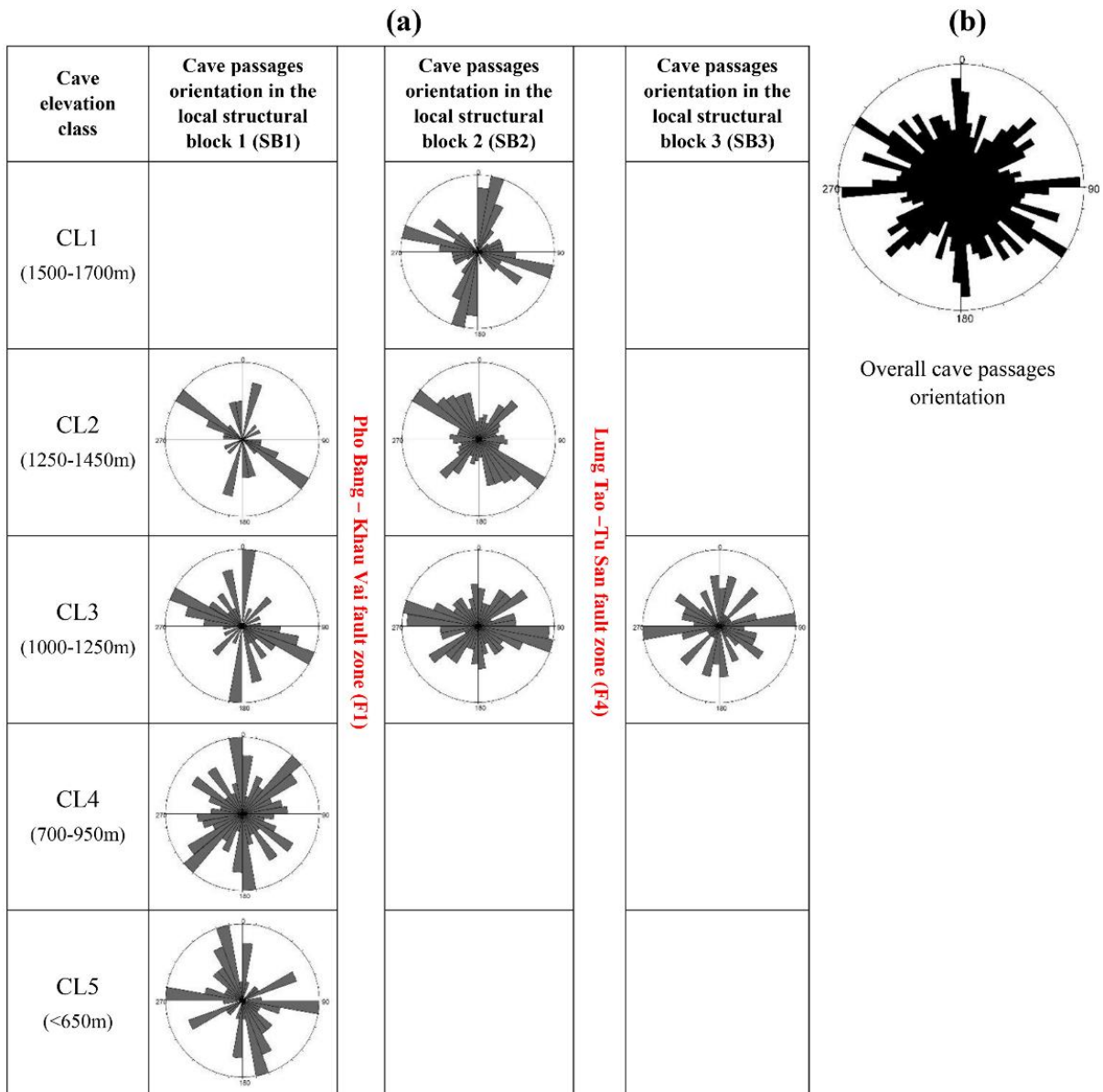


Fig. 2-10 Rose diagrams display (a) the cave passage orientation in different cave groups and (b) the overall cave passages orientation in the study area.

Figure 2-10a shows the rose diagrams of cave groups SB1-CL2, SB1-CL3, SB2-CL1, SB2-CL2 display the main passage orientation in an NW-SE direction and the SB2-CL1 cave group also displays the second main orientation in the NNE-SSW direction. In the cave groups SB1-CL5, SB2-CL3, and SB3-CL3, the main cave passage orientation follows the W-E direction, in which, SB1-CL5 group has the second main orientation in the NNW-SSE direction. In addition, the rose diagram of the SB1-CL3, SB1-CL4 cave groups displays the main passage orientation which is in an approximately N-S direction. And there are two cave groups SB1-CL4 and SB2-CL3 have the second main cave orientation is present in the NE-SW direction.

To sum up, the rose diagram displaying the passage orientation of all cave groups reveals that there are striking similarities in the main orientation of each group regardless of their position. Two distinctive maxima are present at NW-SE and W-E orientations, with two less distinctive maxima at NE-SW and N-S to NNW-SSE orientations.

2.4.2 Discussion

In this study, geometric parameters and the orientation of cave conduits were computed from a database of 49 caves in order to characterize the structure and development of karstification in the Dong Van Karst Plateau. In the following, we summarize and discuss these results.

2.4.2.1 Cave passage orientation in relationship to the geological structure and tectonic periods

Caves are usually young features, so it is possible to link them to Neotectonic activities occurring in the study area. The main passage orientations in cave groups SB1-CL2, SB1-CL3, SB2-CL1, SB2-CL2 are in an approximately NW-SE direction (Fig. 2-10a), which is similar to the direction of the main fault systems in Dong Van Karst Plateau. This result can be explained by the tectonic activities occurring in the Cenozoic that reactivated the NW-SE fault systems, resulting in creating spaces or favorable channels for water to flow and corrosion to dissolve the host rock forming caves that follow this direction. In addition, the SB1-CL4 and SB2-CL3 cave groups also are aligned along the second main orientation in the NE-SW direction. Besides fault control, this result could be because some cave

passages develop under the control of the bedding plane of Triassic siliceous limestone (*T_{1hn}*) which is medium bedded and dips in NE direction.

Littva et al. (2015) used the "Cavitonics" method to explain the relationship between Neotectonics and cave passage orientation which suggests that the orientation of cave passages is perpendicular to the extensional component (σ_3) of the tectonic stress field, which means the same direction as the maximum compressive stress axis (σ_1). Applying this approach to the cave system on Dong Van Karst Plateau, it can be seen that, if Neotectonic faulting is considered a factor controlling the formation and development of a cave system, then the cave passage orientation will have the same direction as the maximum compressive stress fields. In the Neotectonic period, the geodynamic regime in Dong Van Karst Plateau developed according to the two-phase deformation model, sub-latitude compression in the early phase (Eocene-Miocene), and sub-meridian compression in the later phase (Pliocene-Quaternary), therefore, cave passages will be oriented mainly in these two directions.

It is clear that, in the remaining cave groups, the main passages orientation in cave groups SB1-CL5, SB2-CL3, and SB3-CL3 are in an approximately W-E direction, which are similar to the direction of the maximum compressive stress axis in the early phase (Eocene-Miocene). In addition, SB1-CL5 group display the second main orientation in the NNW-SSE direction, SB2-CL1 group also has the second main orientation in NNE-SSW direction and the main passage orientations in cave groups SB1-CL3, and SB1-CL4 is in an approximately N-S direction, which are similar to the direction of the maximum compressive stress axis in the late phase (Pliocene-Quaternary).

2.4.2.2 Relationship between cave levels and planation surfaces on Dong Van Karst Plateau

As mentioned by Palmer (1987), Filipponi et al. (2009), there are some limitations in using horizontal cave levels as an indicator to interpret the karst evolution process because of limited field data analysis, combined with uncertainty as to what constitutes a true cave level such as cave passages developing under the control of a stratigraphic boundary or bedding plane or litho-structural as in the case of an inception

horizons. Therefore, cave levels can be correctly interpreted only where an accurate morphologic and structural analysis is performed in order to exclude such cave passages.

To combine actual observations with geological data, as well as geometrical parameters of cave conduits in the study area, it should be mentioned that there are many caves developed along bedding planes in the Permian ($P_2\bar{d}\bar{d}$) and Triassic (T_1hn) carbonate units, such as Hang Rong ST, Sang Tung 2, Pho Cao 2, Tru Lia. In addition, in the Carboniferous ($C-Pbs$) carbonate unit, there are caves such as Tia Sang, Xa Phin B, Hang Ho, Sang Ma Sao, Bo Doi, and Ma Le 1, 2 which are mainly developed along the stratigraphic boundaries. In fact, these results are limited by the accessibility of caves and the level of cave exploration, because there could be many other cave passages that are not yet discovered. In addition, varied interpretations may have resulted from different experiences and evaluations of speleologists. Therefore, in this calculation, we suggest excluding caves that our study has shown to have developed laterally under the influence of horizontal bedding and/or stratigraphic boundaries.

According to the data in Appendix 2-2b, there are significant changes in horizontal cave passages at different elevation classes after the questionable caves were removed. As a result, the cumulative passage length decreased greatly at altitudes of 850-900 masl, 1000-1150 masl, 1400-1500 masl, and 1550-1700 masl. Most significant was a decrease in cave-passage length to 1315 m at 1050-1100 masl. Next, at elevation class 850-900 masl, the cave passage length decreased strongly, with a decrease of 950 m. In the remaining altitude classes, the passage length slightly decreases from 88 to 410 m.

Appendix 2-2b also shows that the horizontal cave passages are distributed at different elevation classes from 200 to 1550 masl with three peaks. The passage length reaches 894 m at 200-250 masl. At 1200-1250 masl the passage length reaches a maximum is 1651 m, and at 1350-1450 masl the passage length reaches 898 m to 1077 m. In addition, the revised version of the passage distribution in the cave system showed a slight development at 1050-1150 masl with a passage length equivalent to 753-814 m.

The degree of association between horizontal cave passage and planation surface that are formed during tectonically stable periods can be used as a consistent indicator of tectonic periods and karst evolution, as mentioned in the studies of Palmer (1987), Filipponi (2009), Piccini (2011). According to the statistics of elevation distribution of horizontal cave passages after excluding unsuitable caves (App. 2-2b), it can

be seen that in DVKP there are two cave levels that can be related to the planation surface, including cave level with a peak at 1200-1250 masl, equivalent to the planation surface at 1000-1250 masl and cave level with a peak at 1350-1450 masl in comparison to the planation surface at 1250-1450 masl. In addition, there is a peak at the lowest altitude 200-250 masl; however, the cave survey shows that only Na Luong Cave developed at this elevation. This cave is directly connected to Na De spring, a very large karst spring that probably drains large parts of the Dong Van Karst Plateau and forms the upstream end of Nhiem River. These features suggest that this could be the local base level for karst erosion in this area (Fig. 2-11).

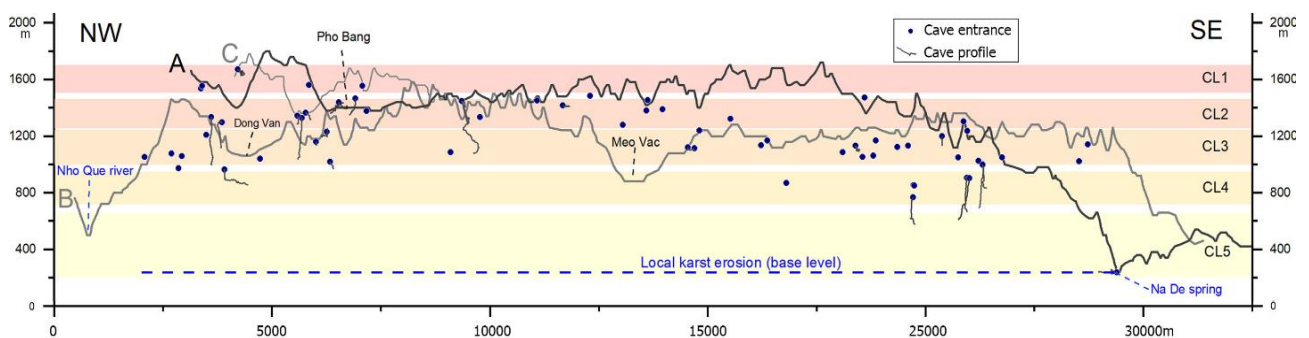


Fig. 2-11 Cross-sections (in Fig. 2-1) showing the development and structure of cave systems and the karstification features on Dong Van Karst Plateau.

Determining whether a cave level may be related to the planation surface needs to be based on a combination of several factors. However, in this study, due to the small number of caves and their limited development in a large karst region, the results obtained are very encouraging, because they represent an aspect of the relationship between the cave level and the planation surface, as well as karst evolution on the Dong Van Karst Plateau. To prove these points quantitatively, the absolute age analysis of cave sediments, stalagmites, etc. at different cave levels, and a comparison with the results of this paper, should be performed in the future.

2.5 Conclusions

This paper has highlighted the relationship between cave systems and the tectonic and geomorphologic development on the Dong Van Karst Plateau, based on analysis and statistics of geometric parameters and orientation of cave passages. Our work has led us to conclude the following:

- Cave classification based on cave conduits geometric parameters shows that caves developed mainly in the vadose zone (27 vadose branchwork caves, 10 mixed caves developed under the control of fault systems, and 12 water-table caves).
- The degree of correlation between cave levels and planation surfaces suggests that the development of horizontal cave passages is related to two levels of planation surfaces, including one at 1250-1450 masl (equivalent to cave level at 1350-1450 masl), and at 1000-1250 masl (corresponding to cave level at 1200-1250 masl).
- The results of geometric parameter analysis of cave conduits in different cave groups show that the karst evolution in the local structural block 3 is mature. In this group, after corrosion to the local base level, the cave system continues to develop horizontally, expanding into lithologically different rocks. Meanwhile, the karst evolution in local structural blocks 1 and 2 are mostly at a youthful stage, with cave systems formed by dissolution, leaching or erosion which are mainly of the isometric form (developed almost vertically), and not yet deepened to the local base level. In these groups, some caves have developed laterally under the influence of a relatively resistant horizontal layer.
- Passage orientation show that the cave system on the Dong Van Karst Plateau formed and developed under the influence of tectonic activity during in the Cenozoic. In terms of cave passage orientation, there are three main distinct trends. The dominant orientation is roughly E-W, coinciding with the direction of the maximum compressive stress axis in the early phase (Eocene-Miocene). Next is a trend roughly N-S with the same direction as the maximum compressive stress axis in the late phase (Pliocene-Quaternary). The last orientation follows the NW-SE direction due to the reactivation of paleo-fault systems having the same direction. In addition, there is a minor trend in the NE-SW direction that follows the dip direction of bedding planes.

Although there are limitations due to the accessibility and the level of cave exploration, this research suggests that cave databases could be used in order to clarify the development and structure of karstification in a region of soluble rocks. Specifically, Jouvès's (2017) approach for quantitative cave

classification based on the geometric parameters of cave conduits is useful for identifying the caves that are usable for tectonic analysis. Additionally, the analysis of cave passage orientation (Littva et al. 2015) represents a simple and useful approach for the study of neotectonics. On the other hand, the degree of correlation of cave levels and planation surfaces in this research once again emphasizes the validity of previous studies (Palmer 1987, Filipponi et al. 2009, Piccini 2011) which suggest that cave levels are among the morphological factors that are consistent indicators of karst evolution. Results presented so far have been very encouraging and could quantitatively demonstrate the association between cave systems and the development and structure of karstification on Dong Van Karst Plateau.

Acknowledgments This work was carried out within the financial support of the German Federal Ministry of Education and Research (BMBF) [grant number 02WCL1291A and 02WCL1415] and was partly sponsored by the Catholic Academic Exchange Service (KAAD). We gratefully acknowledge the Belgian SPEKUL club, as well as the Vietnam Institute of Geosciences and Mineral Resources (VIGMR, Hanoi) for their support during the provision of cave databases. Special thanks are given to David Lagrou, Ho Tien Chung and Doan The Anh for their valuable comments, as well as Dominik Richter, Nguyen Van Dong, Nguyen Cao Cuong, Nguyen Manh Tuan for their help during field work. Finally, we thank editor in chief Wolf-Christian Dullo, as well as reviewer Leonardo Piccini for their thorough review and valuable comments and suggestions.

Appendix 2-1 Summary of cave survey data and cave conduits geometric parameters in Dong Van Karst Plateau

No.	Cave name	Development [m]	Denivelation [m]	Vertical index (V)	Tortuosity (T)	Curvature (K)	Width-height ratio (WH)	Cave entrance elevation [masl]	Average elevation [masl]	Modal elevation [masl]	Formation	Cave type	Local Structural Block
1	Na Luong	1113	-32.7	0.029	1.223	0.067	0.915	238	242	258	C-P <i>bs</i>	MC	
2	Sung Khe 2	389	-192	0.495	1.286	0.148	0.665	768	671	768	T ₁ <i>hn</i>	VB	
3	Sung Khe 1b	183	-57.1	0.313	1.354	0.103	0.478	849	820	849	T ₁ <i>hn</i>	VB	
4	Sung Khe 1a	52	-15.8	0.306	1.151	0.137	0.294	853	845	853	T ₁ <i>hn</i>	VB	
5	Sung Khe 3-4	1030	-296	0.286	1.482	0.264	0.433	903	758	903	T ₁ <i>hn</i>	VB	
6	Ha Su 1	411	-149	0.362	1.186	0.075	1.463	983	967	983	C-P <i>bs</i>	VB	
7	Lung Chinh	504	-306	0.748	2.114	0.214	0.538	1006	844	1006	T ₁ <i>hn</i>	VB	SB1
8	Sung Dia 2	173	-50	0.290	1.270	0.144	0.729	1021	995	1021	C-P <i>bs</i>	VB	
9	Phong Tung	92	-63.7	0.695	1.205	0.083	0.465	1199	1074	1199	C-P <i>bs</i>	VB	
10	Sung Ta 2	162	-52.3	0.322	1.944	0.290	0.764	1084	1060	1086	C-P <i>bs</i>	VB	
11	Pho Cao 1	94	-11.6	0.123	1.431	0.197	2.213	1113	1112	1119	P ₂ <i>dd</i>	WTC	
12	Pho Cao 2019	164	-17.6	0.107	1.055	0.133	2.026	1118	1109	1118	P ₂ <i>dd</i>	WTC	
13	Pho La	195	-51	0.224	1.191	0.114	0.789	1365	1340	1365	C-P <i>bs</i>	VB	
14	Ta Lung 0	280	-141.2	0.504	1.062	0.019	0.592	1470	1399	1470	P ₂ <i>dd</i>	VB	
15	Tia Sang	1154	-107	0.093	1.233	0.078	3.719	963	914	963	C-P <i>bs</i>	WTC	
16	Pai Lung	201	-47	0.233	1.543	0.064	0.715	1017	1000	1017	C-P <i>bs</i>	VB	
17	Sang Chai 1A	501	-115	0.229	1.039	0.040	1.464	1050	992	1050	C-P <i>bs</i>	VB	
18	Kho Thong 1	190	-64.8	0.341	1.479	0.110	0.567	1085	1052	1085	C-P <i>bs</i>	VB	
19	Meo Vac 1	617	-41	0.066	1.300	0.057	1.102	1132	1112	1132	T ₁ <i>hn</i>	MC	
20	Quan Si 1	117	-107.2	0.917	1.178	0.193	0.357	1139	1085	1139	C-P <i>bs</i>	VB	SB2
21	Hang May 2	65	-25.6	0.391	1.224	0.173	0.451	1160	1148	1160	C-P <i>bs</i>	VB	
22	Hang May	598	-57.9	0.100	1.051	0.020	1.411	1230	1224	1253	C-P <i>bs</i>	MC	
23	Lung Pu 1	118	-102.9	0.872	1.088	0.172	0.225	1235	1183	1235	C-P <i>bs</i>	VB	
24	Xa Lung 1	262	-178	0.553	1.585	0.056	0.564	1301	1209	1301	C-P <i>bs</i>	VB	
25	Lung Pu 3	181	-32	0.177	1.633	0.071	0.763	1302	1286	1302	C-P <i>bs</i>	MC	

Continuation of **App. 2-1**

No.	Cave name	Development [m]	Denivelation [m]	Vertical index (V)	Tortuosity (T)	Curvature (K)	Width-height ratio (WH)	Cave entrance elevation [masl]	Average elevation [masl]	Modal elevation [masl]	Formation	Cave type	Local Structural Block
26	Pa Ca 1	475	-293	0.612	2.104	0.073	0.455	1328	1181	1328	C-P <i>bs</i>	VB	
27	Xa Lung 2	1951	-340	0.480	2.553	0.181	0.258	1332	1163	1332	C-P <i>bs</i>	VB	
28	Doan Ket	88	-73.3	0.832	1.059	0.157	0.564	1333	1296	1333	C-P <i>bs</i>	VB	
29	Hang Ong	1679	-341	0.187	1.803	0.154	0.902	1446	1274	1446	T ₁ <i>hn</i>	MC	
30	Pa Ca 2	106	-59	0.557	2.675	0.165	0.208	1342	1299	1342	C-P <i>bs</i>	VB	
31	Dong Nguyet	1143	-78	0.069	1.195	0.075	0.993	1438	1400	1438	T ₁ <i>hn</i>	MC	
32	Xa Phin B	123	-33.2	0.191	1.010	0.057	2.073	1375	1359	1375	C-P <i>bs</i>	WTC	
33	Hang Doi TL	300	-90	0.300	1.195	0.123	0.733	1378	1333	1378	C-P <i>bs</i>	VB	SB2
34	Hang Rong TL	241	-28.5	0.131	1.254	0.164	1.282	1389	1382	1397	C-P <i>bs</i>	MC	
35	Hang Rong ST	404	-10.4	0.026	1.562	0.011	2.408	1415	1411	1415	T ₁ <i>hn</i>	WTC	
36	Sang Tung 2	262	-33	0.126	1.143	0.031	1.714	1450	1436	1450	P ₂ <i>dd</i>	WTC	
37	Lung Tung 1	172	-8.1	0.047	1.009	0.088	1.656	1454	1452	1456	C-P <i>bs</i>	WTC	
38	Xa Phin 3	437	-116	0.186	1.117	0.033	3.377	1464	1407	1464	C-P <i>bs</i>	WTC	
39	Ban Sinh Thau	401	-90	0.224	1.010	0.051	1.261	1485	1441	1485	T ₁ <i>hn</i>	MC	
40	Nhu Sang	926	-22	0.086	1.377	0.050	1.474	1536	1502	1542	C-P <i>bs</i>	MC	
41	Bo Doi	200	-12	0.162	1.129	0.034	1.647	1554	1595	1637	C-P <i>bs</i>	WTC	
42	Sung La Tren 3	97	-63.4	0.656	1.154	0.120	0.509	1561	1529	1561	P ₂ <i>dd</i>	VB	
43	Tru Lia	541	-41.4	0.070	1.269	0.074	3.781	1669	1650	1669	T ₁ <i>hn</i>	WTC	
44	Hang Ho	337	-13.8	0.041	1.394	0.027	2.778	1038	1045	1052	C-P <i>bs</i>	WTC	
45	Ma Le 1	218	-55.9	0.256	1.230	0.022	1.109	1052	1076	1099	C-P <i>bs</i>	VB	
46	Ma Le 2	899	-44.2	0.049	1.293	0.018	0.921	1059	1057	1078	C-P <i>bs</i>	MC	SB3
47	Ma Le 5	610	-47.2	0.077	1.352	0.063	2.030	1077	1059	1080	C-P <i>bs</i>	WTC	
48	Sang Ma Sao	1254	-140	0.112	1.353	0.083	1.701	1138	1185	1249	C-P <i>bs</i>	WTC	
49	Hang Dot Pha	1540	-70	0.045	1.160	0.040	2.327	1208	1217	1245	C-P <i>bs</i>	WTC	

Appendix 2-2 Summary of the statistics of horizontal cave-passage length in Dong Van Karst Plateau

Elevation class [masl]	(a)				(b)			
	Cave passage length (m)				Cave passage length after excluding unsuitable caves (m)			
	Entire DVKP	SB1	SB2	SB3	Entire DVKP	SB1	SB2	SB3
1650 - 1700	294.7	-	294.7	-	-	-	-	-
1600 - 1650	206.6	-	206.6	-	-	-	-	-
1550 - 1600	307.6	-	307.6	-	-	-	-	-
1500 - 1550	567.9	-	567.9	-	567.9	-	567.9	-
1450 - 1500	601.4	-	601.4	-	601.4	-	601.4	-
1400 - 1450	1488.6	-	1488.6	-	898.3	-	898.3	-
1350 - 1400	1171.5	75.2	1096.3	-	1077.3	75.2	1002.1	-
1300 - 1350	492.5	129.4	363.1	-	492.5	129.4	363.0	-
1250 - 1300	405.5	-	405.5	-	405.5	-	405.5	-
1200 - 1250	1651.1	-	809.2	841.9	1651.0	-	809.2	841.9
1150 - 1200	753.5	-	283.4	470.1	753.4	-	283.4	470.1
1100 - 1150	1140.0	201.4	657.0	281.6	792.8	135.8	657.0	-
1050 - 1100	2130.2	32.0	296.4	1801.8	814.9	32.0	296.4	486.5
1000 - 1050	748.4	8.1	275.9	464.4	337.6	8.1	275.9	53.6
950 - 1000	453.7	63.8	389.9	-	447.7	63.8	383.9	-
900 - 950	215.4	25.1	190.3	-	127.4	25.1	102.3	-
850 - 900	967.9	17.9	950.0	-	17.9	17.9	-	-
800 - 850	234.0	234.0	-	-	234.0	234.0	-	-
750 - 800	59.5	59.5	-	-	59.5	59.5	-	-
700 - 750	133.6	133.6	-	-	133.6	133.6	-	-
650 - 700	150.5	150.5	-	-	150.5	150.5	-	-
600 - 650	245.6	245.6	-	-	245.6	245.6	-	-
550 - 600	29.6	29.6	-	-	29.6	29.6	-	-
500 - 550	-	-	-	-	-	-	-	-
450 - 500	-	-	-	-	-	-	-	-
400 - 450	-	-	-	-	-	-	-	-
350 - 400	-	-	-	-	-	-	-	-
300 - 350	-	-	-	-	-	-	-	-
250 - 300	-	-	-	-	-	-	-	-
200 - 250	893.7	893.7	-	-	893.7	893.7	-	-
Total	15343.0	2299.4	9183.7	3859.8	10732.3	2233.8	6646.3	1852.1

Chapter 3

3 Hydrogeology and Hydrogeochemical processes

Reproduced from: Diep Anh Tran, Nadine Goeppert, Nico Goldscheider (2022) Use of major ion chemistry, trace and rare earth elements to characterize hydraulic relations, mixing processes and water-rock interaction in the Dong Van karst aquifer system, Northern Vietnam. Hydrogeology Journal (under review)

Abstract

This paper highlights the effectiveness of the groundwater geochemistry approach in karst hydrogeologic research. In particular, this approach is very useful for initial preliminary studies such as for the Dong Van karst aquifer system in northern Vietnam; analyses of different groundwater chemistry parameters complement each other to clarify hydrochemical processes that are occurring in this karst system. The results of this study show that major ion composition can be used to clarify water chemistry signatures, as well as to identify the mixing processes, and water-rock interactions in aquifers. Meanwhile, trace element concentrations and rare earth element patterns can be used as potential natural tracers when some processes are not revealed through conventional hydrochemical methods. These natural tracers can and also be used to identify contaminant sources and/or contaminant transport processes in karst aquifers. Viewed holistically, the groundwater geochemistry approach provides scientific information to establish a basic hydrogeological conceptual model and estimate the water balance, which has implications for water resources protection and management in karstic systems.

3.1 Introduction

Groundwater from karst aquifers is the major freshwater source for drinking-water supply and agricultural irrigation in many countries and regions throughout the world. The number of karst water consumers is estimated at 678 million, or 9.2% of the world's population (Stevanovic 2019), while the population living on karst areas is estimated at 1.3 billion people (Goldscheider et al. 2020). As pointed out by Tuyet 2001, in Vietnam, limestone accounts for nearly 18% (about 60,000 km²) of the total area, mostly in the northern provinces, while an updated result by Goldscheider et al. 2020 shows that carbonate rocks cover an area of 90,000 km² (occupying 27.2% of the total area). The Dong Van karst plateau (DVKP), located in Ha Giang province, is one of the most prominent karst regions in northern Vietnam, and belongs to the extended part of the South China karst belt (Yunnan karst plateau) (Fig. 3-1a). The Na De spring system (the source of the Nhiem River) is the largest spring in the area, which could be the local base level for karst erosion in the DVKP (Anh et al, 2022) and is probably among the largest karst springs in Southeast Asia (Fig. 3-1c). There is no regular discharge monitoring at this spring. During a one-time measurement during the rainy season, a discharge of 44 m³/s was observed (unpublished data from Ender 2014), but much higher discharge values, probably several hundred m³/s, are expected to occur during extreme high-flow events. There is no specific research on the karst hydrogeological system associated with this major spring. Therefore, research on the hydrogeological characteristics of the Na De spring system and its surrounding area is critical for sustainable groundwater resources management, protection, and exploitation on the Dong Van karst plateau.

Groundwater geochemistry has emerged as an effective tool that can elucidate water sources, hydrochemical processes, and dynamics and to identify contamination input sources in karst aquifers (Lambrakis et al. 2004; Holland and Witthüser 2009; Goldscheider and Drew 2014). The use of major ions to identify the processes controlling groundwater chemistry has become a common method aided by conventional geochemical displays such as Gibbs diagrams, and ion-ratio graphs (Gibbs 1970; White 1988; Goldscheider 2015 and Gao et al. 2019). Previous studies by Güler et al. 2002, Heikinien et al. 2002 applied multivariate statistical methods (e.g. principal components analysis - PCA, and hierarchical cluster analysis - HCA) to compare and partition water samples into homogeneous groups

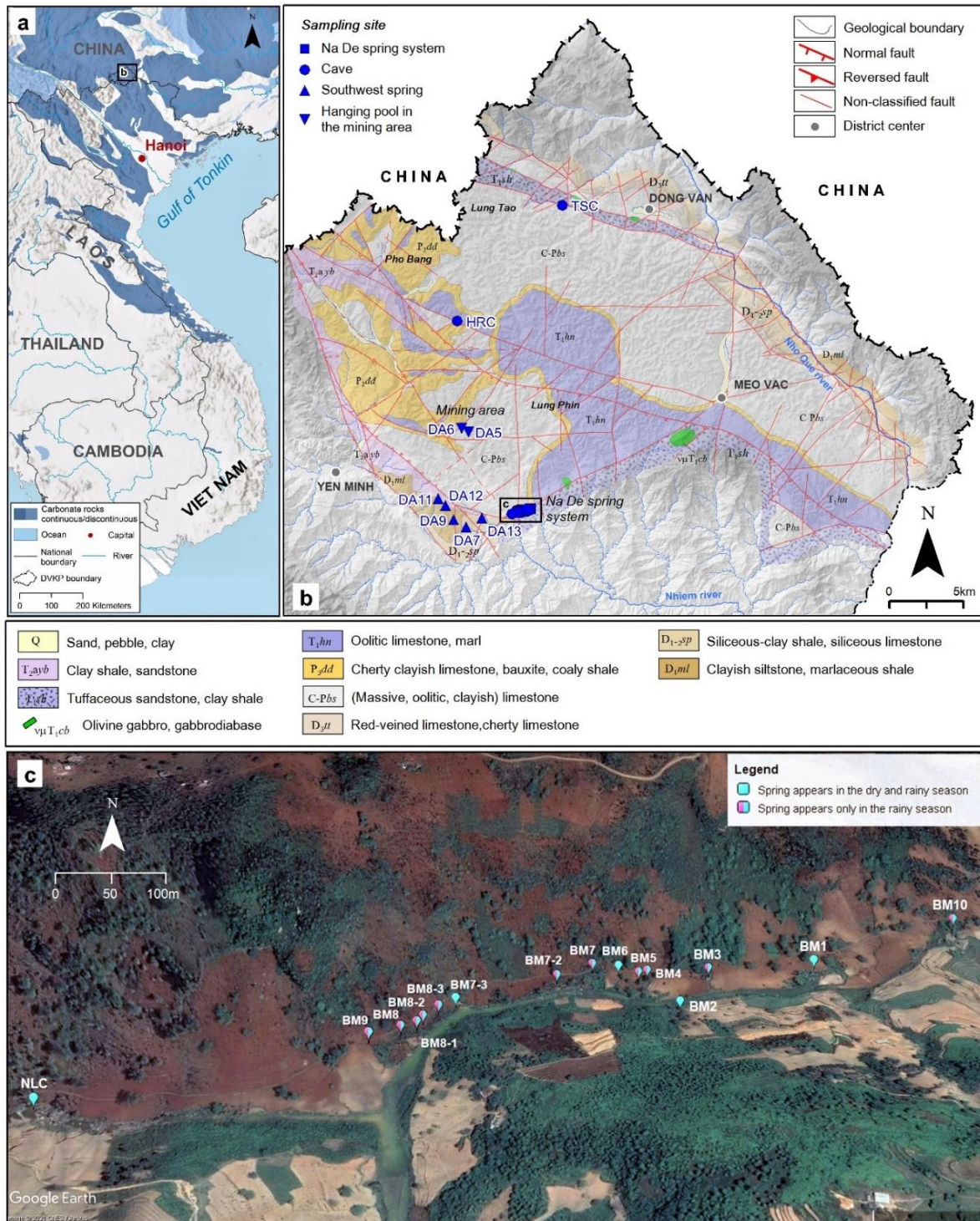


Fig. 3-1 Map of the investigation area; **a**) Location of Dong Van karst plateau in Vietnam and South China karst belt (based on the World Karst Aquifer Map, Goldscheider et al. 2020); **b**) Map of sampling sites on top of geological map of the study area (After Tinh et al. 1976; Updated by KaWaTech project); **c**) Map of distribution of individual springs belonging to the Na De spring system superposed on a satellite image (Source: Google Earth).

based on water physicochemical parameters, providing information on the physical-chemical processes controlling water chemistry, as well as providing insight into underground flow connectivity. In recent

years, many studies have shown that trace elements can be used as potential natural tracers of groundwater origin when some processes are not revealed through conventional hydrochemical methods, such as signatures of major ions and/or stable isotopes. As indicated by Lee et al. 2003; Möller et al. 2004; Han and Liu 2007; Zhou et al. 2012, the rare-earth element (REE) abundances and patterns can be exploited effectively as fingerprints of host aquifers or bedrock as well as indicating paleo-hydrological conditions. Gill et al. 2018 and Cholet et al. 2019 used temporal variability of REE concentrations and patterns to evaluate possible links between different water sources and to quantify mixing contributions.

The main aim of this work is to evaluate the effectiveness of the groundwater geochemistry approach for karst hydrogeological research, with a particular focus on using trace and rare earth elements as natural tracers. The work uses these methods to contribute to a better understanding of the Dong Van karst aquifer system. The specific objectives of this study are: 1) use major ion chemistry to identify and characterize different water types, mixing processes, and water-rock interactions in the aquifers; 2) test the use of trace and rare earth elements as natural tracers for characterizing underground flow connectivity and identifying contaminant transport processes; and 3) establish a conceptual model of the karst aquifer system and produce a water balance of the study region to provide scientific information for water resources management.

3.2 Study site

3.2.1 Geological and hydrogeological settings

The study area is situated in the Dong Van Karst Plateau UNESCO Global Geopark, covering an area of about 620 km², which is composed mainly of carbonate rocks (more than 60%). According to previous and recently updated geological maps, the strata range mainly from Paleozoic to Mesozoic, with local outcrops of Triassic gabbro and diabase along deep faults (Fig. 3-1b). Carbonate rock formations, including Bac Son (C-P *bs*), Dong Dang (P₂ *dd*) and Hong Ngai (T₁ *hn*), are widely distributed in the central part of karst plateau. The Devonian formations including Mia Le (D₁ *ml*), Si Phai (D₁₋₂ *sp*) and Toc Tat (D₃ *tt*) occur in narrow bands, located along the north and northeast. In addition, Triassic

formations, including Song Hien (T_1sh) and Yen Binh ($T_{2a}yb$), are distributed in the South and SW of this area. Tectonically, the investigated area is dissected by many fault systems, but the main one is the NW-SE fault system. In addition, there is the appearance of a fault system with a NE-SW direction, especially sub-latitude and sub-meridian fault systems, formed during a Neotectonic period.

The cave system developed a strong relationship to the tectonic and geomorphologic development processes in this area (Van et al. 2004, Hai et al. 2013, Anh et al. 2022). There are some stream caves such as Na Luong cave, Ma Le cave system, Tia Sang cave and Hang Rong cave, etc. which are important water sources for domestic use and irrigation that have been explored by Belgian SPEKUL club experts and VIGMR speleologists.

The Bac Son formation (Fm.) is composed of homogeneous, massive, partly dolomitized limestone, totaling 700-1000m in thickness, and is hydrologically considered the important karst aquifer in this area, beside the Dong Dang Fm. and Hong Ngai Fm. karst aquifers. In addition, there is also the fractured Si Phai Fm. aquifer (Ender et al. 2018, Lam et al. 2013).

According to published geologic data, Na De spring is located along the boundary between the limestone of Bac Son Fm. (C-Pbs) and terrigenous sediments of Song Hien Fm. (T_1sh) (Tinh et al. 1976). Besides, a study based on cave survey data by Anh et al. 2022 indicates that the Na De spring could be the local base level for karst erosion in the Dong Van karst plateau, which probably drains large parts of this area.

3.2.2 Climatic features

Northern Vietnam's climate is generally of the subtropical monsoon type (Pham 1985). However, the Dong Van karst plateau belongs to the high-altitude region with strongly dissected terrain, and thus the climate is characterized as a temperate zone (Van et al. 2010), and is divided into two seasons: a rainy season (May to October) and a dry season (November to April). According to data collected at the climate station Dong Van District in the period 2015-2020, operated by Vietnam National Centre for Hydro-Meteorological Forecasting (NCHMF), the annual average precipitation is 1537 mm, with the

highest rainfall in June (302 mm average) and lowest in February (12 mm). The annual average temperature is 18.4°C, with the highest reaching 23.6 °C in June and the lowest 11.7°C in December.

3.3 Materials and Methods

3.3.1 Sampling campaigns and sampling sites

Two sampling campaigns were organized between the dry (March) and rainy (June/July) seasons, 2020. A total of 40 water samples were collected from springs (Na De spring system and Southwest springs), in caves (Na Luong cave, Hang Rong cave), the recharge stream (surface flow) of Tia Sang cave (TSC), and hanging pools in the mining area. (Fig. 3-1b).

The Na De spring system (NDSS) is situated in Na De valley in the south of DVKP. This system includes 16 springs, of which 4 springs appear continuously (BM1, BM2, BM6, BM7.3) and 12 springs only flow during the rainy season. (Figs. 3-1c, 3-2a). In this spring system, BM1 is the largest spring and forms the upstream end of Nhiem River (Fig. 3-2c).

Located in the Na De valley, Na Luong cave (NLC) is a river cave developed horizontally in the carbonate rocks of the Bac Son Fm. at an altitude of 238 m a.s.l. (C-Pbs) (Figs. 3-1c, 3-2b). Elsewhere, Hang Rong cave (HRC) has developed in the Hong Ngai Fm. (T₁hn), which consists of layers of argillaceous limestone, siliceous limestone, and medium- to thick-bedded limestone (Figs. 3-1b, 3-2d).

Southwest springs (SW springs) are springs draining in the southwest area of DVKP. This group includes five springs namely DA7, DA9, DA11, DA12, and DA13 that appear along the NW-SE fault zone, which is also the boundary between the carbonate rocks of the Bac Son Fm. (C-P bs) and the terrigenous deposits of the Yen Binh Fm. (T_{2a} yb), Ma Le Fm. (D₁ ml), as well as the shale and siliceous limestone of the Si Phai Fm. (D₁₋₂ sp) (Fig. 3-1b).

The mining area is located northwest of the Na De spring system. Based on survey data, the mined ores are mainly Zinc-Wolframite (Zn-W), which occurs in the soil layers that are derived by in-situ weathering or weathering plus gravitational movement or accumulation overlying the carbonate rock

erosion surface of the Bac Son Fm. (C-P_{bs}) and Dong Dang Fm. (P₂ \overline{dd}) or in the intermontane karst valleys and karst sinkholes. (Figs. 3-1b, 3-2e, 3-2f).

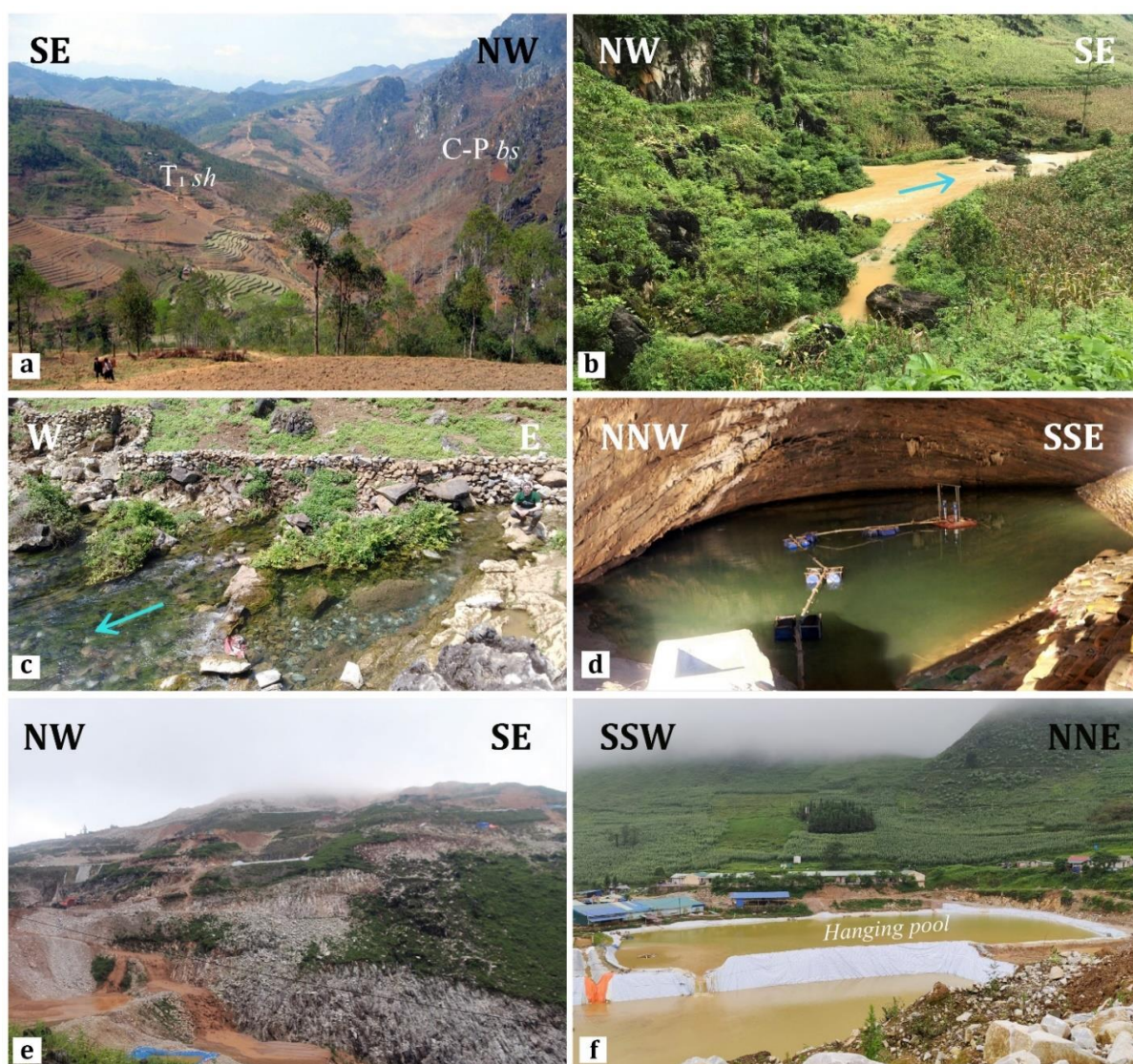


Fig. 3-2 Photos showing different sampling areas in the study area; **a**) Na De valley is located on the boundary between the Bac Son Fm. (C-P_{bs}) and Song Hien Fm. (T_{1sh}) (Photo: David Lagrou); **b**) Discharge area of the underground stream at the entrance of Na Luong cave (NLC) during the rainy season; **c**) BM1 spring is the main spring of Na De spring system during the dry season; **d**) Sampling point in the Hang Rong cave (HRC); **e**) A part of the mining area is located northwest of the Na De spring system; **f**) The hanging pool stores wastewater that is reused for the ore extraction process in the mining area.

3.3.2 Measurements and analysis

A portable multi-parameter device (Multi 3430 IDS, WTW, Weilheim, Germany) was used to measure the pH (IDS SenTix 980). The probe was calibrated on a regular basis with standard buffer solutions. Electrical conductivity (EC) and temperature (T) which were measured with a TetraCon 325 sensor.

Water samples for major ion analysis were filtered with cellulose acetate membrane filters (0.45 μm , 25 mm, Sartorius AG, Göttingen, Germany). Cation samples were collected in conical centrifuge tubes (SuperClear™ 15 ml, Labcon North America, Petaluma, CA, USA), while anion samples were taken using high density polyethylene bottles (30 ml, Rixius AG, Mannheim Germany). Samples for cation analyses were stabilized with nitric acid, and all samples were stored in a refrigerator before being transported to Germany for analysis.

These samples were analyzed in the laboratory of Hydrogeology Division (AGW, KIT, Germany), in which the major cations (Ca^{2+} , Mg^{2+} , K^{+} and Na^{+}), 18 heavy metal elements (Li, Be, Al, V, Cr, Mn, Fe, Co, Ni, Cu, Zn, Ga, As, Rb, Sr, Cd, Sn, Sb, Cs, Ba, Tl, Pb, Bi and U) and 14 rare earth elements (REE) were measured by ICP-MS (Agilent 7800 Quadrupole ICP-MS, Agilent Technologies, Inc., Santa Clara, USA). The anions SO_4^{2-} , NO_3^{-} and Cl^{-} were measured with ion chromatography (Dionex ICS-1100/Dionex ICS-2100, Thermo Fisher Scientific Inc., Waltham, MA, USA). An alkalinity test (111,109, Merck Millipore, Billerica, MA, USA) was used for the direct determination of HCO_3^{-} and CO_3^{2-} in the field. Since the pH values were generally <8.2 , CO_3^{2-} was mainly negligible and total alkalinity could be considered equal to HCO_3^{-} . The calculation of the charge-balance error was carried out with PHREEQC (Parkhurst and Appelo 1999). All analyses with a charge balance error $> 10\%$ were discarded.

3.3.3 Methods

3.3.3.1 Presentation of hydrochemical data

Gibbs diagrams were used to identify the major processes controlling natural groundwater chemistry (Gibbs 1970). A semi-logarithmic plot of the weight ratio of cations [$\text{Na}^{+}/(\text{Na}^{+}+\text{Ca}^{2+})$] or anions [$\text{Cl}^{-}/(\text{Cl}^{-}+\text{HCO}_3^{-})$] versus total dissolved solids (TDS) provides information on the mechanisms controlling water chemistry, such as rock weathering, atmospheric precipitation, and evapotranspiration. All ionic concentrations are expressed in milliequivalents per liter (meq/L). In this study, Gibbs diagrams were established using Origin software (Origin 2020b).

3.3.3.2 Multivariate statistical analysis

Hierarchical cluster analysis (HCA) is a well-proven statistical technique that is proving to be a powerful grouping mechanism for determining whether samples can be grouped into distinct hydrochemical groups that may be significant in a geologic context (Güler et al. 2002; Heikinien et al. 2002; Lambrakis et al. 2004; Holland and Witthüser 2009). In this study, clustering is performed using normalized datasets (over two sampling campaigns), and the results are presented in dendrograms using Origin software. Ward's method (Ward 1963) was used to analyze the distances among linkages for the entire group of observations and the squared Euclidean distances were used to determine the distance between observations. The data were standardized by calculating their standard scores (z-scores) as follows Equation (3-1):

$$z_i = \frac{x_i - \bar{x}}{s} \quad (3 - 1)$$

where z_i = standard score of the sample i , x_i = value of sample, \bar{x} = mean, s = standard deviation. Standardization scales the log-transformed or raw data to a range of approximately ± 3 standard deviations, centered about a mean of zero. Therefore, each variable has equal weight in the statistical analyses.

In this study, 17 variables (physical-chemical parameters) were chosen for multivariate statistical analysis, because they met a primary selection criterion of being representative of water-rock interactions and human inputs: physicochemical parameters (T, pH, EC, TDS), major ions (Na^+ , K^+ , Ca^{2+} , Mg^{2+} , Cl^- , SO_4^{2-} , HCO_3^- , and NO_3^-), and selected trace elements (As, Fe, Zn, Al, and Sr).

3.3.3.3 Normalization and calculation of REE patterns

Rare Earth Elements (REE) including the lanthanide group and yttrium can be separated into three sub-groups according to their atomic weight: light REE (LREE, La–Sm), medium REE (MREE, Eu–Tb), and heavy REE (HREE, Dy–Lu). REE data are typically presented as distribution patterns with the individual REE, listed in the order of their atomic number, as categories on the x-axis and with the corresponding concentrations as normalized logarithmic values on the y-axis. For all water samples in

this study, REE are normalized to the PAAS standard (Post Archean Australian Shales), which is a proxy for average upper continental crust (Taylor and McLennan 1985).

A comprehensive illustration of REE patterns can be identified with a quantitative expression of anomalies that are positive or negative peaks in the REE distribution patterns. Commonly occurring anomalies are Cerium (Ce) anomalies and Europium (Eu) anomalies, which are quantified by Ce/Ce* and Eu/Eu* ratios where Ce* and Eu* are interpolated values based on the measured concentrations of the neighbor elements of Ce and Eu, respectively. These ratios are calculated by the following formulas (McLennan 1989):

$$Ce/Ce^* = \frac{3Ce_n}{2La_n + Nd_n} \quad (3 - 2)$$

$$Eu/Eu^* = \frac{Eu_n}{\sqrt{Sm_n \times Gd_n}} \quad (3 - 3)$$

where the subscript “n” stands for normalized values. Anomalies with Ce/Ce* and Eu/Eu* ratios >1 indicate “positive anomalies”. Anomalies with Ce/Ce* and Eu/Eu* ratios <1 are called “negative anomalies”. In addition, we use the Pr_n/Yb_n ratio as a general descriptor of the slope of the REE pattern, with the ratio Pr_n/Yb_n > 1 indicating LREE enrichment, and Pr_n/Yb_n < 1 indicating HREE enrichment (neither Pr nor Yb behaves anomalously, thus are suitable representative elements).

The occurrence of positive or negative Ce anomalies is typical for oxidizing conditions where Ce is present as Ce⁴⁺ and is therefore less soluble than the other REE (McLennan 1989). By contrast, the Eu anomaly is strongly lithology-dependent (Tricca et al. 1999; Möller et al. 2004; Han and Liu 2007), thus water originating from any aquifer will have Eu anomalies similar to the host rock of that aquifer. In this study, the analysis data of limestones and shale samples in the Lung Cam Permian - Triassic boundary section located in the Dong Van karst plateau from a previous study by Son et al. 2007 was used to understand the relationship between groundwater and exposed lithology.

3.4 Results

3.4.1 Physicochemical characteristics

The water physicochemical analyses of major parameters of all water samples show significant spatial and temporal differences (Table 3-1).

In the NDSS and caves groups, the average value of EC, TDS, Ca^{2+} , and HCO_3^- are high and do not have much seasonal variation. While the water in the SW springs group is characterized by low Ca^{2+} , and HCO_3^- content. Table 3-1 also shows that the concentrations of major parameters in water samples collected at hanging pools in the mining area vary widely depending on the season and location of each sampling site.

Table 3-1 Descriptive statistics of the major physicochemical parameters of water samples in the study area

Sampling area	Number of sample	Value	T (°C)	pH	EC (µS/cm)	TDS (mg/L)	Ca ²⁺ (mg/L)	Mg ²⁺ (mg/L)	Na ⁺ (mg/L)	K ⁺ (mg/L)	HCO ₃ ⁻ (mg/L)	SO ₄ ²⁻ (mg/L)	Cl ⁻ (mg/L)	NO ₃ ⁻ (mg/L)	
Na De spring system & Caves	Dry season	7	Max	20.6	8.5	327.0	265.0	55.8	4.6	2.9	3.0	185.5	9.4	3.6	14.2
		Min	14.4	7.7	148.0	113.2	21.6	1.7	0.9	0.7	82.4	1.3	1.0	1.6	
		Mean	18.7	7.9	292.9	237.7	50.0	3.2	1.4	1.1	165.6	3.9	1.7	10.8	
	Wet season	19	Max	23.2	7.8	317.0	251.9	55.2	3.5	1.9	2.3	176.9	7.2	4.0	15.3
		Min	16.2	7.2	123.0	95.2	18.5	1.2	0.7	0.6	69.3	0.9	1.1	0.9	
		Mean	21.1	7.5	293.1	233.0	50.8	2.3	0.9	0.9	162.2	2.6	2.0	11.3	
SW springs	Dry season	5	Max	20.0	7.7	174.0	129.8	24.7	6.0	3.1	0.5	94.6	5.9	0.8	6.1
		Min	17.7	6.7	94.0	42.6	5.7	2.1	1.8	0.1	25.0	0.6	0.2	1.7	
		Mean	18.4	7.3	135.4	96.2	15.6	4.0	2.4	0.2	67.5	2.7	0.4	3.3	
	Wet season	5	Max	27.5	8.2	168.0	132.2	23.7	4.8	2.2	0.3	97.6	3.0	0.7	9.3
		Min	22.4	5.5	45.0	30.2	5.3	1.0	1.2	0.1	11.9	0.4	0.2	1.6	
		Mean	25.5	6.9	101.2	76.4	12.8	2.9	1.7	0.2	52.7	1.3	0.3	4.5	
Mining area	Dry season	2	Max	16.0	9.3	414.0	287.1	68.3	1.5	3.9	1.0	122.0	81.2	4.8	4.4
		Min	15.3	8.2	129.0	92.3	21.8	0.7	1.1	0.6	45.8	14.6	3.3	4.3	
		Mean	15.7	8.7	271.5	189.7	45.0	1.1	2.5	0.8	83.9	47.9	4.1	4.4	
	Wet season	2	Max	26.3	8.2	231.0	175.6	44.0	0.2	0.8	0.4	112.0	13.6	1.6	3.1
		Min	26.1	7.7	120.0	87.5	21.9	0.1	0.2	0.3	59.5	3.2	0.3	1.9	
		Mean	26.2	8.0	175.5	131.5	33.0	0.1	0.5	0.4	85.7	8.4	1.0	2.5	

The concentrations of SO_4^{2-} and NO_3^- ions show large differences among the sampling areas. The abnormally high value of NO_3^- found in BM2 (15.3 mg/L) is thought to be related to fertilizer pollution in agricultural activities. Whereas the highest SO_4^{2-} value of 9.4 mg/L in the HRC during the dry season is probably related to the alkaline lake structure and evaporation; the oxidation of metal sulfides (e.g., FeS_2 , ZnS , Al_2S_3 , PbS , etc.) in the mining area could be a possible source of SO_4^{2-} . These values are lower than the guideline value set by WHO for drinking water (WHO, 2022).

The Gibbs diagrams (Figs. 3-3a, b) show that most of the water samples of NDSS and caves groups are located in the rock-weathering dominated field. An exception is a sample taken at the recharge stream of Tia Sang cave, which is in the dominant precipitation field in the rainy season. Although they are part of the SW springs group, two springs (DA7 and DA13) fall in the rock-weathering dominated zone. The DA13 water sample is in the dominant precipitation field in the rainy season. Also in this group are three springs (DA9, DA11, and DA12) that are in the precipitation-dominated field. In addition, Figure 3 also shows that the DA5 sample, which is part of the mining area, falls in the rock-weathering dominance field, and sample DA6 is located on the boundary between the precipitation and the rock-weathering dominance zone. It can be seen that the water source for ore extraction is mainly rainwater in the rainy season, while in the dry season, water may be obtained from other water caves near this area. Water is stored in the hanging pools and re-used for the ore-extraction process.

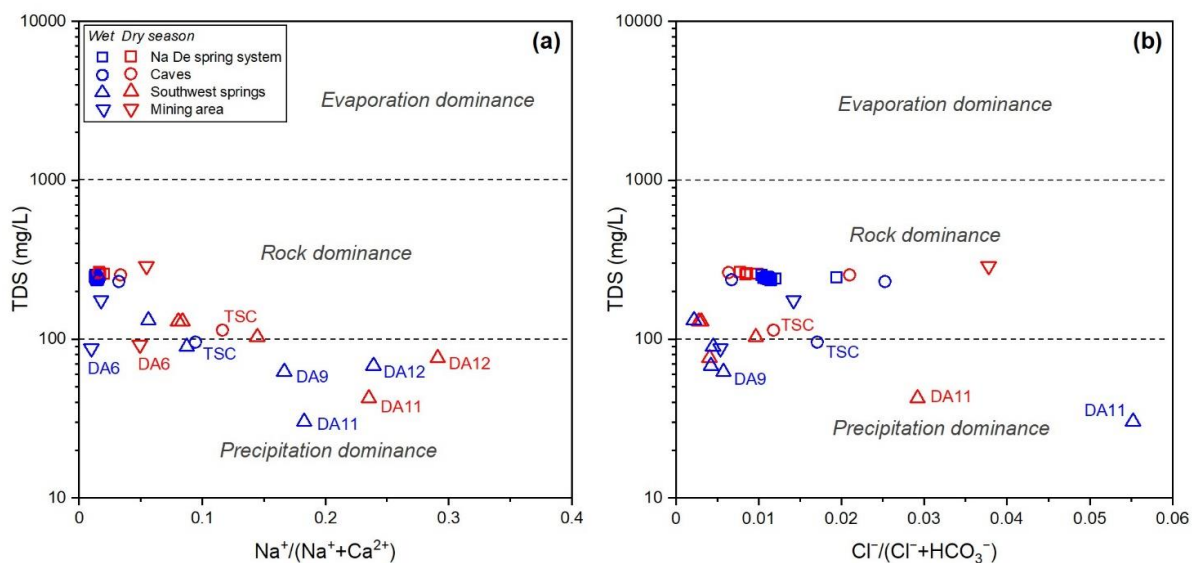


Fig. 3-3 Gibbs diagrams are used to explain the predominant processes of water hydrochemistry in the study area: (a) for cations; (b) for anions.

3.4.2 Water-rock interaction

The interaction of water with its host environment, as well as atmospheric and human inputs, play an important role in forming the chemical compositions of groundwater. The ratios between the major-ions-equivalent concentrations further indicate the sources and the main hydrogeochemical processes that control groundwater chemistry (Gibbs 1970; Goldscheider 2015; Gao et al. 2019).

As mentioned by Hunkeler and Mudry 2014, the dissolution of carbonate and gypsum can provide Ca^{2+} , Mg^{2+} , SO_4^{2-} and HCO_3^- in a groundwater system. If the dissolution of gypsum is the major hydrogeochemical reaction, the equivalent ratio of $(\text{Ca}^{2+}/\text{SO}_4^{2-})$ should be equal to 1. Conversely, if the weathering of carbonates (calcite and dolomite) is the major hydrogeochemical reaction, the ratios of $\text{HCO}_3^-/(\text{Ca}^{2+}+\text{Mg}^{2+})$ should be around 1.

Figure 3-4a indicates that most samples have $\text{SO}_4^{2-}/\text{Ca}^{2+}$ ratios close to 0, while Figure 3-4b shows that the $\text{HCO}_3^-/(\text{Ca}^{2+}+\text{Mg}^{2+})$ ratios are distributed around a 1:1 dissolution line, except for samples from the mining area that have higher SO_4^{2-} contents. This means that the dissolution of calcite and dolomite are the major processes influencing the water chemistry in all sampling areas, whereas the dissolution of gypsum or the oxidation of metal sulfides occurs in the mining area.

The $(\text{Mg}^{2+}/\text{Ca}^{2+})$ index is a useful parameter that can reflect the relative proportion of calcite and dolomite in carbonate rock through which the water sample circulated (White 1988, Nguyet et al. 2016). A ratio of equivalent concentrations $(\text{Mg}^{2+}/\text{Ca}^{2+}) = 1$ represents dissolution of dolomite. In contrast, a ratio $(\text{Mg}^{2+}/\text{Ca}^{2+}) = 0$ represents dissolution of pure calcite. A ratio of $(\text{Mg}^{2+}/\text{Ca}^{2+}) = 0.5$ indicates equilibrium of water with both calcite and dolomite. As shown in figure 3-4c, most of the water samples collected at Na De spring system, caves, and the mining area have $\text{Mg}^{2+}/\text{Ca}^{2+}$ ratios below 0.5, suggesting dominant calcite in carbonate rocks of the areas. Meanwhile, most of the SW springs and TSC also have $\text{Mg}^{2+}/\text{Ca}^{2+}$ ratios less than 0.5 and Ca^{2+} content lower than 1.2 meq/L, which means that dissolution of calcite dominates in the hydrochemical reactions in these springs, but in low concentration. In addition, in this group, sample DA12 is located above the line $(\text{Mg}^{2+}/\text{Ca}^{2+}) = 1$, suggesting that this spring flows through an aquifer that is affected by the dissolution of dolomite.

A study by Ender et al. (2018) indicates that the relation between (Ca^{2+}/Mg^{2+}) and Ca^{2+} can be used to illustrate the hydrochemical processes in different aquifers in the area of Dong Van. Accordingly, the Bac Son Fm. is characterized by high Ca^{2+} concentration and the (Ca^{2+}/Mg^{2+}) index are ranging from approximately 5 to 25, meanwhile, the "Others" group includes springs of the Song Hien, Yen Binh, and Mia Le Fm., which were defined based on their low concentration of Ca^{2+} and their Ca^{2+}/Mg^{2+} ratios. Figure 3-4d shows that the samples at NDSS, NLC, and HRC are located in the Bac Son Fm. karst aquifer, while the SW springs and TSC fall into the "Others" group.

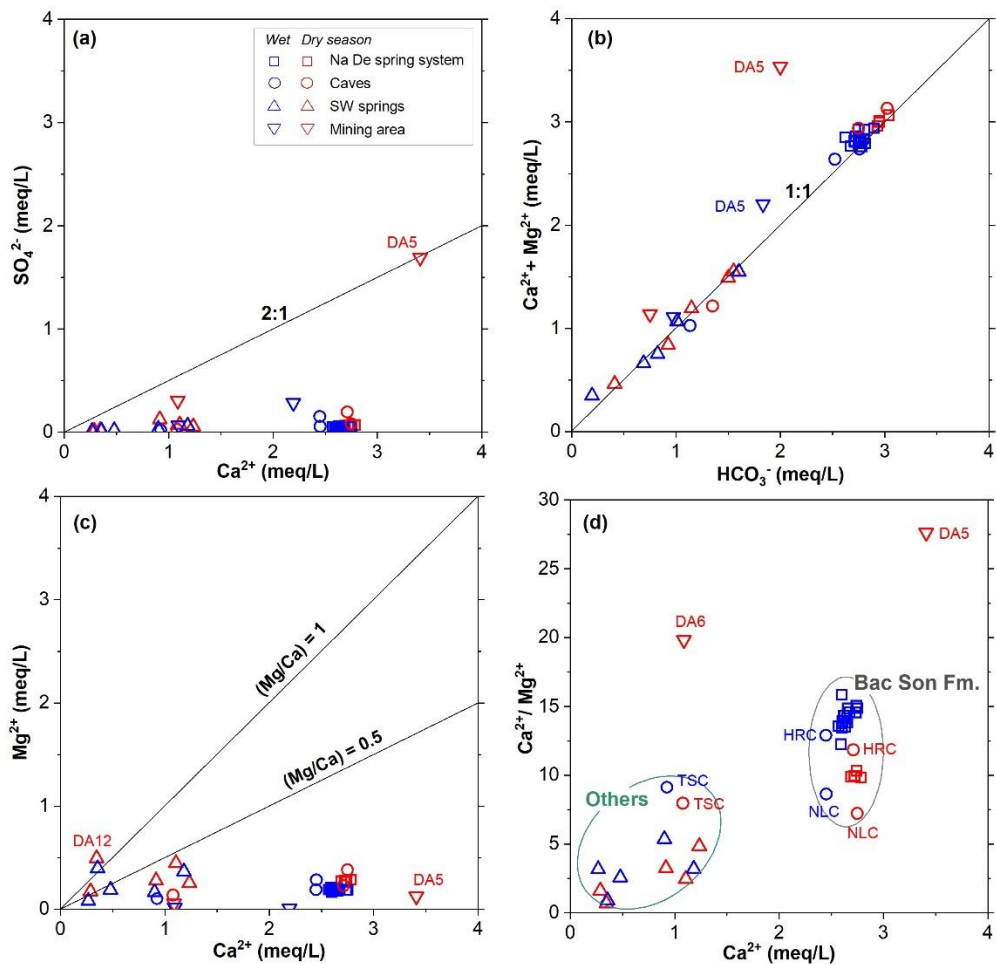


Fig. 3-4 Plots showing the ratios between the major ions of water samples in study area: (a) SO_4^{2-} vs. Ca^{2+} ; (b) $(Ca^{2+} + Mg^{2+})$ vs. HCO_3^- ; (c) Mg^{2+} vs. Ca^{2+} ; (d) (Ca^{2+}/Mg^{2+}) vs. Ca^{2+}

3.4.3 Hierarchical Cluster Analysis

Figure 3-5 presents the dendrograms for 17 variables in the DVKP during both dry and rainy seasons. The nodes represent the grouped clusters, and the lengths of the branches indicate the distances between

the groups. On this basis, water samples were classified into two clusters in both dry and wet seasons. Cluster 1 (CL1) is further sub-divided into two sub-clusters SCL1a and SCL1b during the dry season (Fig. 3-5a), while in the rainy season, Cluster 2 (CL2) was separated into two sub-groups SCL2a and SCL2b (Fig. 3-5b). A summary of the physical-chemical data for each cluster is presented in Table 3-2.

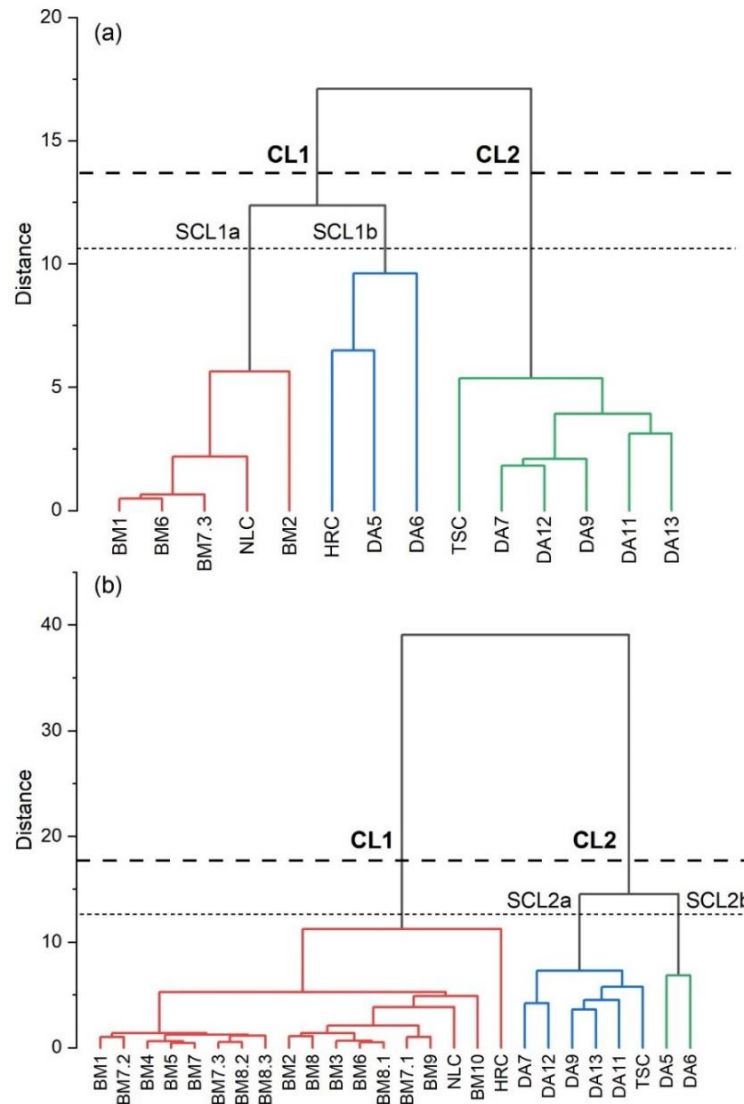


Fig. 3-5 Dendrograms classifying the groundwater samples according to physical-chemical composition. (a) dry season (upper display); (b) rainy season (lower display).

The dendrogram in the dry season (Fig. 3-5a, Tab. 3-2) shows that Cluster 1 combines the samples with signatures of calcium bicarbonate water type. In addition, this group is also characterized by elevated arsenic and aluminum concentrations indicating the influence of a combination of anthropogenic sources. The subdivision of Cluster 1 is based on variations in ion sulfate and heavy metal concentrations, with SCL1b showing highly elevated sulfate, arsenic, iron and aluminum

concentrations compared with SCL1a. Cluster 2 is a collection of samples characterized by low conductivity and little mineralization. These springs are typical of shallow groundwater movement, possibly in the weathered surface zone with a short residence time.

In the rainy season, the dendrogram (Fig. 3-5b) shows that Cluster 1 is the largest group, with a total of 18 samples (Tab. 3-2) that display similar physicochemical parameters to SCL1a in the dry season due to the influence of the same geogenic factors. Cluster 2 is distinguished by low values of conductivity, TDS, Ca^{2+} , and HCO_3^- , while water temperature and the concentrations of arsenic, iron and aluminum were higher than Cluster 1. Cluster 2 was separated into two sub-clusters representing variations in values of pH, EC, TDS, Ca^{2+} , and HCO_3^- , as well as heavy metal concentrations, with SCL2b having significantly higher arsenic and aluminum concentrations compared with SCL2a.

Table 3-2 Mean chemical values for seasonal groups distinguished by hierarchical cluster analysis.

Parameter	Dry season					Rainy season				
	Complete dataset	Cluster 1		Cluster 2	Total CL2	Complete dataset	Cluster 1		Cluster 2	
		Total CL1	SCL1a				SCL1b	Total CL1	Total CL2	SCL2a
Number of samples	14	8	5	3	6	26	18	8	6	2
Temperature (°C)	18.2	18.5	20.1	15.8	17.7	22.3	21.0	25.4	25.1	26.2
pH	7.8	8.1	7.9	8.4	7.5	7.4	7.5	7.2	6.9	8.0
El. Cond. ($\mu\text{S}/\text{cm}$)	233.6	305.6	318.4	284.3	137.5	247.1	302.5	122.5	104.8	175.5
TDS (mg/L)	180.3	241.2	259.5	210.8	99.1	195.1	240.6	92.5	79.5	131.5
Ca^{2+} (mg/L)	37.0	52.3	54.9	48.1	16.6	42.1	52.6	18.5	13.7	33.0
Mg^{2+} (mg/L)	3.2	2.9	3.6	1.6	3.6	2.2	2.3	2.0	2.6	0.1
Na^+ (mg/L)	1.9	1.5	1.0	2.3	2.5	1.0	0.8	1.4	1.7	0.5
K^+ (mg/L)	0.7	1.1	0.8	1.5	0.3	0.7	0.9	0.3	0.3	0.4
HCO_3^- (mg/L)	118.9	155.6	181.8	111.9	70.0	135.3	167.4	63.0	55.5	85.7
SO_4^{2-} (mg/L)	9.7	15.2	3.3	35.0	2.5	2.8	2.7	3.0	1.2	8.4
Cl^- (mg/L)	1.6	2.4	1.5	3.9	0.5	1.6	2.0	0.6	0.5	1.0
NO_3^- (mg/L)	7.2	10.4	12.8	6.3	3.0	9.3	11.9	3.6	3.9	2.5
As ($\mu\text{g}/\text{L}$)	6.5	10.9	5.0	20.7	0.7	3.5	1.3	8.4	0.4	32.3
Fe ($\mu\text{g}/\text{L}$)	13.1	12.8	4.2	27.1	13.5	8.2	4.9	15.6	17.6	9.7
Zn ($\mu\text{g}/\text{L}$)	10.5	12.3	13.3	10.7	8.1	100.9	96.1	111.8	117.0	96.0
Al ($\mu\text{g}/\text{L}$)	42.9	68.5	9.7	166.7	8.7	32.0	24.6	48.8	28.9	108.4
Sr ($\mu\text{g}/\text{L}$)	66.6	61.2	50.0	79.8	73.8	49.0	50.7	45.3	56.9	10.3

3.4.4 Presentation and interpretation of REE data

Normalized patterns of REE for the various water samples from the dry and wet season sampling campaigns are presented in Figure 3-6, expressed both as raw normalized concentrations (a, b), and the average REE pattern for each sampling area as well as each cave (c, d).

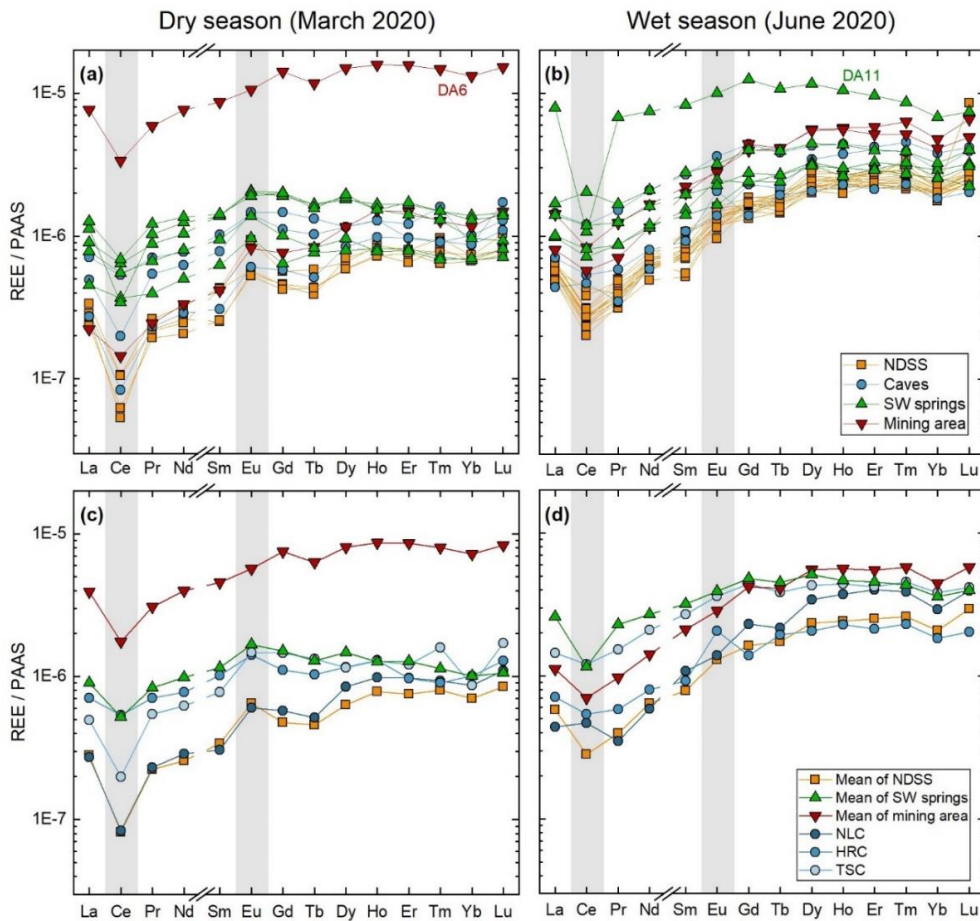


Fig. 3-6 REE abundances in waters normalized to the PAAS standard (Post Archean Australian Shales; Taylor and McLennan 1985) and divided into the samples collected during the dry season in March 2020 (a, c) and wet season in June 2020 (b, d). Panels (a) and (b) show all measured water data without adjustment, while panels (c) and (d) show the mean concentration of each group as well as each cave to emphasize the features in terms of their pattern slope, concentrations, and variations in primary water anomalies (Ce, Eu). Water samples were collected from the Na De spring system (NDSS; orange filled squares); from caves (Caves; blue-filled circles); in the southwest of DVKP (SW springs; green-filled triangles); and at the mining area (red-filled inverted triangles).

In the dry season (March 2020, Fig. 3-6a), the karst groundwater samples at NDSS contrast significantly with the SW springs with lower Σ REE and steeper, highly LREE-depleted REE patterns, as well as more pronounced negative Ce anomalies and stronger positive Eu anomalies. Normalized REE patterns at the cave group showed HREE enrichment at NLC, while slight at TSC and HRC. Ce anomalies are slightly negative at HRC and strongly negative at NLC, TSC, while Eu anomalies were

moderately positive. In addition, samples taken from hanging pools at the mining area showed significant differences in Σ REE. Normalized REE patterns show HREE enrichment at DA5 and moderate HREE enrichment at DA6. Ce anomalies are strongly negative, while Eu anomalies are slightly negative at DA6 and moderately positive at DA5.

During the wet season (June 2020, Fig. 3-6b), total REE concentrations were significantly higher for the NDSS, caves, SW spring samples, and DA5 in the mining area, except for DA6, which has a lower Σ REE concentration, compared to the dry season. Normalized REE patterns from the NDSS group indicate high HREE enrichment, slightly positive Eu anomalies, and moderately negative Ce anomalies. The cave samples show high HREE enrichment, slightly negative at NLC to positive Eu anomalies at HRC, and slight negative Ce anomalies. Compared to the dry season, the SW springs exhibit slight to high enriched HREE, except that DA11 has flatter LREE/HREE patterns, the Eu anomalies vary from mildly negative to slightly positive. The Ce anomalies are mildly positive at DA9, slightly negative at DA7, DA12, DA13, and sharply negative at DA11. The samples at the mining site during the rainy season exhibited a fairly similar REE pattern, characterized by high HREE enrichment, slight negative Eu anomalies, and moderately negative Ce anomalies.

A comparison of average REE patterns (Fig. 3-6c vs. 3-6d) shows that the mining area samples, HRC, and SW springs differ least between dry and rainy seasons, whereas NLC patterns differ most. The NDSS samples and TSC also show some small differences in the Eu and Ce anomalies. Meanwhile, the average Σ REE comparison indicates that the mean total REE concentrations in the rainy season at NDSS, SW springs, NLC, and TSC were significantly higher than in the dry season, while there was only a slight increase at HRC. However, these values in the wet season were significantly lower than in the dry season in the mining area, mainly due to a sharp decrease in DA6, while they increased strongly in DA5. These results indicate that rainwater replenishment, as well as a longer water-rock interaction time, resulted in higher REE concentrations (Gill et al. 2018; Berglund et al. 2019). Meanwhile, sample DA6 in the mining area suggests that the accumulation of wastewater during mining, combined with evaporation in the long term and high pH values, significantly increased the concentration of trace elements in the dry season.

3.5 Discussions

3.5.1 Evaluation of clustering results

For all permutations in the analysis of major ions, and timing for when the data set was expanded to include physical parameters and common trace elements, there was a clear (statistically significant) separation between samples collected from the Na De spring system (NDSS), caves, the mining area, and the SW springs of the Dong Van karst plateau. A reasonable explanation for the similarity of physicochemical parameters between NLC and NDSS is that they belong to the same zones of recharge and discharge. Meanwhile, the SW springs and TSC were identified as typical of shallow groundwater flowing through the weathered surface zone with a short residence time in non-karst formations.

Although Ca^{2+} , Mg^{2+} , and HCO_3^- concentrations do not vary much, HRC is distinct from the NDSS based on its higher SO_4^{2-} content. Meanwhile, the samples taken at the mining site were distinguished from the NDSS by significantly higher concentrations of SO_4^{2-} and heavy metals. However, the abnormally high arsenic concentrations in the mining area and NLC, combined with their location and geologic data, indicate potential connectivity between these sampling sites when arsenic is thought to be transported by groundwater from the mining area to NLC.

There is a large change in clustering patterns during the rainy season when the mining area switches to the same branch with SW springs and TSC (Fig. 3-5b). This is explained by the fact that in the wet season, most of the samples in Cluster 2 are located in the precipitation-dominant field (Fig. 3-3), with TDS, EC, and Ca^{2+} concentrations lower than Cluster 1 (Tab. 3-2). The mining area samples is still distinguished by its high content of heavy metals. It can be seen that these clustering results once again confirm the shallow groundwater pattern of the SW springs and TSC, and also show that rainwater is the main water source for ore extraction processes in the mining area.

In summary, the clustering results are meaningful in grouping and linking water sources. However, the limited number of samples (40) and sampling campaigns (seasonal over a single hydrological cycle) pose mathematical issues which can affect cluster structure. Thus, even if hierarchical cluster analysis yields

statistically significant results, these results are not significant unless they can be reasonably explained by the conceptual groundwater system model, hydrochemical dynamics, as well as geologic data.

3.5.2 Using the concentration of trace elements as a natural tracer

As mentioned by Gill et al. (2018), the consistent contrast in REE features establishes a basis for quantifying the contributions of autogenic and allogenic inputs to groundwater. Therefore, REE patterns can be used as a natural tracer to provide additional information about the characteristics of the aquifer and recharge sources.

The simple comparison of REE systematics exposes differences between SW springs and the karst-dominated waters (Na De spring system, NLC). Specifically, the normalized REE patterns (Figs. 3-6c, d) show that the karst groundwater samples have inherited their REE features from the carbonate rocks, including low Σ REE concentrations, strongly negative Ce anomalies, and high enrichment in HREEs. By contrast, the SW springs have much higher REE concentrations, a much smaller negative Ce anomaly, and a flatter overall REE pattern.

Figure 3-6c shows great similarities in the REE patterns of NLC and NDSS in the dry season, while in the rainy season (Fig. 3-6d), the negative Ce anomaly of NLC was significantly lower, and the HREE enrichment was higher than NDSS (more detail in Appx. 3-1). These results, combined with the ratios of major ion concentrations and spatial relationships strongly suggest that NDSS and NLC belong to the discharge zone of the same karst catchment, but do not preclude the possibility that there is also a connection between NLC and nearby flow systems. In addition, the Ce anomalies of NDSS and NLC become less negative, coupled with increasing total REE concentrations during the rainy season, basically reflecting mixing with sources that were lacking negative Ce anomalies, or that exhibited positive Ce anomalies such as rainwaters and/or water from another catchment.

Excluding the total REE, the REE patterns between the mining area and the NLC in both seasons show great similarities, and there is a difference in Ce anomaly only in the rainy season (more details in Appendix 3-1). Whereas the abnormally high arsenic concentrations in the mining area and NCL combined with their location and geologic data indicate a connection between these sampling sites in the

karst system when arsenic is thought to be transported by water flow from the mining area through fractures or cave systems in the unsaturated zone to NLC (Figs. 3-7a, c).

From a speleological and geological point of view, the HRC sample was taken at the lake (endpoint) of Hang Rong Cave, which developed in the Triassic siliceous limestone of the Hong Ngai Fm. (T_1hn). Thus, the groundwater has the REE distribution patterns of the host rock (Cholet et al. 2019). However, the REE patterns of HRC are fundamentally different from those of the Permian-Triassic limestone and shale samples at the Lung Cam boundary (located in the Dong Van karst plateau) analyzed by Son et al. 2007. In addition, the major ion composition data in the water samples from HRC have similar characteristics to those from the NDSS, which belongs to the Bac Son karst aquifer (Water-rock interaction section, Fig. 3-4d). Moreover, there are also similarities between HRC and NDSS in terms of REE patterns, except for lower negative Ce anomalies, which are thought to be the result of oxidation of Ce^{3+} to Ce^{4+} and subsequent stabilization of carbonate Ce^{4+} complexes in alkaline lake water, the same as in the case of Lake Van (Möller and Bau 1993) or the Abert and Mono lakes (Johannesson et al. 1994). These results would indicate that the HRC has the characteristics of an alkaline lake developed in Triassic siliceous limestones (T_1hn), but mainly associated with the Bac Son (C-Pbs) karst aquifer (Figs. 3-7a, b).

The TSC sample was collected at the drainage into Tia Sang Cave, which is located at the boundary between the terrigenous sediments of the Song Hien Fm. (T_1sh) and the limestone of the Bac Son Fm. (C-Pbs). Notwithstanding the significant differences in major ion composition and water type (as presented in the Hydrogeochemical Processes section), there are several commonalities in the REE patterns between TSC and NDSS during the dry and wet seasons. In particular, the REE patterns in the dry season at both sampling sites show a strong negative Ce anomaly, a moderate positive Eu anomaly, and significant HREE enrichment (Fig. 3-6c), while in the wet season the REE patterns show weaker negative Ce anomalies, lower positive Eu anomalies, and flatter REE distribution patterns (Fig. 3-6d). These results combined with the geologic data lead us to speculate that TSC could be one of the recharge sources of the Na De spring karst catchment. (Fig. 3-7a).

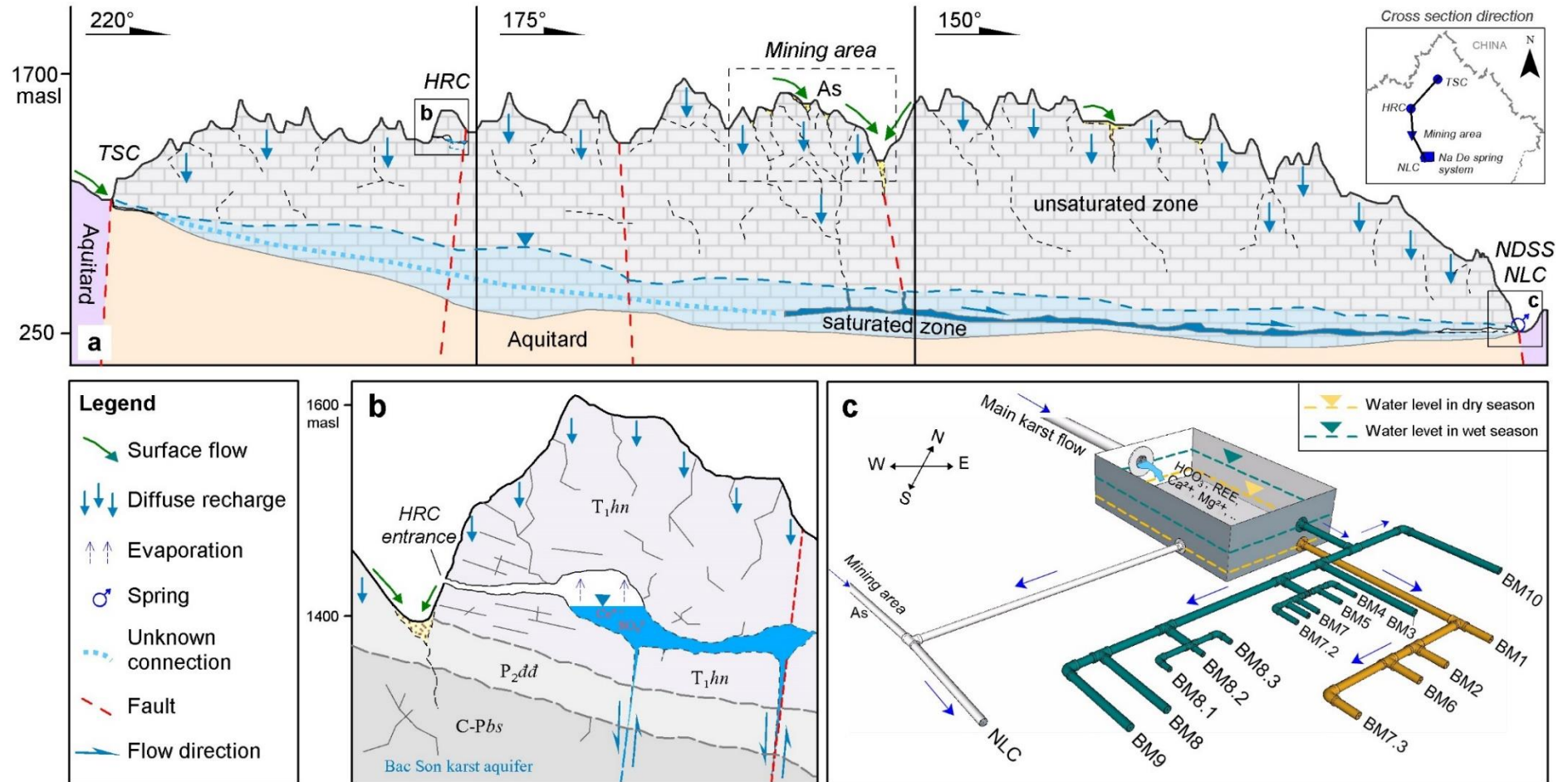


Fig. 3-7 Conceptual model of the Dong Van karst aquifer system: **a)** Cross-section displays the distribution and ability of association between sampling areas based on physicochemical parameters and trace elements in water; **b)** Profile showing the structure of Hang Rong Cave; **c)** Simple conceptual model of Na De karst spring system.

3.5.3 Estimated water balance

Calculation of the water balance is never straightforward for a karst aquifer. It requires deep understanding of hydrogeologic processes that took place in that karst system and the catchment area of the discharge zone. In this section, an estimated water balance is computed based on the established hydrogeologic conceptual model to provide preliminary ideas about the potential catchment area of the Na De discharge zone. The approximate water balance is calculated using the following general equation:

$$Q = R \times A \quad (3-4)$$

where Q = annual average discharge of the spring (m^3/s); R = estimated recharge (mm/year), i.e., the difference between precipitation (P in mm/year) and evapotranspiration (ET in mm/year); A = recharge area (km^2), i.e., the potential catchment area of the Na De discharge zone.

According to the available data (Table 3-3), this calculation includes precipitation during 2015-2020 at the climate station Dong Van District (NCHMF); potential evapotranspiration was calculated based on the hourly PET dataset (hPET) for the global land surface at 0.1° spatial resolution (Singer, et al 2021) over the period 2015-2020 due to the lack of actual evaporation data; the potential catchment area is assumed to be the entire area of the Dong Van karst plateau; and the Na De spring system discharge is a one-time measurement in the wet season (unpublished data from Ender 2014).

Table 3-3 Elements for calculating the water balance on the Dong Van karst plateau.

Potential catchment area (km^2)	Annual average precipitation (Period 2015-2020) (mm/year)	Annual average potential evapotranspiration (Period 2015-2020) (mm/year)	Annual average discharge of the spring (Period 2015-2020) (m^3/s)	The Na De spring system discharge measurement (m^3/s)
620	1537	231	25.6	44

The estimated average annual discharge of the spring is $25.6 \text{ m}^3/\text{s}$, which is lower than the discharge of the Na De spring system, which was recorded at $44 \text{ m}^3/\text{s}$. This means that the Na De discharge zone catchment could be much larger than the potential catchment boundary delineated in the Dong Van karst plateau.

It can be seen that all elements of this water balance are associated with a high degree of uncertainty, particularly the potential catchment area (A), and evapotranspiration (ET). However, this rough estimation could provide an overview of the magnitude and importance of the Na De spring system in the Dong Van karst plateau. Hence, detailed studies need to be implemented in the future in order to improve more knowledge of this karst system.

3.6 Conclusions

This article highlights the effectiveness of the groundwater geochemistry approach in karst hydrogeologic research. In particular, this approach is very useful for preliminary studies in areas like the Dong Van karst aquifer system. This study shows that analytical results of different groundwater parameters (major ions, trace and rare earth elements) can complement each other to clarify hydrochemical processes that are occurring in a karst system. This can form the basis of a hydrogeologic conceptual model, which can inform strategies for the protection and management of karst water resources.

In addition to these general conclusions, this work has led to several specific conclusions about the study area.

Multivariate statistical analysis (hierarchical cluster analysis) of major ion composition clarified water chemistry signatures and provided a scientific basis for comparing and partitioning water samples into distinct hydrochemical groups that may be significant in a geologic context. Specifically, the Na De spring system (NDSS) and Na Luong cave (NLC) belong to the same discharge zone of a karst catchment of the Bac Son karst aquifer (C-Pbs), whereas the SW springs and Tia Sang cave (TSC) were identified as typical of shallow groundwater in non-karst formations.

Trace and rare earth element concentrations and patterns can be used as potential natural tracers of groundwater origin when some processes are not revealed through conventional hydrochemical methods, such as signatures of major ions in the case of Dong Van karst aquifer system. Specifically, it is possible to show a connection between the mining area and Na Luong cave by the abnormally high arsenic concentrations, and similarity in REE pattern, combined with location and geologic data.

Meanwhile, Hang Rong cave has the features of an alkaline lake that developed in Triassic siliceous limestones of the Hong Ngai Fm., but is mainly associated with the Bac Son karst aquifer due to similarity in REE pattern and major ion composition. The commonalities in REE patterns between TSC and the NDSS, combined with geologic data, lead to speculation that it could be one of the recharge sources of the Na De discharge zone.

An initial water balance, while subject to uncertainties, indicates that the Na De discharge zone catchment may extend beyond the boundary of the Dong Van karst plateau.

These findings are subject to some limitations due to the number of samples and sampling campaigns (seasonal over a single hydrological cycle). However, these results are very encouraging and deliver a valuable base for a better understanding of the Dong Van karst aquifer system. Based on that, detailed studies could be considered and implemented in the future such as the artificial tracer test, and long-term monitoring of groundwater.

Acknowledgments We gratefully acknowledge the Vietnam Institute of Geosciences and Mineral Resources (VIGMR, Hanoi) and the Belgian SPEKUL club for their support in providing the geological and cave database. Special thanks are given to Dominik Richter, Niclas Danielzik, Nguyen Van Dong, Nguyen Cao Cuong, Nguyen Manh Tuan for their help during fieldwork. Also, we want to thank the KIT laboratory team (Daniela Blank, Christine Buschhaus and Christine Roske-Stegemann) for their support. Finally, we are grateful to Arthur N. Palmer, Margaret Palmer and Ty Ferre for their language support, as well as the two anonymous reviewers for their valuable comments.

Funding Information This work was carried out within the financial support of the German Federal Ministry of Education and Research (BMBF) [grant number [02WCL1291A](#) and [02WCL1415](#)] and was partly sponsored by the Catholic Academic Exchange Service (KAAD) and the Graduate School of the Centre for Climate and Environment (GRACE).

Appendix 3-1 REE concentration (ng/L) and REE distribution pattern parameters of water samples in the DVKP

Samp. season	Samp. area	Samp. point	La	Ce	Pr	Nd	Sm	Eu	Gd	Tb	Dy	Ho	Er	Tm	Yb	Lu	ΣREE	Ce/Ce*	Eu/Eu*	Pr _n /Yb _n	
Dry season	NDSS	BM1	8.2	3.4	1.6	6.8	1.1	0.5	1.7	0.3	2.1	0.6	1.5	0.3	1.5	0.3	29.8	0.2	1.6	0.3	
		BM2	10.1	6.8	1.9	8.4	1.9	0.8	2.2	0.4	2.3	0.7	1.8	0.3	1.6	0.3	39.5	0.3	1.9	0.4	
		BM6	8.6	6.7	1.5	6.4	1.9	0.5	1.7	0.2	2.4	0.7	1.8	0.3	1.6	0.3	34.8	0.4	1.3	0.3	
		BM7.3	7.0	4.0	1.4	5.4	1.2	0.5	1.6	0.3	2.1	0.6	1.8	0.2	1.5	0.2	27.6	0.3	1.6	0.3	
		Mean	8.5	5.2	1.6	6.7	1.5	0.6	1.8	0.3	2.2	0.6	1.7	0.3	1.5	0.3	32.9	0.3	1.6	0.3	
	Caves	NLC	8.2	5.3	1.6	7.5	1.4	0.5	2.2	0.3	3.0	0.8	2.2	0.3	1.9	0.4	35.7	0.3	1.4	0.3	
		HRC	21.3	34.2	5.0	20.2	4.6	1.3	4.2	0.7	4.1	1.0	2.2	0.3	2.2	0.4	101.7	0.7	1.3	0.7	
		TSC	14.8	12.7	3.9	16.2	3.5	1.3	5.6	0.9	4.1	1.0	2.8	0.5	1.9	0.6	69.7	0.4	1.4	0.6	
	Mining area	DA5	6.7	9.2	1.7	8.7	1.9	0.7	2.9	0.5	4.1	1.2	3.4	0.4	2.6	0.5	44.5	0.6	1.5	0.2	
		DA6	228.6	214.6	41.9	199.1	39.0	9.3	53.9	7.5	52.4	12.6	36.0	4.8	29.1	4.9	933.8	0.4	1.0	0.4	
		Mean	117.6	111.9	21.8	103.9	20.5	5.0	28.4	4.0	28.2	6.9	19.7	2.6	15.8	2.7	489.1	0.4	1.0	0.4	
	SW springs	DA7	27.1	41.1	6.2	27.0	6.3	1.8	7.6	1.1	6.3	1.3	3.8	0.5	3.1	0.5	133.7	0.7	1.2	0.6	
		DA9	13.6	23.6	2.8	13.0	2.8	0.8	2.4	0.5	2.8	0.7	1.9	0.2	1.5	0.2	66.8	0.8	1.5	0.6	
		DA11	33.8	22.0	7.3	32.5	6.2	1.8	7.3	1.1	6.5	1.2	3.9	0.5	2.8	0.4	127.3	0.3	1.3	0.8	
		DA12	38.1	44.0	8.6	35.2	6.4	1.7	7.6	1.0	6.9	1.2	3.2	0.4	2.1	0.3	156.6	0.5	1.1	1.3	
		DA13	23.4	35.3	4.7	20.7	4.3	1.2	3.8	0.5	3.4	0.6	1.8	0.2	1.5	0.3	101.8	0.7	1.4	1.0	
		Mean	27.2	33.2	5.9	25.7	5.2	1.5	5.7	0.8	5.2	1.0	2.9	0.4	2.2	0.3	117.3	0.6	1.3	0.8	
	Wet season	NDSS	BM1	18.1	16.8	3.0	17.5	3.6	1.0	6.5	1.2	9.2	2.0	6.5	0.9	5.2	1.0	92.5	0.4	1.0	0.2
			BM2	14.7	12.9	2.3	12.8	2.3	1.0	5.0	0.9	7.3	1.7	5.3	0.8	4.2	0.8	72.2	0.4	1.4	0.2
			BM3	16.0	14.9	2.2	16.0	3.2	1.3	5.8	1.1	7.7	1.7	5.7	0.8	4.3	0.8	81.5	0.4	1.4	0.2
BM4			17.1	15.8	2.7	16.0	3.4	1.1	6.5	1.2	8.4	2.0	6.4	0.9	4.6	0.9	87.0	0.4	1.1	0.2	
BM5			15.9	15.7	2.4	15.3	3.2	0.8	6.1	1.1	7.7	1.9	5.9	0.9	4.7	2.7	84.4	0.4	0.9	0.2	
BM6			17.8	18.1	2.7	15.7	3.8	1.4	6.2	1.1	8.6	1.9	6.3	1.0	4.8	0.8	90.3	0.5	1.4	0.2	
BM7			19.3	19.4	3.1	18.3	4.8	1.4	7.0	1.2	10.1	2.2	6.5	1.1	4.7	0.8	99.9	0.5	1.1	0.2	
BM7.1			17.3	17.3	2.8	17.3	4.6	1.2	5.6	0.9	7.9	1.9	5.3	0.7	4.5	0.9	88.2	0.4	1.1	0.2	
BM7.2			17.2	17.5	2.7	17.1	2.5	1.1	6.2	1.1	8.0	2.0	5.7	0.8	4.4	0.8	87.3	0.5	1.4	0.2	
BM7.3			19.4	20.1	3.5	20.2	3.9	1.1	7.1	1.2	9.6	2.2	5.9	1.2	5.2	0.9	101.4	0.5	1.0	0.2	
Caves		BM8	16.1	17.3	2.5	16.9	3.2	1.1	5.5	1.2	7.6	1.9	5.0	0.7	4.3	0.8	83.9	0.5	1.2	0.2	
		BM8.1	14.6	14.9	2.6	15.1	3.1	1.0	5.4	1.1	7.2	1.6	5.4	0.8	3.9	0.8	77.5	0.4	1.2	0.2	
		BM8.2	17.6	17.6	2.9	17.8	3.4	1.2	6.6	1.1	8.7	2.1	5.3	0.7	4.7	0.7	90.4	0.4	1.2	0.2	
		BM8.3	19.5	19.8	3.3	16.4	4.8	1.2	6.5	1.3	8.4	2.0	6.4	1.0	4.9	0.9	96.4	0.5	1.0	0.2	
		BM9	17.1	27.8	2.8	15.4	3.5	1.3	6.4	0.9	7.0	1.9	5.0	0.7	4.4	0.8	95.1	0.8	1.3	0.2	
		BM10	19.4	24.4	3.5	18.7	3.2	1.0	6.4	1.0	7.7	1.9	5.4	0.8	4.4	0.9	98.8	0.6	1.0	0.2	
		Mean	17.3	18.1	2.8	16.7	3.5	1.1	6.2	1.1	8.2	1.9	5.8	0.9	4.6	0.9	89.2	0.5	1.1	0.2	
		NLC	13.2	30.0	2.5	15.3	4.9	1.2	8.7	1.4	12.0	3.0	9.2	1.3	6.4	1.3	110.4	1.0	0.9	0.1	
		HRC	21.2	34.3	4.1	20.9	4.1	1.8	5.3	1.2	7.2	1.8	4.9	0.8	4.0	0.7	112.4	0.7	1.8	0.3	
		TSC	43.3	77.0	10.8	54.5	12.1	3.2	16.8	2.5	15.1	3.5	9.6	1.5	8.4	1.3	259.5	0.7	1.0	0.4	
Mining area	DA5	24.0	36.4	5.0	29.8	9.0	2.6	15.1	2.6	19.5	4.6	13.4	2.1	10.4	2.1	176.6	0.6	1.0	0.1		
	DA6	42.6	53.2	8.8	43.4	10.0	2.5	16.8	2.6	19.2	4.4	11.8	1.7	9.0	1.6	227.5	0.6	0.9	0.3		
	Mean	33.3	44.8	6.9	36.6	9.5	2.5	15.9	2.6	19.3	4.5	12.6	1.9	9.7	1.8	202.0	0.6	1.0	0.2		
SW springs	DA7	29.5	45.9	6.2	29.7	6.9	2.2	9.0	1.7	11.4	2.4	7.6	1.0	6.4	1.0	160.9	0.7	1.3	0.3		
	DA9	51.0	129.5	11.8	54.5	12.5	2.8	15.2	2.5	15.6	3.5	9.1	1.3	7.1	1.3	317.6	1.1	1.0	0.5		
	DA11	235.7	68.7	48.3	193.9	37.2	8.8	47.3	6.9	40.4	8.3	22.0	2.8	14.9	2.4	737.6	0.1	1.0	1.0		
	DA12	30.3	52.1	6.2	31.0	6.3	1.5	9.1	1.5	11.0	2.1	6.7	1.1	5.6	0.7	165.3	0.8	0.9	0.3		
	DA13	42.1	75.9	8.8	42.2	8.8	2.0	10.5	1.7	10.9	2.4	6.7	0.9	5.6	1.0	219.4	0.8	1.0	0.5		
Mean	77.7	74.4	16.3	70.2	14.3	3.4	18.2	2.9	17.9	3.7	10.4	1.4	7.9	1.3	320.2	0.4	1.0	0.6			

Chapter 4

4 Recommendations for sustainable water resources management and future research

4.1 Appropriate strategies for sustainable water resources management

The results presented in this study could provide several speculations on karst and cave development as well as hydrogeochemical characteristics and linkability of the karst aquifers on the karst plateau south of Dong Van town, known as the Dong Van Karst Plateau (DVKP). The results have shown that within DVKP, there are almost no or only short surface flows, which disappear soon after the rainy season (most sink underground). Meanwhile, the cave systems developed almost vertically in the vadose zone, of which numerous vertical caves reached depths of up to -341 m in the Hang Ong cave, -340 m in Xa Lung 2 cave, or more than -306 m in the Lung Chinh cave (Masschelein et al. 2007), and not yet deepened to the local base level. In addition, in the southern part of DVKP, at an altitude of 240 masl, Na Luong cave which belongs to the Na De spring system is supposed as the local base level for karst erosion. This means that the water table in this area is at a depth of more than 1000 m above the terrain surface. For most residential areas and villages within the karst plateau, this groundwater table is too deep to extract by common methods such as drilled or dug wells. Plenty of solutions have been applied to address water scarcity in the dry season (as mentioned in Sect. 1.2.3), but they are not effective or sustainable due to high costs, easy damage, and easily polluted water sources. Therefore, adapted water supply strategies such as the KaWaTech project model need to be developed and applied

to meet the increasing water demand that has to be expected due to the economic development and increasing tourism in the whole Geopark area.

In another aspect, from the hydrogeological point of view, results of hydrogeochemical analysis have indicated that the Na De spring system and Na Luong cave belong to the same discharge zone of Bac Son karst aquifer. This spring system forms the source of the Nhiem River, one of the largest discharge zone in the northern part of Vietnam. This information is give evidence of a huge karst catchment area that can cover most or even larger than the area of DVKP. This shows that the Na De spring system area is one of the potential research sites where the "pump used as turbine" (PAT) model can be applied in order to provide sustainable water for highland areas following the concept model of the KaWaTech project or IWRM project in Indonesia (BMBF website).

In addition, there is also a linkability between Na Luong cave and surrounding catchments such as the mining area due to the abnormally high arsenic concentrations which indicate that karst aquifers are susceptible and highly vulnerable to pollution. Therefore, appropriate strategies for the protection, management and sustainable use of water resources need to be established and implemented based on the study and understanding of the Dong Van karst hydrogeological system. In order to address these issues, an urgent strategy that needs to be implemented is to improve awareness among local communities. The aim of this work is to engage the local people in topics related to water and ecosystem conservation; rational water use; or protection of existing water sources and water supply facilities through training, teaching and conventional media (printed media, TV, radio) based on close cooperation between local authorities, schools with environmental NGOs and volunteer groups.

In karst aquifers, water from the surface, including pollutants, penetrates into the ground almost without filtration. Therefore, as a key point to sustainable karst water management, local authorities should develop solutions for planning and treating industrial, domestic, and livestock wastewater before it is discharged into the environment. One of the appropriate wastewater treatment models that could be applied to the DVKP in the future is the decentralized wastewater treatment systems (DWWTS) model which was installed in the Lower Jordan Rift Valley as part of the SMART - IWRM project. This system offers the possibility to introduce wastewater treatment and generate irrigation

water in places that are not connected to centralized treatment plants. The advantage of this technology is providing wastewater treatment infrastructure even in remote and hilly rural communities through the GIS-based assessment (ALLOWS) approach (Fig 4-1) (for more details, see Müller et al. 2011, van Afferden et al. 2015). Furthermore, there should be regulations for the provision and use of environmentally friendly fertilizers and pesticides in agricultural production.

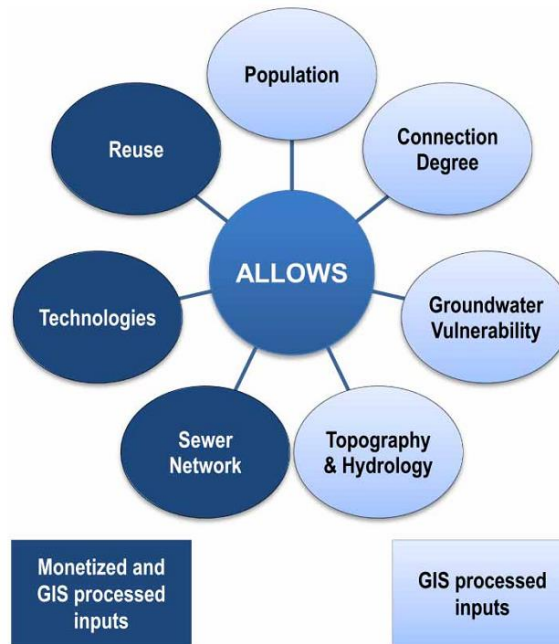


Fig. 4- 1 ALLOWS input data (© van Afferden et al. 2015)

4.2 Outlook for future research

Studying and understanding the processes that take place in the karst systems is a key basis for developing adequate solutions for the protection, management and sustainable use (Ford & Williams 2007). In this thesis, the results basically give the assessments of karst and cave development as well as hydrogeochemical features of the karst aquifers on the DVKP. However, there are still limitations due to accessibility and level of cave exploration, or limited number of water samples and sampling campaigns over a large study site. For these reasons, detailed geological, and hydrogeological investigations, besides speleological expeditions need to be implemented in the future in order to improve more knowledge of the karst system on this plateau.

In order to demonstrate quantitatively the relation between cave level and the planation surface pointed out in this study, dating of the clastic cave sediments at different levels can be used to compare with respectively terrace deposits following an approach proposed by Anthony & Granger (2007). These sediments can be dated by using the differential decay of cosmogenic aluminium-26 (^{26}Al) and beryllium-10 (^{10}Be) in quartz exposed to cosmic radiation at the surface, then buried underground in the cave. In addition, as indicated by Fairchild et al. (2006), Ford & Williams (2007), speleothems or stalagmites can be defined as environmental archives, which have the capacity to effectively record information about climatic and environmental conditions that have prevailed during their formation, in the form of geochemical parameters that are “proxies” for the actual climatic and environmental parameters. Recently, a multi-proxy approach that combines speleothem (stalagmite) stable oxygen and carbon isotopes, trace elements, as well as fabric types in conjunction with monitoring of cave environments has been applied by Hartmann (2020) to reconstruct paleo-climatic in a small karst catchment of Ma Le river, northern of DVKP. In the future, this approach can be widely applied to better understand the paleo-climatic and environmental conditions in relation to the karst evolution processes that occurred in the study site.

Karst aquifers are often geologically and hydraulically complex, therefore, to study and protect a karst aquifer, the catchment area must be identified (Goldscheider & Drew, 2007). However, within the scope of this thesis, the results have essentially not determined accurately the catchment area of the karst aquifer whose discharge zone is the NDSS, which means that numerous appropriate research works are required in the future to progressively determine the catchment area of this discharge zone. Delineation of spring catchments usually relies on classical hydrogeological methods such as three-dimensional geological analysis, spring hydrograph monitoring, water balances, hydrochemical /isotopic methods, geophysical investigations, and artificial tracer tests. However, these methods generally are complex and costly. Where little information about the catchment is available at all, an approximate localization is advantageous as the first step towards an exact delineation, since it facilitates the application of more elaborate methods as mentioned above. There has already been an attempt by Longenecker et al. (2017) to semi-automatically derive approximate catchment boundaries

by correlating karst spring discharge events with global precipitation measurement (GPM) gridded data (NASA, 2016). This approach has demonstrated that is a useful tool for rapidly linking water supplies to their recharge areas which can also be appropriate to apply for the Na De spring system, but also noticed that it could not fully replace conventional hydrogeologic methods. In a recent study, Wunsch (2022) applied convolutional neural networks (CNNs) to simulate karst spring discharge and to directly learn from spatially distributed climate input data (combined 2D–1D CNNs) (Fig 4-2). Besides, by performing a spatial input sensitivity analysis, this approach can further show their usefulness in localizing the position of karst catchments. This approach has indicated that if the exact position of the catchment is unknown, using gridded data has the advantage that a broader region can be taken into account as input to let the model learn the relevant grid cells automatically. In a region where climate stations are sparse like in the Dong Van Karst Plateau, applying the machine learning methods such as artificial neural networks by using gridded meteorological data with a good spatial resolution as well as large-scale availability (e.g., continental – E-OBS or even global – ERA5-Land; see Bandhauer et al. 2021) can provide powerful solution to delineation the Na De discharge catchment.

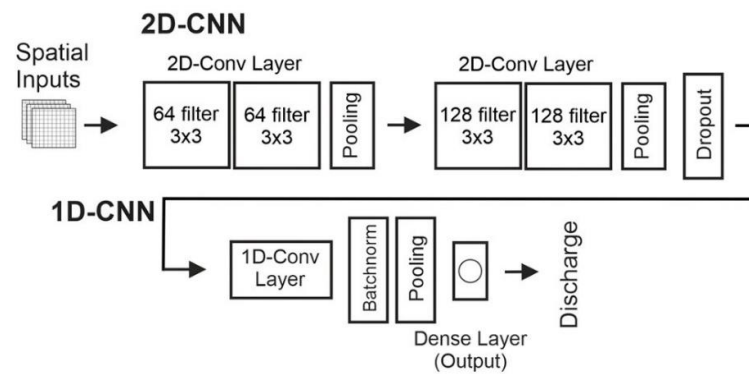


Fig. 4- 2 Model structures applied for modeling karst spring discharge based on gridded meteorological input data. (Modified from Wunsch et al. 2022)

It can be seen that gridded climate data are useful for overcoming missing climate station data as well as contributing to solving different problems in localizing the spatial extent of karst catchments, given sufficiently small grid cell sizes. However, to improve accuracy in the application of these techniques and provide data for future research, a simple ground-based rain gauge system could be established in the expected catchment (Fig. 4-3), besides installing the hydrograph monitoring system for the Na De spring system.

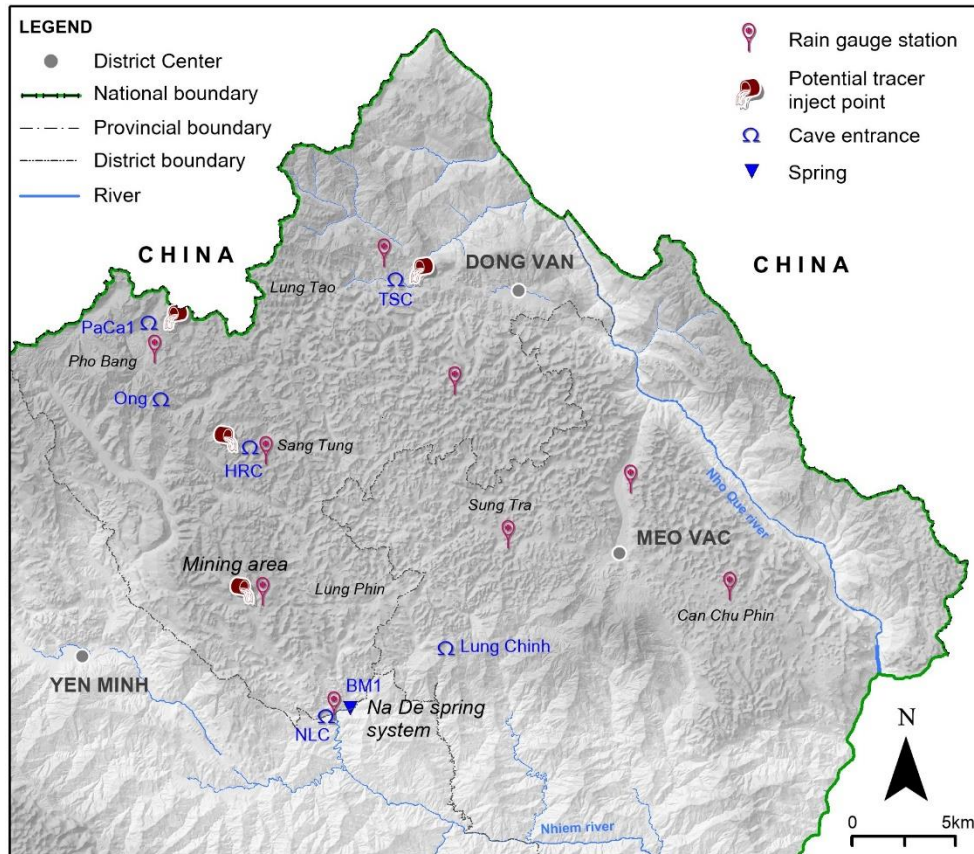


Fig. 4-3 Map of expected ground-based rain gauge network and potential trace inject points.

For a large and complex discharge zone such as the Na De spring system, the installation of a hydrograph monitoring system is necessary for future detailed hydrogeologic research and water resources management actions. Accordingly, the real-time hydrograph analysis is an essential step in assessing and characterizing the behavior and properties of the drainage system, thus the installation requires specific studies and evaluations. Based on the results of this work, the idea concept of a monitoring system for the Na De spring system was established for future application scenarios. Due to NDSS and NLC belonging to the same discharge zone, in which Na Luong cave also has a connection with the surrounding catchments, therefore, this monitoring system will include at least two hydrological monitoring stations, one located at the mainstream namely HMS1 and the other at the discharge flow of Na Luong cave called HMS2 (Fig. 4-4a).

For each station, a multifunction hydrological monitoring system is designed, including at least basic monitoring items such as water level, flow rate, rainfall, air temperature and water physical parameters (T, pH, TDS, EC, oxygen, turbidity). Since the system is located in a remote area without electricity, a

compact monitoring system that uses solar energy with low power consumption, and is suitable for harsh application environments is recommended for installation. In terms of operation and preservation of the monitoring system, a simple wooden or concrete station house should be constructed to protect the equipment installed inside, while serving as a sampling point and temporary staying area during long-term observations such as artificial tracer tests or water quality monitoring. Figure 4-4c shows an example of a simple station house built near the karst flow with groundless, which combines concrete (at the foundation) and wood (World Bank 2018). This model is considered suitable for future applications in the Na De discharge zone.

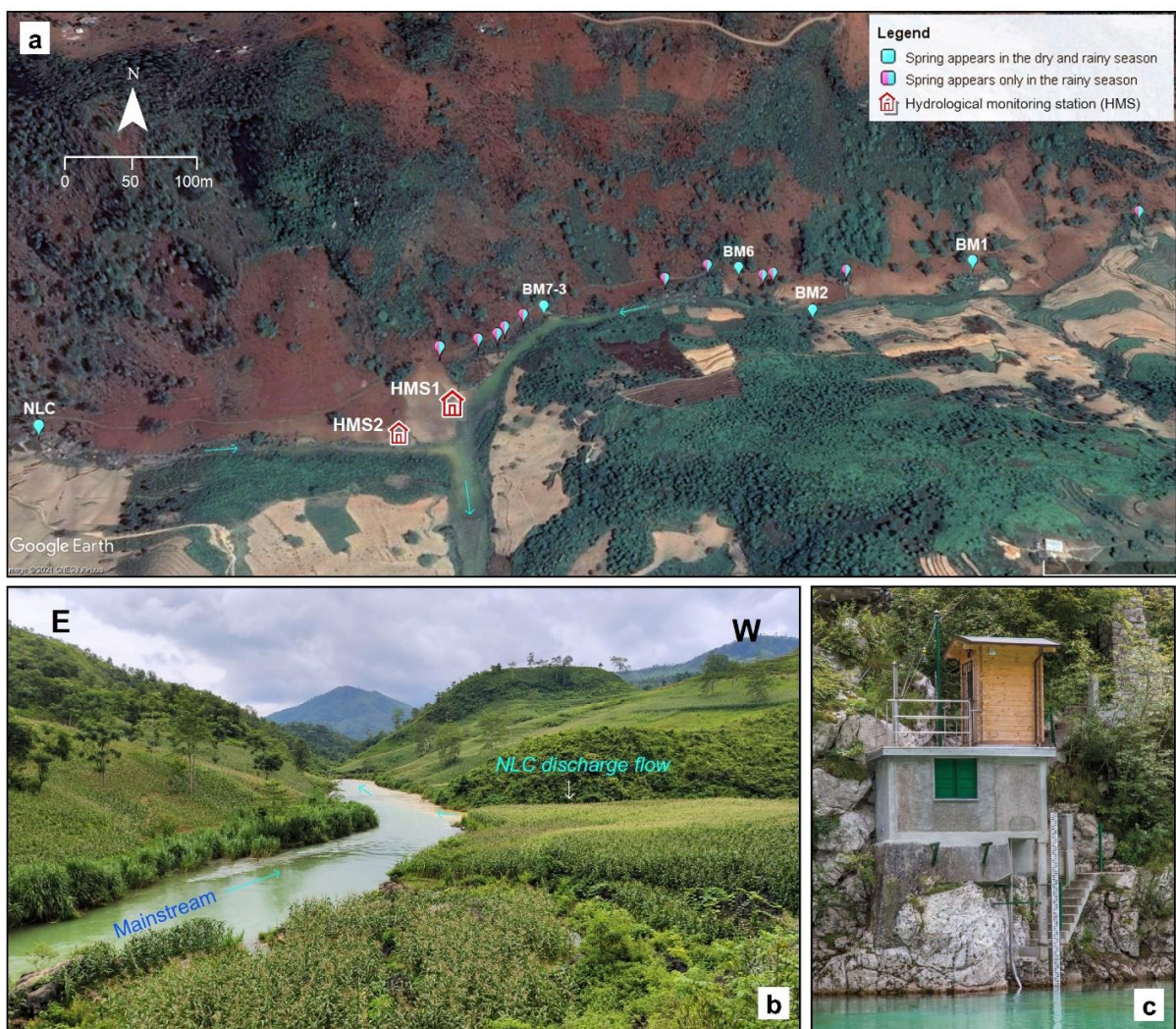


Fig. 4-4 a) Plan of the expected installation location for hydrological monitoring stations of Na De discharge zone; b) View of mainstream and NLC discharge flow from HMS1 expected site; c) An example of a hydrological monitoring station model. (Source: World Bank 2018)

The final step that should be performed to comprehensively evaluate a karst aquifer system is the artificial tracer test. This experiment delivers not only hints and indications but clear and quantitative evidence of underground connections, as well as characterizing the dynamics of the rapid conduit-flow connections. The conduits connect almost infiltration points of the karst system such as swallow holes, sinkholes, doline, and sinking streams to the karst springs. Therefore, to apply this method, more detailed geologic and hydrogeologic investigations are required in the future to identify potential tracer injection points. As pointed out in this study and shown in Figure 4-3, there are several locations that are possible to become the tracer injection points, such as the sinking stream of Tia Sang Cave, the swallow holes in the mining area, and the lake in Hang Rong cave because of the similarity of the hydrochemical signature with the NDSS. In addition, there are also a number of potential injection points including the sinking stream of Pa Ca 1 cave and the underground flow in Hang Ong and Lung Chinh cave. However, this method also has a few limitations when applied in large regionals or systems with long transit times, and the preparation and operation of tracer tests are rather expensive and laborious (Goldscheider 2015). The future implementation of tracer experiment in DVKP requires more detailed investigations as described in this study such as geological mapping, speleological survey, hydrological measurements, the application of hydrochemical methods to obtain more information on aquifer properties, catchment areas, flow, and mixing processes, using trace elements as natural tracers, besides the water balances, isotopic methods and several methods that mentioned above.

Chapter 5

5 Conclusions

Karst research is a huge challenge and requires a profound understanding of the karst system as well as related knowledge such as lithology, tectonics, geomorphology, etc. In this thesis, suitable methods and approaches were applied based on objective conditions and available databases, to better understand the karst development and groundwater resources of a subtropical karst system in Northern Vietnam.

In this region, the KaWaTech and KaWaTech Solutions projects were implemented in order to develop a sustainable freshwater supply by closely integrating several scientific aspects on hydrogeology, hydropower, water production, distribution and supply, water resource protection, and socio-cultural. During these projects, numerous hydrogeologic aspects were considered and addressed, including water availability, discharge variability, water quality, contaminant and sediment transport, and the vulnerability of karst aquifers in the Ma Le valley, Dong Van town, and surrounding areas. The results obtained are valuable in addressing the problem of water scarcity and improving the karst water resources management in Dong Van city, as well as demonstrating that it is a suitable water management model which can be applied in other karst regions. However, these areas belong to the small catchment which is located in the northeastern part of the UNESCO Global Geopark and consist of favorable geological conditions for groundwater availability. Meanwhile, the karst region south of Dong Van town is facing serious water scarcity due to the strongly dissected karst terrain's inability to store surface water and the groundwater level is very deep. In this context, many scientific aspects must be considered, including cave development and distribution in relation to the tectonic and geomorphologic evolution processes, groundwater physico-chemistry relate to the mixing processes and water-rock interaction, water quality, contaminant transport, and the linking of karst flow paths.

To address these issues, extensive fieldwork was carried out and the results from two studies presented in this thesis have been given as follows.

In chapter 2, the karstification conceptual model (Fig. 2-11) was performed to highlight the relationship between cave systems and the tectonic and geomorphologic development on the Dong Van Karst Plateau and provide a basis for further investigations. Accordingly, the cave classification based on the cave conduit's geometric parameters indicated that the karst evolution in this area is in a youthful stage, with cave systems developed mainly of the isometric form (developed almost vertically) in the vadose zone, and not yet deepened to the local base level. The degree of correlation between cave levels and planation surfaces suggests that the development of horizontal cave passages is related to two levels of planation surfaces at 1000-1250 and 1250-1450 masl. Meanwhile, at an altitude of 240 masl, the Na Luong cave which belongs to the Na De spring system could be the local base level for karst erosion. Additionally, cave passage orientation shows that the cave system formed and developed under the influence of tectonic activities in the Cenozoic. The dominant orientation trend is roughly in the East-West direction and occurred in the early phase (Eocene - Miocene). Next is a trend roughly North-South that occurred in the late phase (Pliocene - Quaternary). The last orientation trend follows the NW-SE direction due to the reactivation of paleo-fault systems in the same direction.

Chapter 3 highlights the effectiveness of the groundwater geochemistry approach in karst hydrogeologic research. In particular, this approach is very useful for preliminary studies in areas like the Dong Van karst aquifer system. This study shows that analytical results of different groundwater parameters (major ions, trace and rare earth elements) can complement each other to clarify hydrochemical processes that are occurring in a karst system. This can form the basis of a hydrogeologic conceptual model (Fig. 3-7), which can inform strategies for the protection and management of karst water resources. Specifically, the major ion composition and cluster analysis indicate that the Na De spring system and Na Luong cave belong to the same discharge zone of Carboniferous karst aquifer, while the southwestern springs and Tia Sang cave were identified as typical of shallow groundwater movement in the weathered surface zone in non-karst formations. In addition, it is possible to show a connection between the mining area and Na Luong cave by the

abnormally high arsenic concentrations, and similarity in REE pattern, combined with location and geologic data. Meanwhile, Hang Rong cave has the features of an alkaline lake that developed in Triassic siliceous limestones of the Hong Ngai Fm., but is mainly associated with the Bac Son karst aquifer due to similarity in REE pattern and major ion composition. The commonalities in REE patterns between TSC and the NDSS, combined with geologic data, lead to speculation that it could be one of the recharge sources of the Na De discharge zone. An initial water balance calculation, while subject to uncertainties, indicates that the Na De discharge zone catchment may extend beyond the boundary of the Dong Van karst plateau.

In summary, the results presented in this thesis have essentially clarified the development of karst and caves, as well as the hydrogeochemical processes and connectivity ability of karst aquifers on the Dong Van Karst Plateau. Although there are still some incompleteness, the results obtained are rather positive, which provides the basis for future detailed hydrogeologic studies in this area.

Declaration of authorship

Study 1 (Chapter 2)



Citation: Diep Anh Tran, Nadine Goeppert, Arthur N. Palmer, Nico Goldscheider (2022) Development and structure of karstification of the Dong Van Karst Plateau UNESCO Global Geopark, North Vietnam based on cave survey data. International Journal of Earth Sciences, <https://doi.org/10.1007/s00531-022-02190-5>

Declaration of authorship: Diep Anh Tran (Diep) performed investigations, and gathered and analyzed the data, proposed the methodology in close consultation with Arthur N. Palmer, Nico Goldscheider, and Nadine Goeppert. Diep wrote the manuscript. The manuscript was reviewed and edited by all authors.

Study 2 (Chapter 3)

Citation: Diep Anh Tran, Nadine Goeppert, Nico Goldscheider. Use of major ion chemistry, trace and rare earth elements to characterize hydraulic relations, mixing processes and water-rock interaction in the Dong Van karst aquifer system, Northern Vietnam. Hydrogeology Journal (Under review)

Declaration of authorship: Diep Anh Tran (Diep) performed investigations, and gathered and analyzed the data, proposed the methodology in close consultation with Nico Goldscheider, and Nadine Goeppert. Diep wrote the manuscript. The manuscript was reviewed and edited by all authors.

References

- An, L.D., Bao, D.V., (2008). Dong Van - Meo Vac Karst Plateau: A valuable karst geomorphology heritage. *Journal of Earth Sciences*, 30 (4) Addendum: 534-544, (2008). (in Vietnamese).
- Anh, T.D, Goepfert, N., Palmer, A.N., Goldscheider, N. (2022) Development and structure of karstification of the Dong Van Karst Plateau UNESCO Global Geopark, North Vietnam based on cave survey data, *Int J Earth Sci (Geol Rundsch)* 111: 1573–1592, <https://doi.org/10.1007/s00531-022-02190-5>
- Anthony, D.M. & Granger, D.E. (2007) A new chronology for the age of Appalachian erosional surfaces determined by cosmogenic nuclides in cave sediments. *Earth Surface Processes and Landforms: The Journal of the British Geomorphological Research Group*, 32(6), pp.874-887. <https://doi.org/10.1002/esp.1446>
- Audra, P. & Palmer, A.N. (2017) The pattern of caves: controls of epigenic speleogenesis. *Geomorphology Revues*, 17(4), 1–40.
- Bandhauer, M., Isotta, F., Lakatos, M., Lussana, C., Båserud, L., Izsák, B., Szentes, O., Tveito, O. E., & Frei, C.: Evaluation of Daily Precipitation Analyses in E-OBS (V19.0e) and ERA5 by Comparison to Regional High-Resolution Datasets in European Regions. *Int. J. Climatol.*, 42, 727–747, <https://doi.org/10.1002/joc.7269>, 2021.
- Berglund, J.L., Toran, L., Herman, E.K. (2019) Deducing flow path mixing by storm-induced bulk chemistry and REE variations in two karst springs: With trends like these who needs anomalies?, *J. Hydrol.* 571: 349-364, <https://doi.org/10.1016/j.jhydrol.2019.01.050>
- BMBF website <https://www.wasserressourcen-management.de/en/293.php>
- Chen, Z. (1993) Discussion on the principles, contents and methods for mapping geomorphologic maps of China. *Acta Geographica Sinica*, 48(2): 105–112. (in Chinese)

- Cholet, C., Steinmann, M., Charlier, J.B., Denimal, S. (2019) Characterizing fluxes of trace metals related to dissolved and suspended matter during a storm event: application to a karst aquifer using trace metals and rare earth elements as provenance indicators, *Hydrogeol. J.* 27(1): 305-319, <https://doi.org/10.1007/s10040-018-1859-2>
- Coldewey, W. G. (n.d.) (2019). Hydrogeology. *Springer Textbooks in Earth Sciences, Geography and Environment*. <https://doi.org/10.1007/978-3-662-56375-5>
- Collon, P., Bernasconi, D., Vuilleumier, C., Renard, P. (2017) Statistical metrics for the characterization of karst network geometry and topology. *Geomorphology* 283:122–142. <https://doi.org/10.1016/j.geomorph.2017.01.034>.
- Dovjikov, A.E., My, B.P. and Vashilevshkaya, E.D. (1965) Geological Map of North Vietnam, Scale 1:500 000, with Memoir 650 pp. *Science and Technics Publishing House*, Hanoi.
- Elango, L., Kannan, R. (2007) Rock–water interaction and its control on chemical composition of groundwater. *Developments in environmental science*, 5: 229-243, [https://doi.org/10.1016/S1474-8177\(07\)05011-5](https://doi.org/10.1016/S1474-8177(07)05011-5)
- Ender, A. (2014) Fieldtrip report in Dong Van Karst Plateau, North Vietnam on July 2014 of TP2-AWG subproject under Vietnamese-German Cooperation for the Development of Sustainable Karst Water Technologies Project (Unpublished).
- Ender, A., Goeppert, N., Grimmeisen, F., & Goldscheider, N. (2017) Evaluation of β -d-glucuronidase and particle-size distribution for microbiological water quality monitoring in Northern Vietnam. *Science of the total environment*, 580, 996-1006. <https://doi.org/10.1016/j.scitotenv.2016.12.054>
- Ender, A., Goeppert, N., & Goldscheider, N. (2018a) Spatial resolution of transport parameters in a subtropical karst conduit system during dry and wet seasons. *Hydrogeology Journal*, 26(7), 2241-2255. <https://doi.org/10.1007/s10040-018-1746-x>

- Ender, A., Goepfert, N., Goldscheider, N. (2018b) Hydrogeological controls of variable microbial water quality in a complex subtropical karst system in Northern Vietnam, *Hydrogeol. J.* 26(7): 2297-2314. <https://doi.org/10.1007/s10040-018-1783-5>
- Fairchild, I.J., Smith, C.L., Baker, A., Fuller, L., Spötl, C., Matthey, D. (2006) Modification and preservation of environmental signals in speleothems. In: *Earth-Science Reviews* 75 (1–4), pp. 105–153. <https://doi.org/10.1016/j.earscirev.2005.08.003>
- Ford, D.C., (1971) Geologic structure and a new explanation of limestone cavern genesis. *Transactions of the Cave Research Group of Great Britain.* 13 (2), 81–94.
- Ford, D. & Williams, P.D. (2007) Karst Hydrogeology and Geomorphology, *John Wiley & Sons*, 562, <https://doi.org/10.1002/9781118684986>
- Filipponi, M., Jeannin, P. Y., & Tacher, L. (2009) Evidence of inception horizons in karst conduit networks. *Geomorphology*, 106(1–2), 86–99. <https://doi.org/10.1016/j.geomorph.2008.09.010>
- Gao, Z., Liu, J., Feng, J., Wang, M., Wu, G. (2019) Hydrogeochemical characteristics and the suitability of groundwater in the alluvial-diluvial plain of southwest Shandong Province, China, *Water (Switzerland)* 11(8):1577, <https://doi.org/10.3390/w11081577>
- General Statistics Office of Vietnam (2021) Statistical Yearbook of Viet Nam. 1056p. *Statistical Publishing House.*
- Gibbs, R.J. (1970) Mechanisms controlling world water chemistry, *Science* 170(3962): 1088-1090.
- Gill, L.W., Babechuk, M.G., Kamber, B.S., McCormack, T., Murphy, C. (2018) Use of trace and rare earth elements to quantify autogenic and allogenic inputs within a lowland karst network, *Appl. Geochemistry* 90: 101-114, <https://doi.org/10.1016/j.apgeochem.2018.01.001>
- Gillieson, D. (2005). Karst in southeast Asia. *The Physical Geography of Southeast Asia.* Oxford University Press, Oxford, 157-176.

- Global Geoparks Network (2019) Dong Van Karst Plateau UNESCO Global Geopark annual report 2019. http://www.globalgeopark.org/UploadFiles/2020_11_3/Dong-Van-Annual-Report-2019-final.pdf
- Global Geoparks Network (2020) Dong Van Karst Plateau UNESCO Global Geopark annual report 2020 http://www.globalgeopark.org/UploadFiles/2020_11_3/Dong-Van-Annual-Report-2020-final.pdf
- Goldscheider, N. (2015) Overview of Methods Applied in Karst Hydrogeology. In: Stevanović Z (eds) Karst Aquifers - Characterization and Engineering, Professional Practice in Earth Sciences. Springer, Cham. p 127-145, https://doi.org/10.1007/978-3-319-12850-4_4
- Goldscheider, N. (2019) A holistic approach to groundwater protection and ecosystem services in karst terrains. *Carbonates and Evaporites*, 34(4): 1241-1249, <https://doi.org/10.1007/s13146-019-00492-5>
- Goldscheider, N., Chen, Z., Auler, A. S., Bakalowicz, M., Broda, S., Drew, D., Hartmann, J., Jiang, G., Moosdorf, N., Stevanovic, Z., & Veni, G. (2020) Global distribution of carbonate rocks and karst water resources. *Hydrogeol. J.* 28(5), 1661-1677 <https://doi.org/10.1007/s10040-020-02139-5>
- Güler, C., Thyne, G.D., McCray, J.E., Turner, A.K. (2002) Evaluation of graphical and multivariate statistical methods for classification of water chemistry data, *Hydrogeol. J.* 10(4): 455–474, <https://doi.org/10.1007/s10040-002-0196-6>
- Ha Giang Department of Planning and Investment (2021) Explain the construction planning of Ha Giang province to 2030, vision to 2050. (In Vietnamese) <http://skhdt.hagiang.gov.vn/index.php/tin-tuc/chi-tiet/357>
- Ha Giang People's Council (2020) Resolution No. 39/NQ-HDND dated December 9, 2020, The approval of Ha Giang province's socio-economic development plan for the period of 2021-2025. (In Vietnamese) <http://dbnd.hagiang.gov.vn/index.php?nv=laws&op=view-1079-39-NQ-HDND>
- Ha Giang Statistics Office (2021) Ha Giang Statistical Yearbook 2020. *Statistical Publishing House*, 575p.

- Han, G., Liu, C.Q. (2007) Dissolved rare earth elements in river waters draining karst terrains in Guizhou Province, China, *Aquat Geochem* 13(1): 95-107, <https://doi.org/10.1007/s10498-006-9009-1>
- Hai, T.T., Bat, D.V., Chi, N.K., Que, D.H. & Quyen, N.M. (2013) Structural controls on the occurrence and morphology of karstified assemblages in northeastern Vietnam: A regional perspective. *Environmental Earth Sciences*, 70(2), 511–520. <https://doi.org/10.1007/s12665-011-1057-1>
- Häuselmann, P., Jeannin, P. Y., & Bitterli, T. (1999) Relationships between karst and tectonics: Case-study of the cave system north of lake thun (bern, switzerland). *Geodinamica Acta*, 12(6), 377–388. <https://doi.org/10.1080/09853111.1999.11105357>
- Hartmann, A. (2020) Speleothem-based reconstruction of the Paleohydrology in the tropical western Pacific. *Department of Civil Engineering, Geo- and Environmental Sciences of the Karlsruhe Institute of Technology (KIT)*. Ph.D. thesis, 426 p.
- Heikkinen, P., Korkka-Niemi, K., Lahti, M., Salonen, V.P. (2002) Groundwater and surface water contamination in the area of the Hitura nickel mine, Western Finland, *Env Geol* 42(4): 313-329, <https://doi.org/10.1007/s00254-002-0525-z>
- HGDONRE (2021) Project Summary Report: Investigate and assess the current status of water use and identify sources of water pollution; assess the quality of domestic water sources in four mountain districts, propose solutions for sustainable water use to meet climate change. (In Vietnamese) <http://stnmt.hagiang.gov.vn/baiviet?id=1143>
- Holland, M., Witthüser, K.T. (2009) Geochemical characterization of karst groundwater in the cradle of humankind world heritage site, South Africa, *Env Geol* 57(3): 513–524. <https://doi.org/10.1007/s00254-008-1320-2>
- Hunkeler, D. & Mudry, J. (2014) Hydrochemical methods. In: Goldscheider, N. & Drew, D. (eds) *Methods in karst hydrogeology, IAH: International Contribution to Hydrogeology*, 26. Taylor and Francis, London. p 93-121, <https://doi.org/10.1201/9781482266023>
- Huyen, D.T. (ed) (2007) Phanerozoic stratigraphy in the Northeast part of Vietnam. *Center for Information and Archives of Geology, Geological Survey of Vietnam*. 537 p. (inVietnamese)

- Jacoby, B. S., Peterson, E. W., Kostelnick, J. C., & Dogwiler, T. (2013) Approaching Cave Level Identification with GIS: A Case Study of Carter Caves. *ISRN Geology*, 2013(Figure 1), 1–7. <https://doi.org/10.1155/2013/160397>
- Janvier, P. & Phuong, T.H. (1999) Vertebrates (Placodermi, Galeaspida) of the Lower Devonian of the Lung Côt-Mia Lé section, Hà Giang province, Vietnam, with complementary comments on vertebrate deposits of the eastern Bac Bo Devonian (*Les vertébrés (Placodermi, Galeaspida) du Dévonien inférieur de la coupe de Lung Côt-Mia Lé, province de Hà Giang, Viêt Nam, avec des données complémentaires sur les gisements à vertébrés du Dévonien du Bac Bo oriental*). *Geodiversitas*, 21(1), pp.33-67 (in French)
- Jaskolla, F., Volk, P. (1986) Use of Cave-maps for tectonic surveys. *Int. J. Speleol.* 15, pp. 15-40.
- Jeannin, P.Y., Groves, C., Häuselmann, P. (2007) Speleological investigations. In: Goldscheider, N., Drew, D. (Eds.), *Methods in Karst Hydrogeology*. Taylor & Francis, London, pp. 25–44.
- Johannesson, KH., Lyons, W.B., Bird, D.A (1994) Rare earth element concentrations and speciation in alkaline lakes from the western USA, *Geophys. Res. Lett.* 21(9): 773-776, <https://doi.org/10.1029/94GL00005>
- Jouves, J., Viseur, S., Arfib, B., Baudement, C., Camus, H., Collon, P., & Guglielmi, Y. (2017) Speleogenesis, geometry, and topology of caves: A quantitative study of 3D karst conduits. *Geomorphology*, 298, 86–106. <https://doi.org/10.1016/j.geomorph.2017.09.019>
- Kambesis, P. (2007) The importance of cave exploration to scientific research. *Journal of Cave and Karst Studies*, 69(1), 46–58.
- Khang, P. (1985) The development of karst landscapes in Vietnam. *Acta Geol. Pol.* 35(3–4): 305–319.
- Klimchouk, A., (2009) Morphogenesis of hypogenic caves. *Geomorphology* 106 (1–2): 100–117. <https://doi.org/10.1016/j.geomorph.2008.09.013>.
- Klimchouk, A., Auler, A.S., Bezerra, F.H.R., Cazarin, C.L., Balsamo, F., Dublyansky, Y. (2016) Hypogenic origin, geologic controls and functional organization of a giant cave system in

- Precambrian carbonates, Brazil. *Geomorphology* 253:385–405. <https://doi.org/10.1016/j.geomorph.2015.11.002>
- Labib, M. A., Haryono, E., & Sunarto. (2019) The development of cave passage in Donomulyo, Malang-Indonesia. *E3S Web of Conferences*, 76, 1–7. <https://doi.org/10.1051/e3sconf/20197604010>
- Lam, N.V., Ngoc, N.K., Hoan, H.V., Tuan, T.Q., Nga, V.T. (2013) Characteristics of groundwater in karstic region in northeastern Vietnam. *Environ. Earth Sci.* 70(2): 501–510. <https://doi.org/10.1007/s12665-012-1548-8>
- Lambrakis, N., Antonakos, A., Panagopoulos, G. (2004) The use of multicomponent statistical analysis in hydrogeological environmental research, *Water Res.* 38(7): 1862-1872, <https://doi.org/10.1016/j.watres.2004.01.009>
- Lee, S.G., Lee, D.H., Kim, Y., Chae, B.G., Kim, W.Y., Woo, N.C. (2003) Rare earth elements as indicators of groundwater environment changes in a fractured rock system: evidence from fracture-filling calcite, *Appl. Geochemistry* 18(1): 135-143, [https://doi.org/10.1016/S0883-2927\(02\)00071-9](https://doi.org/10.1016/S0883-2927(02)00071-9)
- Littva, J., Hók, J., & Bella, P. (2015) Cavitonics: Using caves in active tectonic studies (Western Carpathians, case study). *Journal of Structural Geology*, 80, 47–56. <https://doi.org/10.1016/j.jsg.2015.08.011>
- Bontridder, L.D. (2010, 2019) Cave database in Ha Giang. (Unpublished data)
- Longenecker, J., Bechtel, T., Chen, Z., Goldscheider, N., Liesch, T. & Walter, R. (2017) Correlating Global Precipitation Measurement satellite data with karst spring hydrographs for rapid catchment delineation. *Geophysical Research Letters*, 44(10), pp.4926-4932. <https://doi.org/10.1002/2017GL073790>
- Masschelein, J., Coessens, V., Lagrou D., Duser, M., & Van, T.T. (eds) (2007) Northern Vietnam 1993-2006 (Belgian-Vietnamese speleological projects in the provinces of Bac Kan, Ha Giang, Hoa Binh, Lai Chau and Son La). *Berliner Höhlenkundliche Berichte*.

- McLennan, S.M. (1989) Rare earth elements in sedimentary rocks: influence of provenance and sedimentary processes. In: Bruce RL, McKay GA (eds) *Geochemistry and Mineralogy of Rare Earth Elements*, *Mineral. Soc. Am., Washington, DC*. p 169-200, <https://doi.org/10.1515/9781501509032-010>
- Moldovan A, Hoaghia MA, Kovacs E, Mirea IC, Kenesz M, Arghir RA, Petculescu A, Levei EA, Moldovan OT (2020) Quality and health risk assessment associated with water consumption - a case study on karstic springs. *Water (Switzerland)*, 12(12):3510, <https://doi.org/10.3390/w12123510>
- Molnar, P; England, P; Martinod, J, (1993) Mantle dynamics, uplift of the Tibetan Plateau, and the Indian Monsoon. *Reviews of Geophysics*, 3(4): 357-396 .
- Möller P, Bau M (1993) Rare-earth patterns with positive cerium anomaly in alkaline waters from Lake Van, Turkey, *Earth Planet. Sci. Lett.* 117(3-4): 671-676, [https://doi.org/10.1016/0012-821X\(93\)90110-U](https://doi.org/10.1016/0012-821X(93)90110-U)
- Möller P, Dulski P, Savascin Y, Conrad MJCG (2004) Rare earth elements, yttrium and Pb isotope ratios in thermal spring and well waters of West Anatolia, Turkey: a hydrochemical study of their origin, *Chem. Geol.* 206(1-2): 97-118, <https://doi.org/10.1016/j.chemgeo.2004.01.009>
- Müller, R. A., Cardona, J., Subah, A., Abbassi, B., van Afferden, M. (2011) Decentralized wastewater treatment in arid areas and options for a large scale implementation in Jordan. In: *Proceedings of the International Conference on Integrated Water Resources Management (IWRM)*, 12-13 October 2011, Dresden, Germany. (https://www.iwrm2011.de/_media/Mueller.pdf)
- NASA (2016) Global Precipitation Measurement, NASA. (Available at www.nasa.gov/mission_pages/GPM/main/index.html, accessed 11/4/2016)
- Nguyet, V.T.M., Thanh, V.P., Hai, V.D., Roi, N.D., Tra, D.T.T. (2016) Hydrogeochemical characterization and groundwater quality of the Dong Giao karst aquifer in Tam Diep, Ninh Binh, Vietnam, *Acta Carsologica* 45(3): 233–242, <https://doi.org/10.3986/ac.v45i3.3588>

- Nhan, D.D., Lam, N.V., Long, H.C.H., Thuan, D.D., Minh, D.A., & Anh, V.T. (2013) Hydrological characteristics of karstic groundwater in the northeast Viet Nam as studied by isotopic techniques. *Environmental earth sciences*, 70(2), 521-529. doi 10.1007/s12665-011-0943-x
- Oberle, P., Stoffel, D., Walter, D., Breiner, R., Vogel, M., Müller, H.S., Nestmann, F. (2017) Innovative Technologien zur Wasserförderung und-verteilung in Gebirgsregionen. *Bautechnik* 94: 514-525, <https://doi.org/10.1002/bate.201700066>
- Osborne, R. (2001) Halls and Narrows: Network caves in dipping limestone, examples from eastern Australia. *Cave & Karst Science* 28 (1), pp 3-14.
- Palmer, A. N. (1987) Cave levels and their interpretation. *NSS Bulletin*, 49(2), 50–66.
- Palmer, A. N. (1991) Origin and morphology of limestone caves. *Geological Society of America Bulletin*, 103(1), 1–21. <https://doi.org/10.1130/0016>
- Palmer, A. N. (2009) Cave exploration as a guide to geologic research in the appalachians. *Journal of Cave and Karst Studies*, 71(3), 180–192. <https://doi.org/10.4311/jcks2008es0042>
- Pardo-Igúzquiza, E., Duran-Valsero, J.J., Rodriguez-Galiano, V. (2011) Morphometric analysis of three-dimensional networks of karst conduits. *Geomorphology* 132 (1–2): 17–28. <https://doi.org/10.1016/j.geomorph.2011.04.030>
- Parkhurst, D.L., Appelo, C.A.J. (1999) User's guide to PHREEQC (Version 2): A computer program for speciation, batch-reaction, one-dimensional transport, and inverse geochemical calculations, *Water-resources investigations report*, 99(4259): 312.
- Phuong, T.H. (2000) Devonian, Carboniferous stratigraphy in the Dong Van section, Ha Giang Province (Địa tầng Devon, Carbon trong mặt cắt Đồng Văn, Hà Giang). *Journal of Geology, series A, Appendix/2000*, p. 2-9. Hanoi. (inVietnamese)
- Piccini, L. (2011) Recent developments on morphometric analysis of karst caves. *Acta Carsologica*, 40(1), 43–52. <https://doi.org/10.3986/ac.v40i1.27>

- Prime Minister of Vietnam (2017) Decision No. 438/QĐ-TTg dated April 7, 2017, Approving the Construction planning of Dong Van Karst Plateau Global Geopark, Ha Giang Province to 2030. (In Vietnamese)
- Reiter, F. & Acs, P. (1996). TectonicsFP software. <http://www.tectonicsfp.com>
- Richter, D., Goeppert, N., Zindler, B., & Goldscheider, N. (2021). Spatial and temporal dynamics of suspended particles and E. coli in a complex surface-water and karst groundwater system as a basis for an adapted water protection scheme, northern Vietnam. *Hydrogeology Journal*, 29(5), 1965-1978. doi:10.1007/s10040-021-02356-6
- Richter, D., Goeppert, N., & Goldscheider, N. (2022). New insights into particle transport in karst conduits using comparative tracer tests with natural sediments and solutes during low-flow and high-flow conditions. *Hydrological Processes*, 36(1), e14472. doi.org/10.1002/hyp.14472
- Shanov, S., & Kostov, K. (2015) Cave and Karst Systems of the World Dynamic Tectonics and Karst. *Springer*. <https://doi.org/10.1007/978-3-662-43992-0>
- Singer MB, Asfaw DT, Rosolem R, Cuthbert MO, Miralles DG, MacLeod D, Quichimbo EA, Michaelides K (2021). Hourly potential evapotranspiration at 0.1 resolution for the global land surface from 1981-present, *Sci Data* 8(1):224, <https://doi.org/10.1038/s41597-021-01003-9>
- Son, T.H., Koeberl, C., Ngoc, N.L., Huyen, T.D. (2007) The Permian-Triassic boundary sections in northern Vietnam (Nhi Tao and Lung Cam sections): Carbon-isotope excursion and elemental variations indicate major anoxic event, *Palaeoworld*, 16(1-3): 51-66, <https://doi.org/10.1016/j.palwor.2007.05.010>
- Stevanović, Z. (2019) Karst waters in potable water supply: a global scale overview, *Environ Earth Sci* 78(23):662, <https://doi.org/10.1007/s12665-019-8670-9>
- Taco van Ieperen (1990). On Station software. <http://cancaver.ca/Survey/OnStation>

- Tam, V. T., & Batelaan, O. (2011) A multi-analysis remote-sensing approach for mapping groundwater resources in the karstic Meo Vac Valley, Vietnam. *Hydrogeology Journal*, 19(2), 275-287. doi 10.1007/s10040-010-0684-z
- Tapponnier, P., Lacassin, R., Leloup, P. H., Schärer, U., Dalai, Z., Haiwei, W., Xiaohan, L., Shaocheng, J., Lianshang, Z., & Jiayou, Z. (1990) The Ailao Shan/Red River metamorphic belt: Tertiary left-lateral shear between Indochina and South China. *Nature*, 343(6257), 431–437. <https://doi.org/10.1038/343431a0>
- Taylor, S.R. & McLennan, S.M. (1985) The continental crust: its composition and evolution, Blackwell, Oxford, UK Press.
- Thach, N.N., Hai, P.N., Canh, P.X., Hang, N.T.T., Lam, N.V., & Thuy, D.T.T. (2013). Application of multimedia methodology for investigation of karst water in highland regions of Ha Giang Province, Vietnam. *Environmental earth sciences*, 70(2), 531-542. doi 10.1007/s12665-013-2617-3
- Tinh, H.X. (1976). Report on Geological Mapping and Mineral resources assessment at 1:200,000 scale of Bao Lac map group. *Department of Geology and Minerals of Vietnam, Hanoi* (in Vietnamese)
- Tri, T.V., Chien, N.V., Cu, L.V., Hao, D.X., Hung, L., Khuc, V., Luong, P.D., Ngan, P.K., Nhan, T.D., Quy, H.H., Thanh, T.D., Thi, P.T., Tho, T., Thom, N., Tung, N.X., Uy, N.D. (1977). Geology of Viet Nam–North Part (Địa chất Việt Nam – Phần Miền Bắc). *Scientific and Technical Publishing House Ha Noi*, p. 355. (in Vietnamese)
- Tri, T.V., Khuc, V, (editors) (2009). Geology and Earth Resources of Vietnam. *Natural Sciences and Technology Publishing House*, Hanoi
- Tricca, A., Stille, P., Steinmann, M., Kiefel, B., Samuel, J., Eikenberg, J. (1999) Rare earth elements and Sr and Nd isotopic compositions of dissolved and suspended loads from small river systems in the Vosges mountains (France), the river Rhine and groundwater, *Chem. Geol.* 160(1-2): 139-158, [https://doi.org/10.1016/S0009-2541\(99\)00065-0](https://doi.org/10.1016/S0009-2541(99)00065-0)

- Truong, D.N., Huyen, T.D., Khien, N.X., Phuong, T.H. (2004). On the Permian/Triassic boundary in Viet Nam. *Journal of Geology (Department of Geology and Minerals of Viet Nam)*. B/24: 1-9. Hanoi.
- Tuyet, D. (2001) Characteristics of karst ecosystems of Vietnam and their vulnerability to human impact, *Acta Geol. Sin. (English edn.)* 75(3): 325–329, <https://doi.org/10.1111/j.1755-6724.2001.tb00539.x>
- UNESCO (2021) Dong Van Karst Plateau UNESCO Global Geopark, Viet Nam <https://en.unesco.org/global-geoparks/dong-van-karst>
- van Afferden, M., Cardona, J.A., Lee, M.Y., Subah, A. and Müller, R.A., 2015. A new approach to implementing decentralized wastewater treatment concepts. *Water Science and Technology*, 72(11), pp.1923-1930. <https://doi.org/10.2166/wst.2015.393>
- Van, T. T., Lagrou, D., Masschelein, J., Dugar, M., Ke, T. D., Viet, A., Quyet, D. X., Thang, D. Van, Chung, H. T., & Anh, D. T. (2004). Karst water management in Dong Van and Meo Vac districts, Ha Giang province, Vietnam. Contribution of geological and speleological investigations. *Trans-KARST 2004*, 265–271.
- Van, T.T. (ed) (2010). Investigate and research geological heritages and propose building a Geopark in the North of Vietnam. *Archives in Vietnam Institute of Geosciences and Minerals Resources, Hanoi* (in Vietnamese).
- Wagner, T., Fritz, H., Stüwe, K., Nestroy, O., Rodnight, H., Hellstrom, J., & Benischke, R. (2011). Correlations of cave levels, stream terraces and planation surfaces along the River Mur-Timing of landscape evolution along the eastern margin of the Alps. *Geomorphology*, 134(1–2), 62–78. <https://doi.org/10.1016/j.geomorph.2011.04.024>
- Wang, E., Burchfiel, B. C., Royden, L. H., Chen, L., Chen, J., Li, W., & Chen, Z. (1998). Late Cenozoic Xianshuihe-Xiaojiang, Red River, and Dali fault systems of Southwestern Sichuan and Central Yunnan, China. In *Special Paper of the Geological Society of America* (Vol. 327). <https://doi.org/10.1130/0-8137-2327-2.1>

- Ward, J.H.Jr. (1963) Hierarchical Grouping to Optimize an Objective Function, *J Am Stat Assoc* 58: 236–244.
- White, W.B. (1988) *Geomorphology and hydrology of karst terrains*, Oxford University Press.
- World Bank (2018). *Assessment of the State of Hydrological Services in Developing Countries*. (Available at <https://www.gfdr.org/en/publication/assessment-state-hydrological-services-developing-countries>).
- World Health Organization (WHO) (2022) *Guidelines for drinking-water quality: fourth edition incorporating the first and second addenda*, <https://www.who.int/publications/i/item/9789240045064>
- Wunsch, A., Liesch, T., Cinkus, G., Ravbar, N., Chen, Z., Mazzilli, N., Jourde, H. and Goldscheider, N., (2022) Karst spring discharge modeling based on deep learning using spatially distributed input data. *Hydrol. Earth Syst. Sci.*, 26(9), pp.2405-2430, <https://doi.org/10.5194/hess-26-2405-2022>
- Zhou, H., Greig, A., Tang, J., You, C.F., Yuan, D., Tong, X., Huang, Y. (2012) Rare earth element patterns in a Chinese stalagmite controlled by sources and scavenging from karst groundwater. *Geochim. Cosmochim. Acta.* 83: 1-18, <https://doi.org/10.1016/j.gca.2011.12.027>